Republic of Iraq

Ministry of Higher Education

And Scientific Research

University of Kerbala

College of Engineering

Department of Civil Engineering

Effects of Topography, Land use and Climate change on storm water drainage under Different Rainfall Intensities in AL-Ameer District in city of AL-Najaf

A thesis submitted to the

Department of Civil Engineering University of Kerbela in Partial Fulfillment of the Requirements for the Degree of Master of Science in Civil Engineering (Infrastructure Engineering)

By

Salam Naji Hussein

B.Sc. in Civil Eng. / University of Technology (2006)

Supervised by

Prof. Dr. Basim Khlail Nile

Assist. Prof. Dr. Haider Mohammed Naima Zwain

October 2021 A.D.

بِسْمِ اللَّهِ الرَّحْمَٰنِ الرَّحِيمِ

نَرْفَعُ دَرَجَاتٍ مَنْ نَشَاءُ

وَفَوْقَ كُلِّ ذِي عِلْمٍ

عَلِيمٌ

صدق الله العلي العظيم

سورة يوسف - الآية (6)

Abstract

Stormwater drainage system flooding is a major problem in urban development that can be affected by land use, climate change, and topography. Flood problems can be successfully assessed using simulation models such as the Stormwater Management Model (SWMM). In this study, the generation of intensity-duration-frequency (IDF) curves integrating the impact of climate change for the Najaf Governorate in Iraq was performed for the first time. In addition, the impacts of different conditions of land-use (50, 75, and 100%), climate change (2, 5, 10, and 25 years), topography slope (0.5% to 0.4%, 0.3%, 0.2%, and 0.1%), and concentration time (downstream and upstream) on the stormwater drainage system were evaluated using SWMM simulation.

Results indicated that by increasing the sub-catchment area from 50 to 100%, there was an increase in total runoff from 20,380 to 37350 m^3, and total flooding from 10,513 to 26032 m^3, respectively. In response to climate change, changing the return period from 2 to 5 years increased total runoff from 14,120 to 27,110 m^3 (representing 48% of the increase), and total flooding increased from 5,914 to 17,591 m^3 (representing 66.66% increment). Generally, sub-catchment slope positively affected flooding at all rainfall intensities, but had less effect at low rainfall intensities. In a two years return period, the effect of sub-catchment slope was limited with high flood reduction, whereas low sub-catchment slope had a little effect on flooding at return period of 10 and 25 years. Finally, the rise of the sub-catchment slope is observed leading to a further increase in runoff, which leads to flooding. The results also showed that the flood time occurs downstream before the upstream, indicating that the downstream region

suffers from topographic and design problems. This was illustrated by manhole R315 flooding before manhole R15 because the slope of the sub-catchment is in the opposite direction of flow in pipes, as well as the depth of the manhole, is short.

To conclude, as flooding locations and magnitudes were identified, the system fails to discharge stormwater under some critical conditions, and the adverse effect of the climate change on the stormwater drainage system was more than the effects of land-use. Also, the designers must match the sub-catchment with network pipe slops to reduce floods.

Supervisor Certificate

I certify that this thesis entitled "**Effects of Topography, Land use and Climate change on storm water drainage under Different Rainfall Intensities in AL-Ameer District in city of AL-Najaf**", which is prepared by "Salam Naji. Hussein", is under my supervision at University of Karbala in partial fulfillment of the requirements for the degree of Master of Science in Civil Engineering (Infrastructure Engineering).

Signature:

Name: Prof Dr. Basim K . Nile

(Supervisor)

Signature:

Name: Assist. Prof. Dr. Haider Mohammed Naima Zwain

(Supervisor)

LINGUISTIC CERTIFICATE

I certify that this thesis entitled "**Effects of Topography, Land use and Climate change on storm water drainage under Different Rainfall Intensities in AL-Ameer District in city of AL-Najaf**", which is prepared by "Salam Naji .Hussein ", is under my linguistic supervision. It was amended to meet the English style.

Signature: Dhiya

Linguistic Supervisor: Deyaa Khalil Nile

Date: / / 2021

EXAMININATION COMMITTEE CERTIFICATION

We certify that we have read the thesis entitled **"Effects of Topography, Land use and Climate change on storm water drainage under Different Rainfall Intensities in AL-Ameer District in city of AL-Najaf"** and as an examining committee, we examined the student "Salam Naji .Hussein" in its content and in what is connected with it, and that in our opinion it is adequate as a thesis for degree of Master of Science in Civil Engineering (Infrastructure Engineering).

Signature:
Prof. Dr. Basim Khlail Nile
(Supervisor)

Signature:
Assist Prof Dr. Haider Mohammed Naima Zwain
(Supervisor)

Signature
Prof. Dr. Mussa H. Jasim
(Member)

Signature
Assist Prof. Dr. Ahmed S. Naji
(Member)

Signature
Prof. Dr. Jabbar H.Al-Baidhani
(Chairman)

Approval of the Department of Civil Engineering

Signature:

Name: Dr. Raid R. A. Almuhanna
(Head of civil Engineering Dept.)
Date: 1 / 11 / 2021

Approval of Deanery of the College of Engineering -University of Karbala

Signature:

Name: Assist Prof. Dr. Laith Sh. Rasheed
(Dean of the College of Engineering)
Date: / / 2021

ACKNOWLEDGMENTS

First, thanks to Allah his majesty, for completing this work. This project would not have been possible without the assistance of many individuals. I am grateful to those people, who donated their time and advice, especially my supervisors **Prpf. Dr. Basim Khalil Nile and Assit.Prpf.Dr. Haider Zwain** for their guidance, advice, invaluable remarks and fruitful discussions throughout the preparation of my thesis.

I also wish to express my deep appreciation and gratitude to the employees of the Sanitation Directory in Najaf, as well as the Urban Planning Department, the Geographical Information Systems (GIS) Department.

I would also like to express my deepest gratitude to my mother and wife for their support, as well as I wish God's mercy and forgiveness for my father, without whom hope would not have been fulfilled.

Many others are not mentioned explicitly here; their efforts are equally appreciated.

Table of Content

List of Tables

List of Figures

Abbreviations

Abbreviation	Description
GIS	Geographic Information System
PVC	Polyvinyl Chloride
D.S.N	Directorate of the Sewage of Najaf
SWMM	Storm Water Management Model
IDF	Intensity-Duration-Frequency curve
USGS	U.S Geological Survey
SSA	Storm and Sanitary Analysis
R	Correlation coefficient
DEM	Digital Elevation Model
TIFF	Format File Tagged Image
USEPA	United States Environmental Protection Agency
SCS	Soil Conservation Service
ILLUDAS	I lliuoise urban drainage area simulator
SSA	Autodesk Storm and Sanitary Analysis 2015
USEPA	the United States Environmental Protection Agency
IDM	Indian Meteorological Department
G.A.M.S.M	the General Authority for Meteorology and Seismic Monitoring

CHAPTER ONE

INTRODUCTION

1.1 Background

Drainage systems have been used since the beginning of the third millennium BC. studies of practical technical solutions to problems of water transfer have a long history, as they first appeared in Mesopotamia, Egypt, India, Hellas, and China as a fusion of technology between philosophy and science (Yannopoulos et al., 2015).

Urban floods have become a common threat to urban areas, causing loss of life and massive property damage, Urban growth generally causes hydraulic hazards, due to the sealing of natural surfaces and directing of the natural underground drainage network to the pipes, thus increasing surface runoff (Qi et al., 2020).

Infrastructure is adversely impacted by the flooding of storm systems in urban areas. Climate change increases the amount of runoff by increasing the intensity of rainfall, hence, it's the most significant parameter that influences the rate of flooding. Urban growth also increased urbanization and produced an increase in impermeable areas, which in turn reduced the rate of infiltration that causes the amount of runoff, peak flow, and concentration-time to increase(Nile, 2018).

The Modeling used to assess urban floods relies on topography and urban engineering. Urban surface features that range from major features are included (e.g. construction) to minor features (e.g. sidewalks, etc.) have been included in flood modeling approaches for various purposes of urban hydrology and flood assessment (Leandro et al., 2016a).

The implications of employing high-resolution data for urban drainage modeling, increases the acquisition of accurate results(Schubert et al., 2008). In addition to observed increases in high-intensity, in short-term precipitation events that generate pluvial flooding, nuisance flooding is a source of concern due to the combined effects of urban areas' high exposure potential (Westra et al., 2014).

Floods can also occur when drainage is inadequate, such as when rainfall exceeds the storm design level, or when storm sewers back up due to overcrowding or the presence of clogs (such as leaves) that prevent water from flowing from the streets to the stormwater system (Rosenzweig et al., 2018).

The effective drainage of the rain network has a powerful link with drain duration and concentration-time Sub-catchment that affects velosity and peak runoff releases. Besides, urbanization affects hydrology, which is characterized by the rise in peak flooding values This triggers a rise in runoff volume and reduces the time lag (Ogden et al., 2011).

many parameters on the performance of storm network to get many options such as water flooding and water depth. The model is commonly used for drainage system planning, analysis, and design in metropolitan areas. The model comes with a Windows environment that allows you to edit data, perform simulations, and view the results in the form of themed maps, graphs, tables, profile plots, and statistical reports (Gironás et al., 2010).

AL-Ameer District as a case study is distinguished by its religious and tourist nature, which caused the migration of citizens from various cities to it. Urbanization in the study area [Al-Ameer district, Najaf] transformed most of the lands from the pervious sand into an paved impervious area, and the effect of the topography increases the velocity of runoff, which leads to an increase in urban floods. As a result, controlling the amount of flooding in urban areas became an important issue in order to reduce the cost of damage to the infrastructure.

1.2 Statement of the problem

The case study is Al-Amir district, which is located in the northeastern part of Al-Najaf Al-Ashraf city, Iraq. The study area suffers from the flooding of the rainwater drainage system during the rainy seasons. Because of the topography of the land represented by the high slope and the establishment of the airport road at a level higher than the study area, which ranges nearly a meter higher than the study area, the area has become relatively low, and thus leads to rainwater gathering in the downstream, which leads to damage to infrastructure and property. Further, urban expansion and an increase in the intensity and amount of precipitation to values higher than that of the design increased the discharge stormwater drainage system requirements in the study area. This increase coupled with the velocity of surface runoff exceeded the drainage capacity of the network and led to the occurrence of floods .

1.3 Objectives of the study

The study's main goal is to assess floods in the Al-Ameer District's stormwater drainage system. Simultaneously, the research attempts to:

- Produce an Intensity-Duration-Frequency (IDF) curve for Al-Najaf city for the first time.
- To create a model to simulate the performance of Al-Ameer District stormwater drainage system using (SWMM).
- To evaluate a model the effects of different land-use, climate change, topography slope, and concentration time on the system performance.

- To Provide technical support by modeling solution scenarios to mitigate the flooding effects in the study area.

1.4 Scope of the study

The steps to work in this study could be summarized as the following:

a) This study is a case study conducted in Al-Ameer District of Najaf, Iraq. This District is facing many changes in recent years that lead to severe flooding.

b) This study relied on the available hydrological data, residential unit areas, slopes, and storm drainage network extensions.

c) The maximum flow of water entering the study area from the neighboring areas during the period in which the maximum precipitation coincides was taken into consideration.

d) The information from the Department of Urban Planning was used to identify commercial, industrial and public places.

e) Information provided by the (D.S.N) was used regarding the diameters and lengths of pipes and manholes and their levels.

f) Rainwater Management Model (SWMM5.1) and Geographic Information of the GIS system were used as tools to facilitate the data entry process.

1.5 Engineering Significance

Through this study, it is possible to help engineers and decision makers through some of the following procedures:

1) There is a lack of hydrological data, and from this study, an IDF will be drawn that will help researchers and designers to predict the amount of future rainfall.

2) The conclusion of a mathematical model that helps designers in analyzing, designing and evaluating the rainwater drainage system without resorting to engineering programs.

3) Through this study, the network was evaluated and the flood areas and flood quantities were determined, and this helps decision makers to take proactive measures to reduce floods.

4) Find some solutions and scenarios to reduce recurrent floods during the rainy seasons.

1.6 Thesis structure

The thesis is divided into five chapters:

- Chapter one shows the background, problem statement, objectives of the study, study scopes, the methodology of this thesis, thesis structure, and summary of chapter one.
- Chapter two listed the literature review of the different sections. The first section is related to the factors influencing stormwater, the second section associated with the curve of the Intensity-Duration-Frequency (IDF) and the relation with the SWMM model.
- Chapter three describe the subjects: states the study area, Intensity-Duration-Frequency curve (IDF), SWMM, the properties of collected data, and stormwater .
- Chapter four illustrates the results of the SWMM model and a suggested scenario that present concerns for future work.
- Chapter five consists of the conclusions and the recommendations for the topic.

CHAPTER TWO
LITERATURE REVIEW

2.1 Introduction

This chapter presents the main factors that affected urban flooding in the literature Review. These factors were climate change, represented by the effects of different rainfall intensities, urbanization, land-use, the effect of topography and misuse of the drainage system. Besides, this chapter will present previous studies related to urban flood modeling by SWMM.

2.2 Storm Sewers

Rain sewers are underground pipes used to efficiently and easily transmit stormwater from urban areas into natural bodies of water such as streams and lakes. Usually, they are used in highways, and parking areas. Urban planners handled stormwater before the construction of rain sewers, by channeling it into a system of swales along streets and alleys and ultimately into streams, a technique still in use in underdeveloped countries today(Gribbin, 2013).

Since the water stayed on the ground surface, it resulted in inconvenience and transmission of illness .The introduction of storm sewers allowed land development with modern transportation advances practically unencumbered by stormwater issues. Storm sewers have been used in urban areas over the past century to transport sewage waste as well as stormwater in the same pipes. Combined sewers are called such systems and have now been almost removed in favor of independent storm sewers and sanitary sewers. Figure (2.1) depicts these basic elements of a stormwater drainage system (Gribbin, 2013).

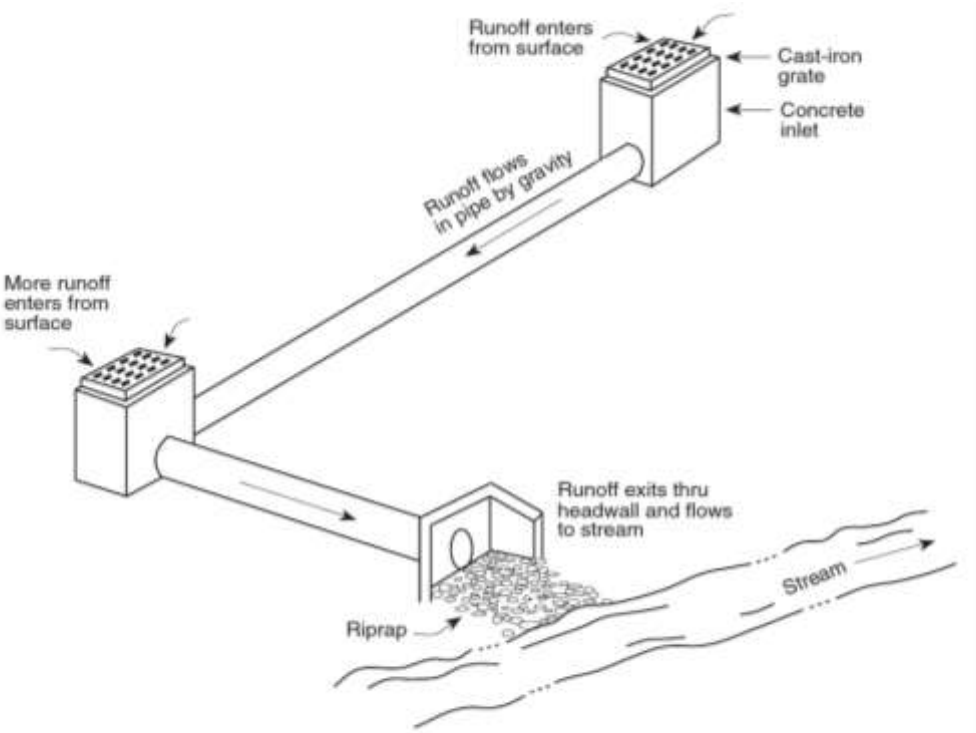

Figure 2.1: Basic elements of a storm sewer system(Gribbin, 2013).

In many countries, urban flooding caused by stormwater runoff was a problem. The hydraulic design and efficiency of sewage pipes must be improved, which will help reduce the effects of floods in urban areas. (Wang et al., 2018) had studied circular slope pipes, where the overcritical flow descends into steep topography and forms a controlled hydraulic jump downstream, which papers flow procedures. The movement of jumping and the consequent throttling of flow in a circular pipes is not well understood yet. Based on momentum theory, this study formulates and solves the problem of hydraulic jump in a circular slope pipe using iterative methods. The solutions require an undulating jump and a direct jump in the filling ratio and the downstream area. For the first time, the pipe slope dependence of Froude's number was measured. It is possible to obtain two different fill ratios for a given slope (or equivalent diss).

Storm channels provide important data for flood modeling, but it is also necessary to simplify the tension between massive data volumes and the existing computational resources to balance it. To develop rational generalization techniques, the sensitivity of flood simulation to the accuracy of storm sewer system data must be explored. In this study, in terms of total inland drainage flow and flood impacts, the effect of using the stroke computation method for generalizing storm ducts on flood simulation was analyzed. The results of the three study basins showed that the different dynamics of the sewer system did not have a significant effect on the average outflow of the single drainage area, but it did so for the multiple drainage areas. Besides, the harmful floods were mainly scattered over the main pipes, which can be identified by the simplified sewer system (Yang et al., 2018).

(Hassan et al., 2017) had studied the behavior of stormwater drainage system in the Middle East region (Karbala City, Iraq), while has been evaluated in order to predict future flooding hazards caused by climate change, especially in the event of insufficient sewer connections. For Karbala's storm drainage network simulation, the analysis used the SWMM model. From 2008 to 2016, continuous hourly data on rainfall intensity was used. It was concluded that the system was adequate as planned, without consideration of excess sewage due to an illegitimate sewer connection. The results showed that the SWMM was effective in modeling urban flood forecasting, and urban flooding could not be predicted perfectly without surface runoff routing.

2.3 The Relation between Urbanization and Flooding

Changes in land use and a rise in the difference in level (land slope) enhance the risk of urban floods, which increases the volume of surface runoff and shortens the time at peak discharge (Figure 2.2)(Butler et al., 2018).

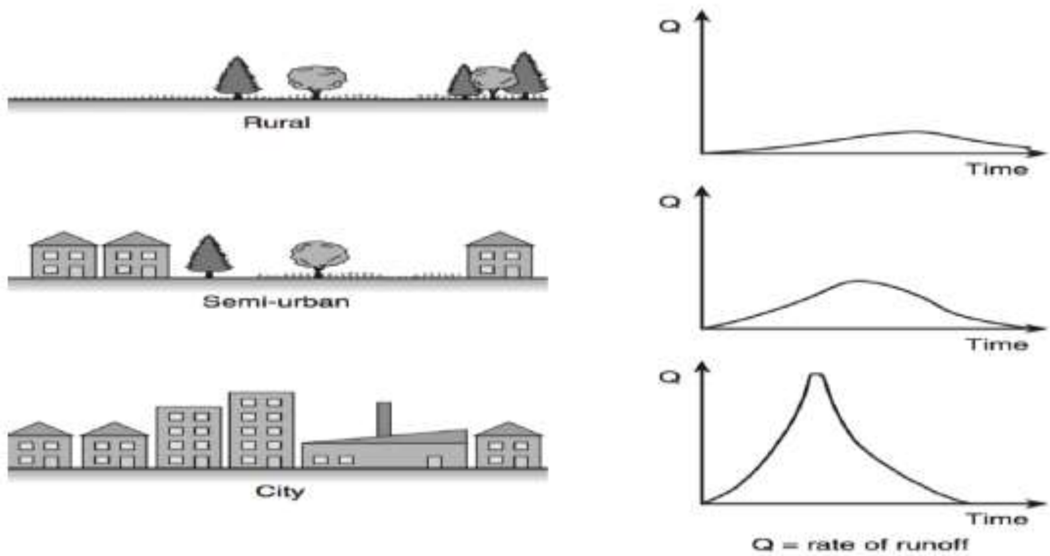

Figure. 2.2:The effect of land use change on flooding phenomena(Butler et al., 2018).

In Los Angeles the urban area, (Sheng & Wilson, 2009) reported that owing to the drop in the infiltration rate as a result of the shift in the land use cover, there was a loss of 90 % of the precipitation as a runoff. Although 25% of rainfall in non-urban forested areas retains the residual amount of water lost due to infiltration and evaporation as a runoff. Some of the runoff losses through evaporation or absorbed by plants when rainfall non-urban areas; some infiltrates through soil and convert to groundwater storage, and some runs off the ground (Figure 2.3.a) shows that. Urbanization involves covering the impermeable surface of the natural earth. The impermeable surface increases the amount of surface runoff and decreases the rate of infiltration, thus increasing the total volume of water flooding during or rapidly after precipitation (Figure 2.3.b) (Butler et al., 2018).

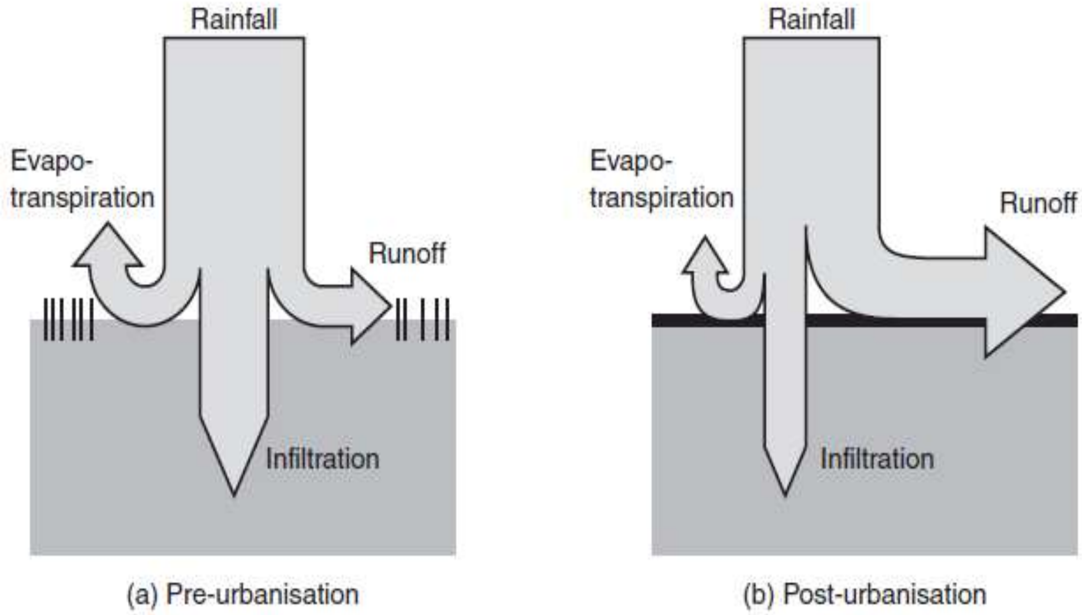

Figure. 2.3 (a&b): The effect of urbanization on the hydrology cycle) (Butler et al., 2018).

2.4 Factors affecting the design of stormwater systems

2.4.1 IDF curve

The rainfall curves (IDF) are graphical representations of the probability of a specific average rainfall intensity happening during a given time period(Nhat et al., 2006). The IDF curves provide a mathematical relationship between rainfall intensity (I) Duration (d), and return period (T) (or equal to the annual excess frequency (f), allowing the return period of an observed rainfall event to be calculated or, conversely, the rainfall intensity corresponding to that return period to be estimated (Elsebaie, 2012). Design storms resulting from IDF curves are commonly used in water management engineering for modeling urban drainage systems, evaluating the durability of hydraulic infrastructure, and assessing regional flood hazards (Sun et al., 2019).

The usual steps for deriving the IDF curves are, as shown in Figure (2.4), as follows (Nhat et al., 2006).

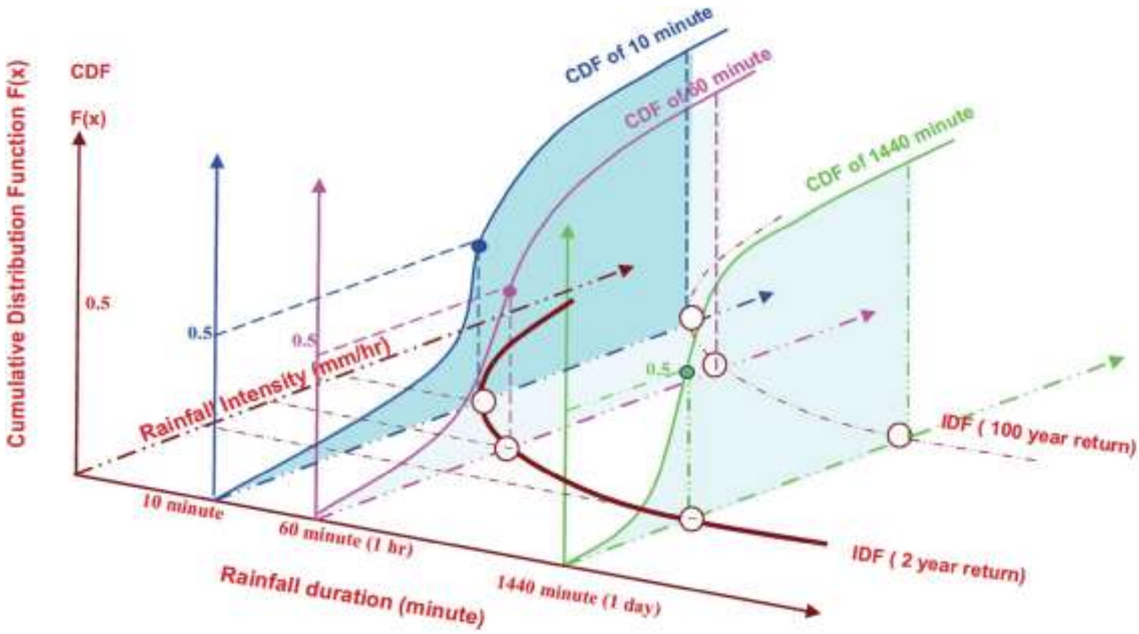

Figure 2.4: Derivation of IDF curves schematic diagram (Nhat et al., 2006).

2.4.2 Empirical Intensity for IDF Equations

The IDF formulas are empirical equations that define the relationship between maximum rainfall intensity (as a dependent variable) and other factors of relevance, such as rainfall period and frequency (as independent variables). There are several extensively used functions in the literature of hydrological applications; four fundamental types of equations used to explain the relationship between rainfall intensity and Duration are presented as follows (Chin, 2019).

Talbot Equation $i = \frac{C * T^m}{d + b}$ **[2.1]**

Bernard Equation $i = \frac{C * T^m}{d^e}$ **[2.2]**

Kimijima Equation $i = \frac{C * T^m}{d^e + b}$ **[2.3]**

Sherman Equation $i = \frac{a}{(T + b)^C}$ **[2.4]**

Where 'i' is the rainfall intensity (mm/hour);
d is the duration (minutes);
T return period in years c, b, e and m are the constant parameters related to the metrological conditions.
It can be seen from these empirical equations that rainfall intensity reduces as rainfall duration increases for a particular return period. All of the functions have been extensively used in hydrology applications.

2.4.3 Empirical Reduction Formula

To estimate the IDF curves for Baghdad city, (Al-Awadi, 2016) has been using the Indian reduction equation (IDM) in the Estimation of Short Duration Rainfall. Various frequency analysis technical procedures were used to develop the relationship between rainfall intensity, storm duration, and return periods from the rainfall data. These technologies are: Gumbel, Log normal, and Log Pearson Type III distributions. Nonlinear regression analysis was also used to estimate the IDF equation coefficients for different return periods.

2.5 Effect of land use on stormwater drainage system

Urbanization has resulted in a rise in impervious surface areas, which have resulted in 30 major hydrological effects around the world (Bell et al., 2016). Changes in land use, land cover, and lack of green space have a negative effect on quantity runoff , runoff velocity, peak flood duration, and magnitude, which increase the risk and magnitude of urban flood disasters, are the most direct of these influences(Pauleit et al., 2005).

(Kong et al., 2017a) studied assessed flood control capacities for applying large-scale LID techniques in urban sub-catchment in central Illinois using a personal computer stormwater management model (PCSWMM). Two flood gauges based on surface runoff were used to identify floods (43 m^3/s) and significant floods (95 m^3/s). Four land-use scenarios for urban development were analyzed to estimate the influence of urbanization on surface runoff and flooding. According to modeling data, increasing urban land use from 50% to 94 % between 1992 and 2030 increased average annual runoff and flood events by more than 30%, implying that urbanization without effective management would raise flooding risk by more than 30%.

In areas where urbanization has risen, stormwater runoff issues and impacts are most apparent. Land use adjustments have a significant impact on both the amount and consistency of runoff from stormwater. Urbanization can drastically alter the natural hydrology of a region if not properly designed and controlled. The increased of impermeable cover reduces the amount of rainwater that can infiltrate into the soil naturally and increases the volume and rate of runoff of stormwater, the changes are contributing to more frequent and serious floods and possible public and private property damage. Usually, under natural conditions, 10% of stormwater falling on a piece of the property flows into streams, rivers, or lakes off the ground surface. The remaining either results in evaporation into the air or infiltration into the soil which provides groundwater replenishment Figure (2.5). Site layout increases the number of surfaces that are impervious. Since the percentage of impermeable surfaces increases, the percentage of runoff rises(Miles, 2014).

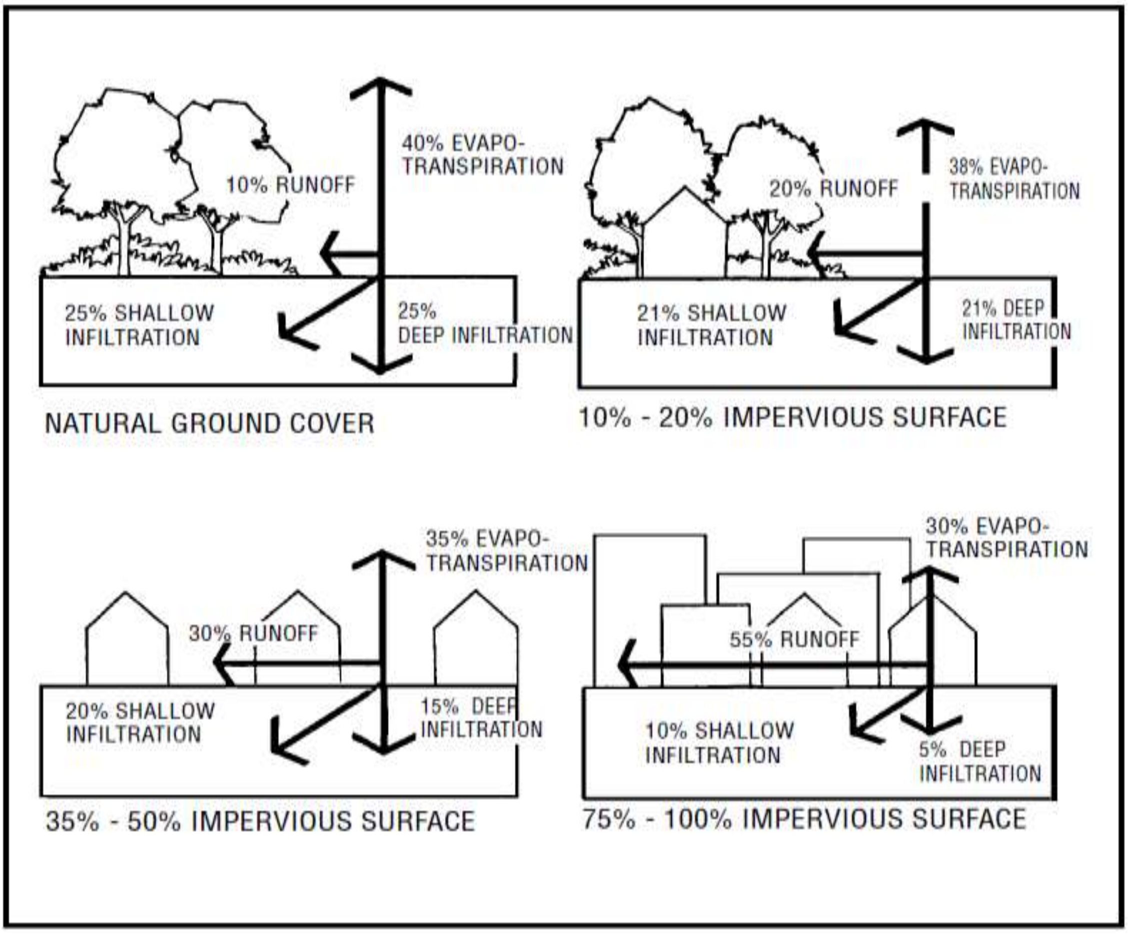

Figure 2.5: Changes in Runoff Flows Resulting from Paved Surfaces (Miles, 2014).

The rate of runoff and stream flow following a storm event often shows significant rises in post-predevelopment conditions relative to pre-development conditions Figure (2.6). The higher and faster peak discharge of runoff and stream flow, causing downstream flooding and stream bank erosion, can overload the capacity of the stream or river. Every year, local governments expend millions of dollars rectifying the harm caused by unregulated stormwater pollution to public and private land. During heavy rainfall, damage to public and private property happens in heavily developed areas. This damage involves washouts of highways, culverts, and water and sewer lines, flooded homes and yards, sediment and debris accumulation on properties and roads, and bridge damage. The Sediments clog stream channels, culverts, and pipelines with sediment as stream banks erode, leading to flooding problems. Sediments are washed into wetlands, lakes, and other impoundments, decreasing their water holding capacity and requiring expensive measures to clear them (Miles, 2014).

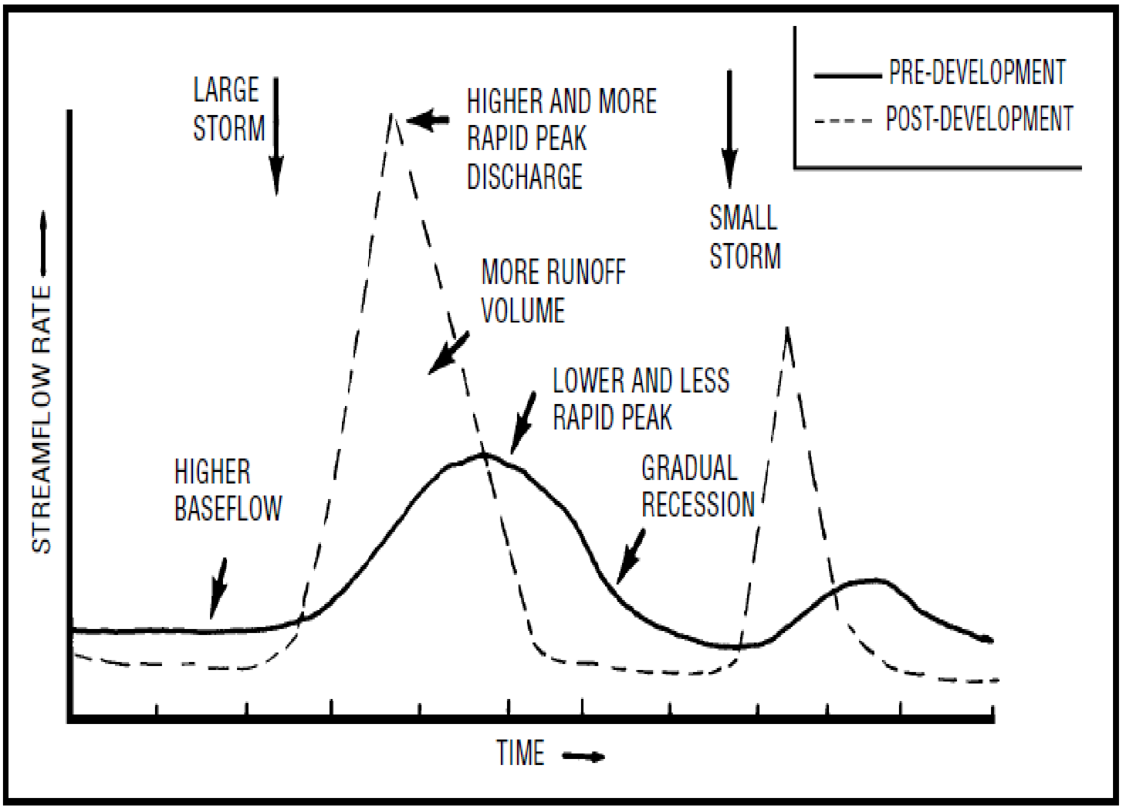

Figure 2.6: Pre Versus Post Development Stream flow Rates (Miles, 2014).

2.6 Effect of Topography on the Design of Stormwater Systems.

One of the vital elements of hydrological activity is topography. Topography geometry can take on complex forms with various slopes and curvature profiles (Agnese et al., 2007). Topography geometry, characterized by elevation, slope, ramp length, and curvature, has a significant effect on runoff and exerts significant influence over the basin's hydrological response, determining the boundary conditions under which water and sediment transport processes can take place (Hallema et al., 2016).

(Troch et al., 2003) found that converging surfaces drain more slowly than diverging surfaces due to the lower flow at the basin's exit. The topography and urban area geometry produce prediction of urban flooding. For diverse objectives of urban hydrology and flood assessment, urban surface features ranging from major characteristics (e.g. structure) to minor characteristics (e.g. sidewalks, road curbs, etc.) have been used in flood modeling methodologies (Leandro et al., 2016b).However the implications for practical 1D-2D urban drainage modeling of high-resolution data usage combined with optimization procedures have not been studied so far.

2.7 Climate Changes effect on storm sewer

The distinction between climate change and climate variability, where the former signifies a long-term change in climate, is very important to remember, while the latter is the normal change in climate from one time to the next. Climate variability tends to have a very strong influence on different hydrological processes (Kundzewicz & Robson, 2004).

Stormwater drainage system flooding can be exacerbated by climate change. The Al-Abbas neighborhood in Karbala, Iraq, was selected as a case study for the present study(In this research Storm Water Management Model [SWMM] has been used to simulate the flooding of the storm drainage network in Al-Eskari quarter, Kerbala, Iraq.). To forecast the severity of the future period 2017-2070 and to research the effect of climate change on such a prediction, historical data for the period 1980-2016 was used. The results suggested that 46.48 mm/hour would exceed the maximum intensity of the precipitation in the year 2067. This value is three times the intensity of the design. With time, the percentage of manholes grows. For each particular time span during the 53-year study design period, five design phases were chosen to demonstrate the variability in manhole flooding. In the first phase, for example, the flood rate decreased by 39.2% in 2070, while in the second phase the rate increased by 14.2%, the third phase increased six times, the fourth phase did not shift, and the fifth phase increased by around 6% relative to the beginning period 2017 (Hassan et al., 2017).

In evaluating the hydraulic capacity of urban drainage systems, the growth of urbanization, and the likely rise in severe rainfall due to climate change were the most important impacts. Clear evidence also suggests that sewage surcharge and flooding opportunities and threats are increased due to global warming.(Solomon et al., 2007).

(Sansom & Renwick, 2007) had studied the assessment of the impact of future climate change, it was found that this effect can result in both floods and droughts. The result of using general circulation models (GCMs) to estimate climate change in New Zealand was an increase in rainfall intensity as a result of increased rainfall due to climate change.

(Elshorbagy et al., 2018) simulated and quantified the inevitable natural weather variability and its impact on the uncertainty of extreme events. When water ponding/flooding is a key concern, the study's main finding was that the distribution of rain throughout the storm event may be more relevant than the overall rainfall depth. Furthermore, risk assessments must be adapted to the type of infrastructure under consideration, according to the findings.

In general, the urban area is projected to different effects due to climate changes. In this regard, low-intensity precipitation events will not damage the urban stormwater drainage system directly, but it is possible that this may multiply the effect of following precipitations if pervious areas can become saturated and may affect the levels of groundwater. On the other hand, extreme precipitation and very high-intensity events are likely to cause increased surface floods, basement floods, combined sewer overflow and influx to treatment instruments. Even if the entire precipitation volume reduced, the increased peak intensity will cause quick runoff, and the satisfactory infiltration ability might not be obtainable (Olsson et al., 2009).

2.8 Software Used for Stormwater Systems

Rainfall simulation is a well-known simulation method that has been used for a long time. The rainfall simulator is also based on technological advancements and information on rainfall and the relationship between rain and the ground. There are several different types of rainfall simulators in use now all around the world. Rainfall simulation can also be used to investigate the impact of particular management actions on the properties of a certain material, or to improve our understanding of processes like erosion, rainfall network analysis, and design, runoff, and infiltration (Haris et al., 2016).A list of the stormwater management techniques most used is as follows:

2.8.1 Info Works

Info Works River Simulation (InfoWork RS) is hydrodynamic modeling software that allows users to model open channels, floodplains, hydraulic structures, and embankments in their entirety. Both event-based and conceptual hydrological methods can be used to simulate rainfall-runoff utilizing spatial plan views, sectional views, long sections, spreadsheets, time-varying graphical data, and incomplete interactive data displays. Complete flood-mapping capability is offered based on a sophisticated flood-interpolation model layered on an imported ground model (Salarpour et al., 2011).

InfoWorks RS integrates a powerful flow simulation engine, hydrological and hydraulic models, GIS capability, and database storage into a single environment. An "Integrated Network Model" integrates data storage via a GIS to the software suite for hydrological/hydraulic modeling incorporated in InfoWorks RS as the main system architecture (Mah et al., 2007).

2.8.2 MIKE URBAN

Hydraulic modeling in urban contexts is a common MIKE URBAN application. It focuses on stormwater runoff, as well as its discharge through open or closed pipes and on the ground.

- Mike Urban is in charge of collection system master planning.
- Hydraulic rehabilitation plans for wet weather management to reduce overflows.
- Management of capacity and operational upkeep.
- Inflow and infiltration that are influenced by rainfall.
- Flood- response planning for metropolitan areas.

The user can have a better understanding of rainfall-runoff and discharge processes in metropolitan settings by using hydraulic models.

Detailed cost-benefit evaluations also allow consultants and engineers to construct scenarios to optimize existing infrastructure, resulting in logical and repeatable city planning operations. The best-known mathematical answers to the physical properties of the system are used to create MIKE URBAN models. Hydraulic processes are thus handled with extreme precision. One of the reasons MIKE URBAN is the best choice for designing or optimizing cost-intensive infrastructure projects is this (Bisht et al., 2016).

2.8.3 Autodesk Storm and Sanitary Analysis 2015 (SSA)

It's easy to understand and use the Autodesk Storm and Sanitary Analysis tools. A number of different sources can be used to rapidly create simulation models. CAD and GIS files can be used to import network components. The network model can be created interactively by pointing and clicking with a mouse. Manholes, pipes, pumps, weirs, ditches, channels, catch basin inlets, and detention ponds are all represented with graphical symbols. The app allows you to connect, insert, delete, or transfer any network feature interactively at any time, automatically updating the model. Selecting and moving a manhole, for example, transfers all linked pipes, ditches, channels, and other structures. Pipes can be curvilinear, and lengths can be measured automatically. GIS and CAD files of streets, plots, and houses, as well as scanned aerial ortjumphoto TIFF photos and charts, can be imported and displayed as a background image. You can use this function to easily digitize a network model, validate the network layout, or improve the performance modeling results. You can also use the Plan View to quickly evaluate the specified input data and output modeling results by pointing to or clicking any network manhole, pipe, pump, weir, ditch, channel, catch basin inlet, or detention pond(Kim et al., 2015).

2.8.4 SWMM

The USEPA Storm Water Management Model (SWMM) was developed in 1971 and widely has been used in thorough hydrological and hydraulic modeling of stormwater and the sub catchment for over 30 years.

This software can simulate the passage of precipitation from the ground to a channel or pipe network. SWMM simulated single occurrences as well as a long continuous period of events. The SWMM version has been freeware for a long time and is maintained by a large number of individuals and organizations. The SWMM engine has been rewritten and is now known as SWIMM 5, which is maintained by the USEPA. Every sub-cluster in this hydrological model is represented by a sub-cluster (Lockie, 2009).

The (SWMM) of the USEPA is one of the most extensively used numerical models for simulating urban runoff and drainage. Hundreds of thousands of sub-catchments are involved in a typical SWMM project, with more than 20 parameters connected with six separate physical processes for each sub-catchment (Behrouz et al., 2020).

(Jiang et al., 2015) made a comparison by using a combination of SWMM or other urban hydrology model with synthetic hydrograph methods like (Soil Conservation Service) SCS–SWMM or Clark–(illiuoise urban drainage area simulator) ILLUDAS or use traditional synthetic hydrograph methods such as SCS–SCS or Clark–Clark to estimate the urbanization influence on the hydraulic performance for the same stormwater drainage system and same location in Korea. The result of the comparison stated that the using of SWMM model give appropriate and predictable results for the influence of the urbanization approximate to reality .The results of SWMM can be used for design purpose comparing with the traditional synthetic hydrograph methods. SWMM gave a good result even for simulation of an un calibrated natural sub catchment areas.

2.8.5 DR3M

Distributed Routing Rainfall-Runoff Model (DR3M) is one of the storm water modeling. This software is created to simulate the storm runoff. It can simulate the routing storm either in system or pipes or natural channel. By using rainfall as an input, this software model the detail simulation of storm runoff according to user period time selected.

DR3M is commonly is used to simulating the storm runoff for small urban basins. To calculate the infiltration and pervious area rainfall excess the Green-Ampt equation is used. The disadvantage of this software is it does not simulate interflow and base flow of the basin. Daily precipitation, daily evapotranspiration, and short-interval precipitation are required for data requirement. To optimize and calibrate the model short interval discharge is needed (Survey U S G, 2020).

2.8.6 HSPF

Hydrological Simulation Program-Fortran (HSPF) simulating the extended periods of time the hydrologic processes on pervious and impervious land surfaces and in streams and well-mixed impoundments. HSPF uses continuous rainfall and other meteorological records to compute stream flow hydrographs. This software is used to simulate one or many pervious or impervious unit areas discharging to one or many river reaches or reservoirs. Any time series for frequency-duration analysis can be done. From 1 minute to 1 day at any time that divides equally into 1 day can be used. HSPF also can simulate any period from a minute to hundreds of years. This software is generally used to evaluate the effects of land-use change, reservoir operations, point or nonpoint source treatment alternatives, or flow diversions (U S Geological Survey, 2008)

Programs which available separately, will support data in pre-processing and post processing for statistical and graphical analysis of data saved to the Watershed Data Management (WDM) file. The model contains hundreds of process algorithms developed from theory, laboratory experiments, and empirical relations from instrumented watersheds. HSPF simulated sediment routing by particle size, channel routing, reservoir routing, and constituent routing. Meteorological records of precipitation and estimates of potential evapotranspiration are required for watershed simulation. Physical measurements and related parameters are required to describe the land area, channels, and reservoirs (U S Geological Survey, 2008).

2.8.7 XP-SWMM

Fully two-dimensional (2D) models have long been used to simulate river and coastal hydraulics, and they have lately become a viable choice for simulating urban floods. 2D models are more accurate as a stormwater management tool, and they offer results that are significantly more easily accepted and understood by managers, decision-makers, and other stakeholders. A 2D hydrodynamic simulation engine has been integrated into XP-user-friendly SWMM's graphical interface, which guides the user through the preprocessing of input data, model calculation, and display of model results. The 1-dimensional river model built in the previous instruction is given a 2D component in this tutorial. Polylines and polygons are used to add 2D objects. The model is solved when the 2D job control settings are set. There are animations showing velocity and water depth (Phillips, et al,. 2005).

*There are other programs, including MOUSE, DRAIN, ... etc.

2.9 Dimensional and Similitude Analysis

Defining dimension analysis is a very effective method to use in analyzing and understanding engineering problems. For computing dimensionless parameters, the dimensionless analysis provides a response to the set of parameters affecting the problem. Using Buckingham's π

theory, this meta-analysis can be performed. The number of independent parameters involved in the problem is reduced by dimensional analysis,As a dimensionless class, these independent parameters are expressed. Often such dimensional combinations are ratios of significant physical quantities involved in the problem of interest. Its main purpose in modeling and experimentation is to reduce the number of independent variables, simplify the solution, and generalize their results (Reddy & Reddy, 2014).

2.9.1 The π-Theorem

Many statements have been practically considered about the π-theorem. In fact, any of the texts which have been mentioned above on dimensional analysis or every basic text in fluid mechanics have some statement of it. It is worthy to mention that this given statement is adapted and modified from the original paper of Buckingham (Buckingham, 1914). The Buckingham's π-theorem can be stated as follows: Any dimensionally homogeneous equation of the form.

$$F(Q1,Q2,Q3,\ldots\ldots Qn)=0 \qquad [2.5]$$

that is dimensionally homogeneous, defines a relation among (n) different kinds of quantities such as: Q1,Q2,... Qn, which involves ($k < n$) as essential dimensions, if this equation is a correct and complete one, is reducible to the form.

$$F(\pi_1, \pi_2, \ldots, \pi_n) = 0 \qquad [2.6]$$

Where the symbol (F) is some unknown function to be calculated by experiment, at the same time each π-term is considered as a dimensionless product which is made up of the Q's, also each π-term should consist of less than k + 1 variables (here just one need may be changed from term to term and where there just k variables will be common to every π-terms), where i = n - k, which is considered as the number of dimensionless products which derived from the (n) quantities by involving (k) essential dimensions. (Wong, 1978) claimed that if Q1, Q2, Q3 . . , Qk are all the Q's common to all π-terms, then the i dimensionless products could be written in the following way (Wang, 2021).

$$\pi_1 = Q_1^{x1}\ Q_2^{y1}\ Q_3^{z1}\ \ldots.Q_k^{k1}\ P_1,$$

$$\pi_2 = Q_1^{x2}\ Q_2^{y2}\ Q_3^{z2}\ \ldots.Q_k^{k1}\ P_1, \qquad \textbf{[2.6]}$$

$$\ldots\ldots\ldots$$

$$\pi_i = Q_1^{xi}\ Q_2^{yi}\ Q_3^{zi}\ \ldots.Q_k^{ki}\ P_i.$$

evaluate and Analyzing the performance and drainage capacity of the stormwater drainage system in light of climate change and the impact of topography and assessing the network performance in the framework of the proposed improvements to provide technical support to decision-makers The results will address flood problems and help improve the drainage capacity of the stormwater drainage system.

2.10 Gap of Knowledge

The IDF relationships are essential for the designing of hydraulic structures for future planning and management and there is no available data for the study area. The intent is to determine IDF relationship for the area, Rain gauge stations are not so frequent in the study region. Under this condition, the engineers are bound to use IDF relationships. The effects of topography and climate change on the existing stormwater system in the study area have not been analyzed. The use of the SWMM program is to evaluate the rain drainage networks and identify problems and solutions can also be found.

2.11 summary

Previous studies indicated that the SWMM model was effective and able to simulate urban flooding and produce results close to reality. It can also provide decision-makers with technical support in planning, management improvement, and hydraulic rehabilitation plans for urban flood control in order to reduce effort and economic losses and help them make sound decisions towards the implementation of development. Studies have identified a critical role for the SWMM in the design, planning, evaluation, and analysis of the storm, sewer system, and subscriber. The impact of urbanization and climate change on urban floods can be simulated and analyzed by SWMM. In this study, a rain runoff simulation model in Al-Ameer, Najaf, Iraq was based on the SWMM model. It aims to

CHAPTER THREE

STUDY METHODOLOGY

3.1 Introduction

The research methodology directs the researcher to do the work from start to finish, collect data directly, analyze data, interpret results, and draw conclusions. The purpose of this chapter is to discuss the methods used to model stormwater drainage system in the case study of AL-Ameer District, and simulate effects of changes in land-use, climate change, topography, and time of concentration, as well as solution scenarios to mitigate flooding problems. The chapter is divided into several sections: description of the study area, data collection, methods used in modelling, and discussion of model inputs. Figure (3.1) illustrates the methodology layout adopted in this study in the present study.

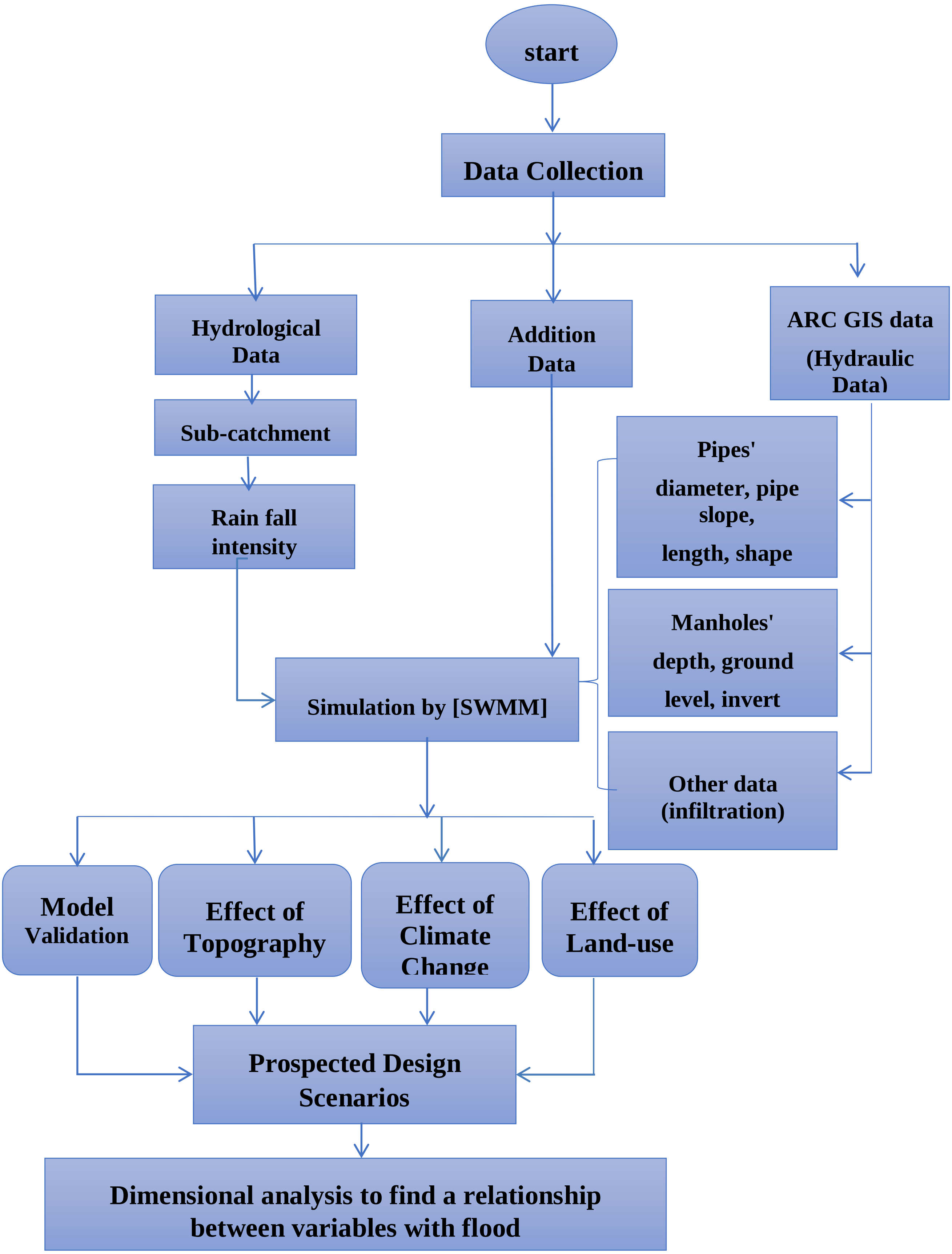

Figure 3.1: Methodology layout of the study work.

3.2 The Study Area

3.2.1 Description of the Study Area

Al-Najaf Governorate is located 165 km southwest of Baghdad, Iraq (32° 01' 33.38" N and 44° 20' 46.50" E). The climate is arid to semi-arid with, an average temperature of 24 °C, Average annual rainfall is 99 mm/year, evaporation of 3483 mm/year, average wind speed of 10 km/hr, and humidity of 41% (Zwain et al., 2021). As shown in Figure 1, the the study area of AL-Ameer District is located close to the center of An Najaf Governorate, with longitude and latitude (32˚ 00′ 28″ N and 44˚ 21′ 51″ E).

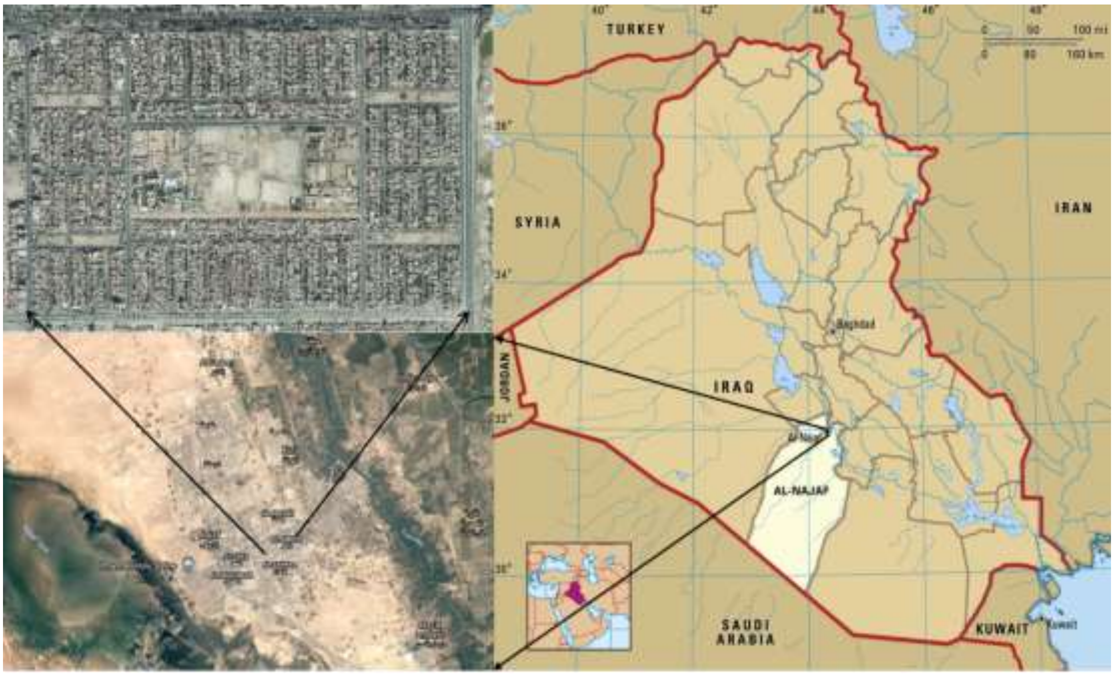

Figure 3.2: Case study location of AL-Ameer District in Al-Najaf, Iraq (Google map, 2021).

3.2.2 Study Area Land-Use

Determining the land use characteristics of a given area is essential to calculate the amount of surface runoff that cannot be infiltrated by the land surface. In this case study, the area land-use has been defined into three main parts; gardens, paved spaces, and buildings. Gardens constitute 10% of the total land area, paved areas constitute 10%, while the third part represents buildings such as schools, hospitals, and residential homes, which constitute 80% of the total land-use area. Figure (3.3) shows the area land-use of the case study of AL-Ameer District and surroundings. The total area is about 1.64 km^2,0.557 km^2 from the study area are pervious (34% of the total area) and 1.083 km^2 are impervious (about 66% of the total area).

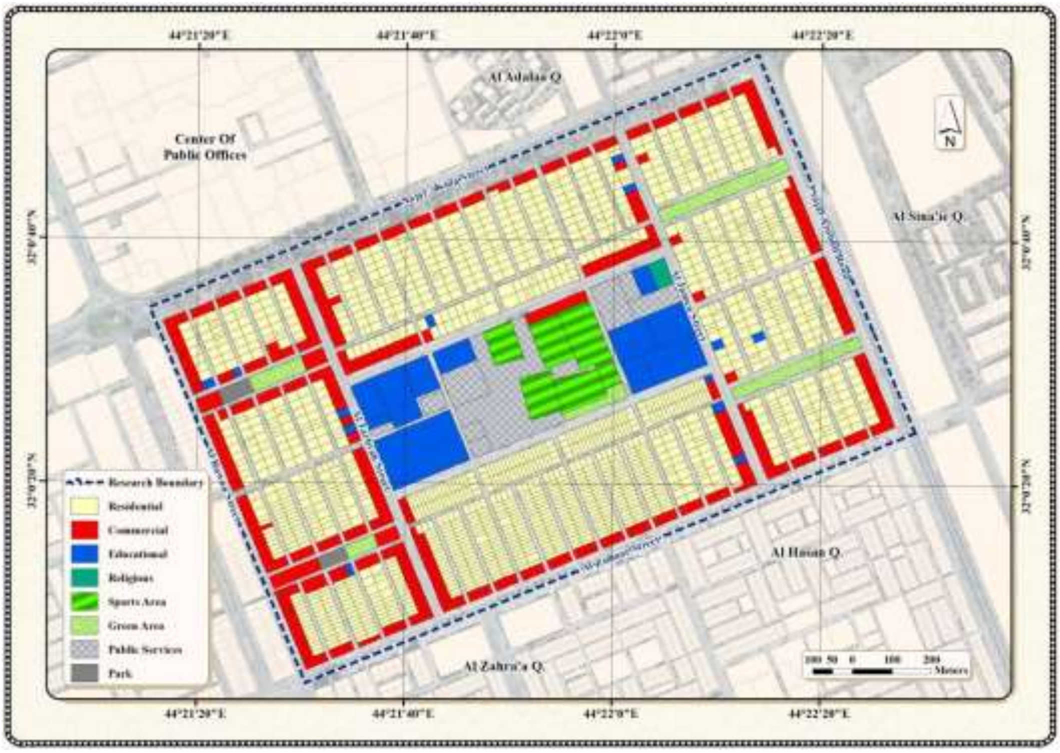

Figure 3.3: Land-use map of AL-Ameer District and surrounding areas (Al-Najaf Directorate of Urban Planning 2010).

3.2.3 Study Area Topography

Figure (3.4) shows the topography of AL-Ameer District and the surrounding areas. The topography of Al-Najaf city helps the flow of drainage water by gravity. The presence of high slopes leads to the discharge of surface runoff towards the downstream, leading to the accumulation of stormwater in the lower areas at the right side end of the study area. The land is on elevation that ranges from 40 to 46 m above sea level.

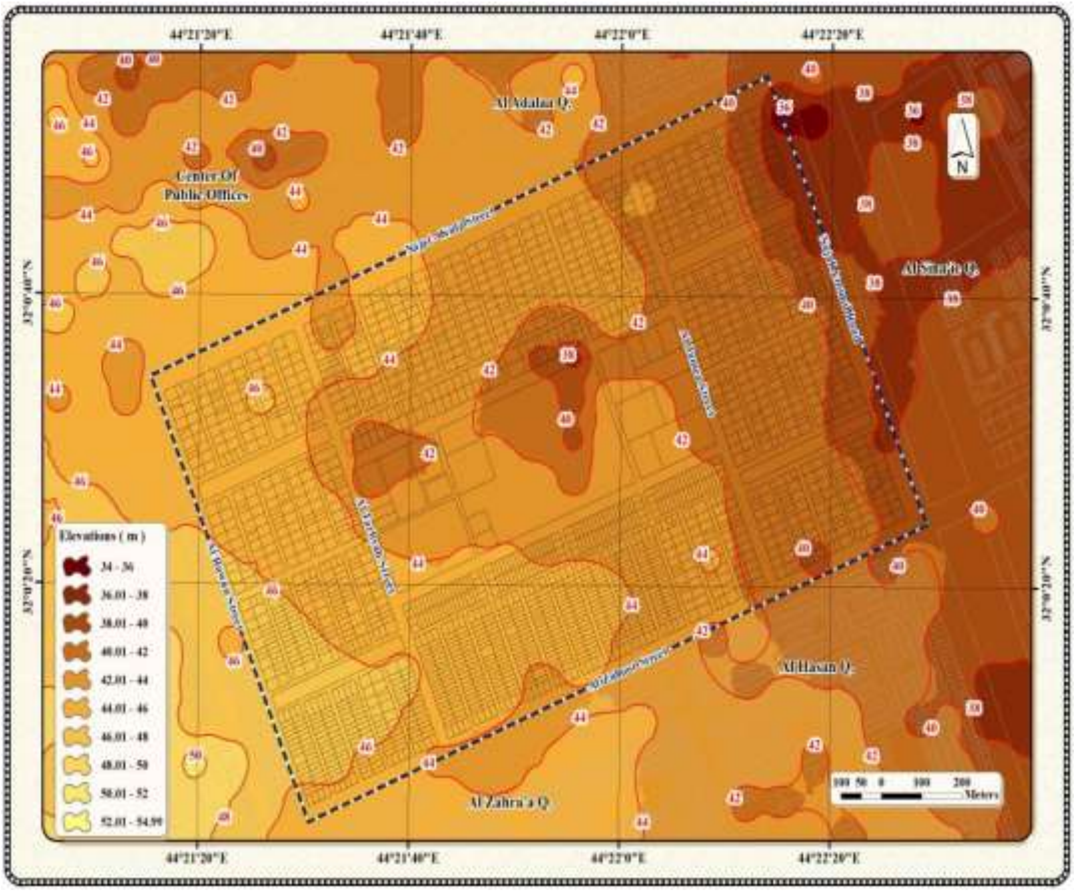

Figure 3.4: Topography of AL-Ameer District and surrounding areas (USGS website 2020).

3.2.4 Flooding problems in the Study Area

The study area AL-Ameer District, Najaf, Iraq has a stormwater drainage system covering the entire region. This stormwater drainage system suffers from floods during rainy days, which happens for many reasons such as change in land-use, network design problems, and climate change. The topography of the study area, represented by the slope of the sub-catchment and the increase of non-permeable areas, leads to an increase in the speed of surface runoff. This will increase in surface runoff velocity, in which runoff does not enter the drainage gutters in sufficient quantities. In recent years, the precipitation intensity has increased above the design intensity. Furthermore, the stormwater drainage system was not designed to contain high rainfall intensities in recent years, in addition to lack of maintenance. An increase in surface runoff volume and decrease in system drainage capacity lead to frequent floods, especially in downstream. Flooding leads to damage in public and private properties and causes serious accidents. Figure (3.5) shows an example of flood event that occurred in on November 29, 2020 with a precipitation depth of about 55mm during the two hours .

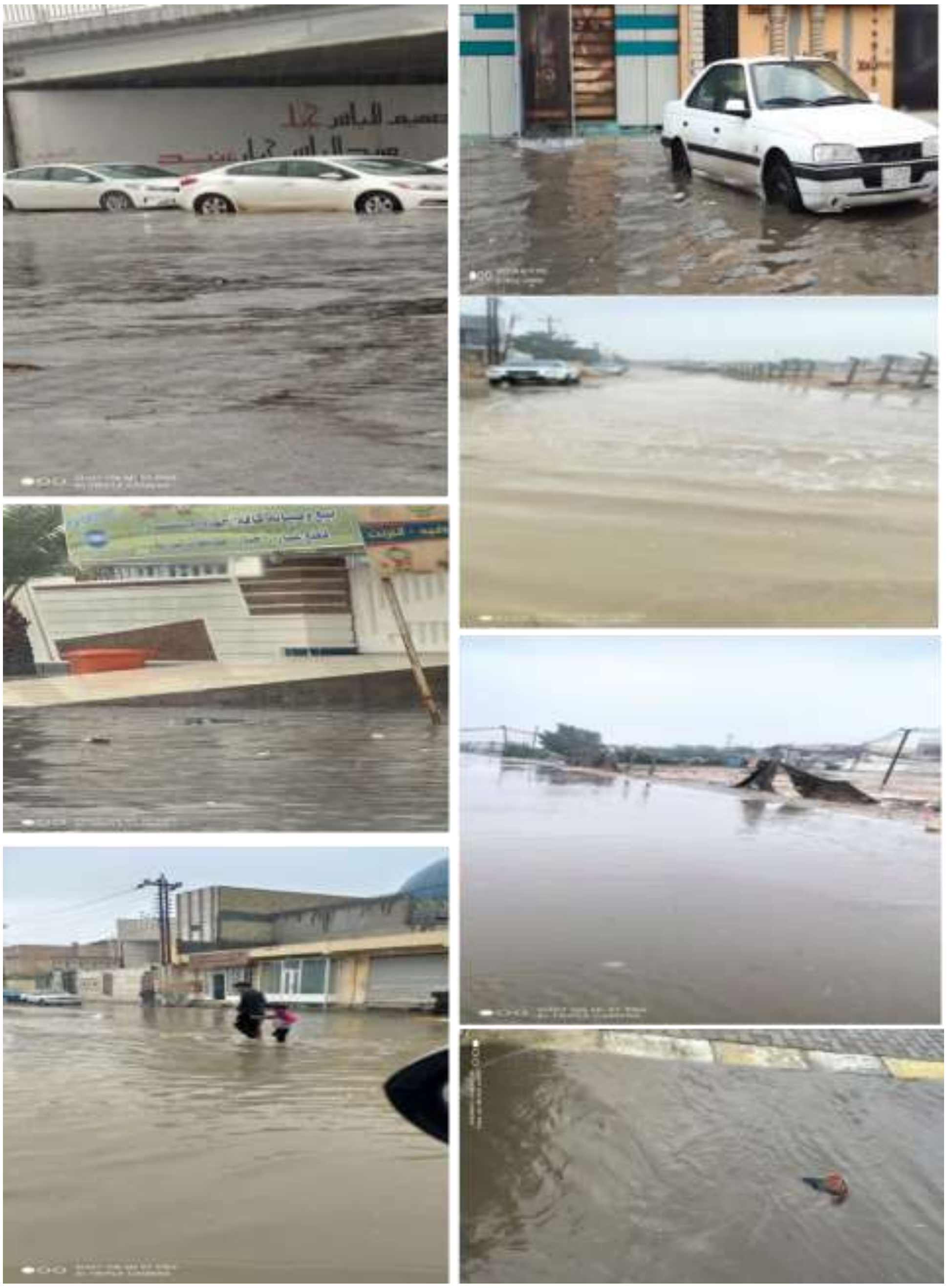

Figure 3.5: Flooding in AL-Ameer District of Al-Najaf, Iraq (29/11/2020).

3.3 Rainfall Intensity Analysis

The relationship between precipitation intensity and frequency (IDF) is one of the most used tools in many anti-flood engineering projects. The IDF curves express the relationship between precipitation intensity, duration, and return period. In order to construct the IDF curves in Al-Najaf, a historical series of maximum rainfall intensity is required with a higher time accuracy (within 1 minute time interval) (Nhat et al., 2006). The steps for an IDF drawing using Easy Fit 5.6 and Microsoft EXCEL 2016 can be illustrated as follows:

1. Finding the maximum daily rainfall per year, as shown in Table 3.1.

Table 3.1: Maximum Daily Rainfall Recorded in Najaf Governorate During 1989-2018 (G.A.M.S.M).

Year	Maximum Daily Rainfall (mm)	Year	Maximum Daily Rainfall (mm)	Year	Maximum Daily Rainfall (mm)
1989	5	1999	8.2	2009	12.6
1990	12	2000	10.7	2010	10.9
1991	8.8	2001	17.3	2011	13.8
1992	16.2	2002	15.2	2012	18.2
1993	34.4	2003	19	2013	64.5
1994	42	2004	8.7	2014	22.2
1995	11.5	2005	27.7	2015	32.9
1996	17.9	2006	22.6	2016	26.6
1997	21.1	2007	12.8	2017	8.6
1998	12.4	2008	26.8	2018	19.3

* The year 2019, 2020 and 2021 are not available in (G.A.M.S.M).

2. The maximum precipitation of 5, 10, 20, 30, 60, and 120 minutes are evaluated using the IMD reduction formula (Rathnam et al., 2001) as shown below in [Equation 3.1], and calculated data are listed in Table 3.2.

Table 3.2: Maximum daily precipitation depth for time duration.

Year	Precipitation Depth (mm)					
	5 (min)	10 (min)	20 (min)	30 (min)	60 (min)	120 (min)
1989	0.757	0.954	1.202	1.376	1.733	2.184
1990	1.817	2.289	2.885	3.302	4.160	5.242
1991	1.333	1.679	2.115	2.421	3.051	3.844
1992	2.453	3.091	3.894	4.458	5.616	7.076
1993	5.209	6.563	8.269	9.466	11.926	15.026
1994	6.360	8.013	10.096	11.557	14.561	18.345
1995	1.741	2.194	2.764	3.164	3.987	5.023
1996	2.711	3.415	4.303	4.925	6.206	7.819
1997	3.195	4.026	5.072	5.806	7.315	9.216
1998	1.878	2.366	2.981	3.412	4.299	5.416
1999	1.242	1.564	1.971	2.256	2.843	3.582
2000	1.620	2.041	2.572	2.944	3.710	4.674
2001	2.620	3.301	4.159	4.760	5.998	7.557
2002	2.302	2.900	3.654	4.182	5.270	6.639
2003	2.877	3.625	4.567	5.228	6.587	8.299
2004	1.317	1.660	2.091	2.394	3.016	3.800
2005	4.195	5.285	6.658	7.622	9.603	12.099
2006	3.422	4.312	5.433	6.219	7.835	9.872
2007	1.938	2.442	3.077	3.522	4.438	5.591
2008	4.058	5.113	6.442	7.374	9.291	11.706
2009	1.908	2.404	3.029	3.467	4.368	5.504

2010	1.651	2.080	2.620	2.999	3.779	4.761
2011	2.090	2.633	3.317	3.797	4.784	6.028
2012	2.756	3.472	4.375	5.008	6.310	7.950
2013	9.767	12.306	15.504	17.748	22.361	28.173
2014	3.362	4.236	5.336	6.109	7.696	9.697
2015	4.982	6.277	7.908	9.053	11.406	14.371
2016	4.028	5.075	6.394	7.319	9.222	11.619
2017	1.302	1.641	2.067	2.366	2.981	3.756
2018	2.923	3.682	4.639	5.311	6.691	8.430

$$p_t = p_{24} * \left(\frac{t}{24}\right)^{\frac{1}{3}} \qquad [\mathbf{3.1}]$$

Where:

Pt is the required precipitation depth for the specific duration in mm, P24 is precipitation per day in mm, while t is the time duration in hours where the depth of precipitation is required.

For example:

$$p_5 = 5 * \left(\frac{5}{24 * 60}\right)^{1\backslash 3} = 0.757\, mm$$

3. Using the software Easy Fit 5.5 and based on the data in Table 3.2 and Gumbel Distribution and selecting the probability for 2, 5, 10 and 25 years, the probability of rain per minute can be obtained, as shown in Table 3.3.

Table 3.3: The rainfall intensity is converted to mm/hr.

Return Period (Years)	Rainfall Intensity (mm\hr)					
	5 (min)	10 (min)	20 (min)	30 (min)	60 (min)	120 (min)
2	29.55	18.61	11.73	8.95	5.64	3.55
5	47.46	29.90	18.84	14.37	9.06	5.70
10	61.27	38.60	24.32	18.56	11.69	7.36
25	80.79	50.90	32.06	24.47	15.41	9.71

4. From data in Table 3.3, IDF curve for Al-Najaf Governorate is generated.

3.4 SWMM Model

The runoff module in SWMM deals with precipitation flow over a number of sub-catchments to produce runoff, which is then transported through a series of pipes, manholes, pumps stations, storage, and so on by the routing module. Geology data (soil type), land use data, hydraulic data [drainage system dimension and spatial distribution], and climate data (basically pre-industrial) are all needed for modeling.

3.4.1 Data input into SWMM

The SWMM is a dynamic precipitation runoff model with different intensities and different events. Use the principles of maintaining mass, momentum, and water balance where appropriate (Rossman, 2010). Accurate data entry is essential. This section will describe all hydrological and hydraulic data computational practices affecting the study area.

3.4.2 Hydrological Data

Collecting field data for the case study of Al-Ameer District from the Sewage Department of Najaf Governorate. These data include pipes, inspection manholes, floor areas, as well as service data, green areas, and their characteristics. Collected data was plotted in GIS ARCMAP as a bitmap, line, and polygon files. After the data were plotted and revised, the network was imported into the SWMM software.

3.4.2.1 Rain Gage

Rain Gages provide data on precipitation for one or several sub-catchment areas in a research area. Data of rainfall may come from an external file or from a user-defined time series. It support a number of different popular rainfall file formats and a standard user-defined format (Rossman, 2010). The principal input properties of rain are shown below:

- Type of rainfall data (e.g., intensity, or volume).
- Recording intervals of time (e.g., by hours, 10-minutes, etc).
- Rainfall data source (either by inserting a time series or via an external file).
- Precipitation data source name.
- In this paper, the name is inserted as Rain Gage-01.

3.4.2.2 Sub-catchment Properties

The sub-catchment is the area drained by a network of connected pipes or by streams, and the runoff generated in this area from the drainage to a single outlet (Khadka & Basnet, 2019). The sub-catchment is divided into Pervious and Impervious surfaces that are divided into two areas: one with depression storage and the other with no storage. The impervious area only loses precipitation in the depressive storage area and the rest turns into a street runoff or pipework, but in the pervious region, runoff can infiltrate through the upper soil area (Rossman, 2010). The characteristics of sub-catchment, such as land-use, drainage path, and topography, divide the drainage area into rectangular sub-catchments that is a general practice in hydrological models but the spatial precision of dividing the drainage basin has little influence on the runoff outcomes (Park et al., 2008).

The surface runoff in SWMM simulation is the total runoff from a set of sub-catchments that received precipitation, then SWMM transfers this total surface runoff to pipes system and manholes, whereas SWMM model determine the runoff for each sub-catchment and discharge in each pipe. After defining study area characteristics, the SWMM system diagram can be drawn. In this study area, the total catchment area is about 1.64 km^2 and it is consisted of 43 sub-catchments, as shown in the Figure (3.6).

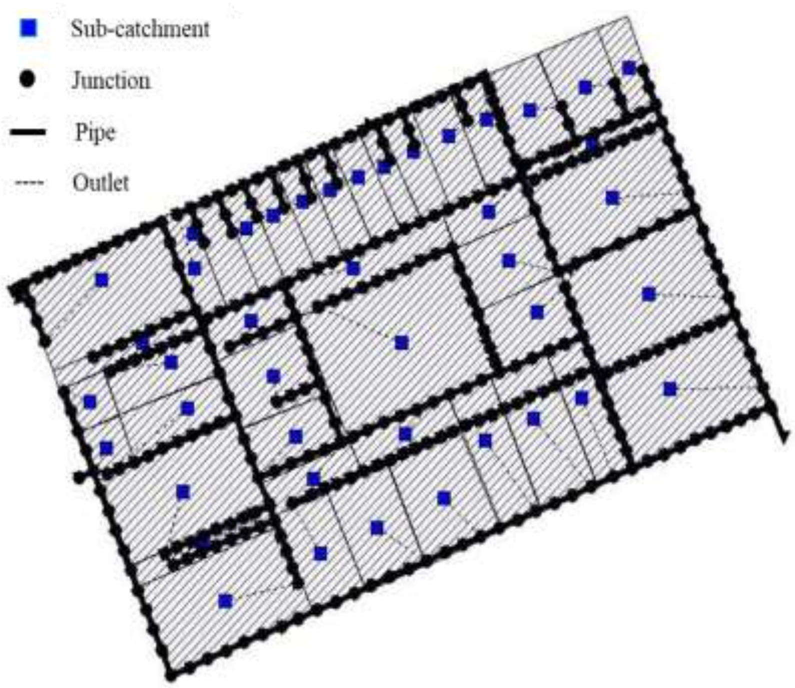

Figure 3.6: Distribution of study area sub-catchments, junctions and pipes(SWMM).

3.4.2.3 Sub-catchments Area and Width

The study area aerial image was provided by Al-Najaf Sewage Department, which shows the spatial distribution and helps to estimate the sub-catchment area by measurement tools in GIS ARCMAP. There was no real physical meaning to the sub-catchment display (Cantone & Schmidt, 2011). The width can be calculated as surface area divided by the length of the runoff with the latter being the length of the longer surface flow path (Shen & Zhang, 2014). The width can be calculated by equations, as shown in equation[3.2] :

$$\mathbf{W = \frac{A}{Lmax}} \quad \mathbf{[3.2]}$$

Where:

A = The area of sub-catchment (m^2)

Lmax = The maximum runoff length in sub-catchment.

where:

Dp and Paut= The distance between the outlet point of the sub-catchment and another arbitrary point. This arbitrary point represents the farthest point to the outlet and should be one of the verteces of the sub catchment, as described in Figure (3.7).

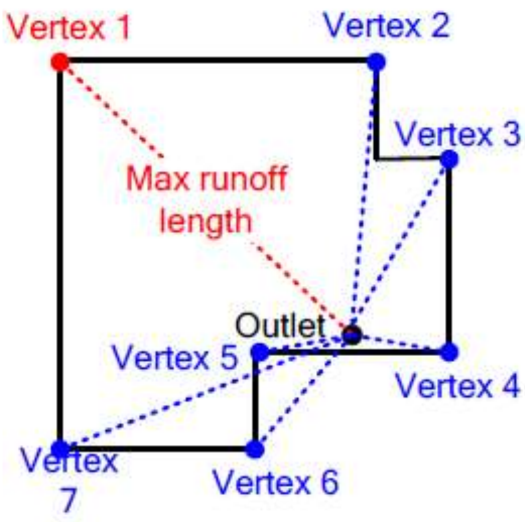

Figure 3.7: The calculation of maximum runoff length(Shen & Zhang, 2014).

3.4.2.4 Sub-catchment Slope

The sub-catchment surface slope is one of the most important properties that influence the surface runoff flow velocity. The sub-catchments slope can be found by the difference in elevation between upstream and downstream of each sub-catchment divided by the length of the sub-catchment. In this study, the slope was calculated by fieldwork due to lack of available data, its average slope value was 0.5%.

3.4.2.5 Pervious and Impervious surfaces

The sub-catchment area can be divided into two parts: pervious and impervious surfaces. The impervious zone is divided into two areas where one has depression storage and the other has not. Meanwhile, total depression storage depth is the depression storage depth for pervious and impervious areas and the values were taken based on the table (3.4) (Federation & Engineers, 1992). The impervious area only loses precipitation in storage depression and the rest turns into a surface runoff or flows down the pipes. However, in the former region, surface runoff can infiltrate through the upper soil region (Rossman, 2010). The proportion of impermeability has indirect effects on receiving downstream and a direct effect on the local water surface (Chabaeva et al., 2009). The percentage of the excluded area can be estimated directly from the aerial photo and the supplementary land use map from urban planning by dividing the area of the unimplemented area by the total sub-catchment area. The unimplemented percentage is 66% approximately in the study area. Also, the depth of depression storage was taken for the pervious and impervious areas, 5 and 2 mm, respectively.

Table 3.4: The depth of depression storage for various land use (Rossman., 2010) .

Typical Depression Storage Values		
Land Cover	Depression Storage	
	(inches)	(mm)
Impervious Surfaces	005-0.10	1.25-2.50
Lawns	0.10-0.20	250-5.00
Pasture	0.20	5.00
Forest Litter	0.30	7.50

3.4.2.6 Manning Roughness

In hydrological modeling, manning roughness is one of the most powerful parameters. The values for each sub-catchment are based on the form of land-use. Manning roughness values are tabulated in Table 3.5 (Pendergast & McCuen II, 1996) for various overland forms. In this study, Manning Roughness was taken as 0.013 approximately.

Table 3.5: The Manning roughness coefficient for overland(McGhee & Steel, 1991).

Surface	n
Smooth asphalt	0.011
Smooth concrete	0.012
Ordinary concrete lining	0.013
Good wood	0.014
Brick With cement mortar	0.014
Vitrified clay	0.016
Cast iron	0.016
Corrugated metal pipes	0.024
Cement rubble surface	0.024
Fallow soils (no residue)	0.06
Cultivated soils	
Residue cover < 20%	0.06
Residue cover > 20%	0.17
Range (natural)	0.13
Grass	
Short, prarie	0.16
Dense	0.24
Bermuda grass	0.41
Woods	
Light underbrush	0.40
Dense underbrush	0.80

3.4.2.7 Time Series

Rain gauges provide precipitation data for single or several sub-catchment areas in the search area. Data of rainfall may come from an external file or user-defined time series. Several different common precipitation input file formats can be used, as well as the standard format defined by the user. Figure (3.8) shows an example of one of the input models for the time series.

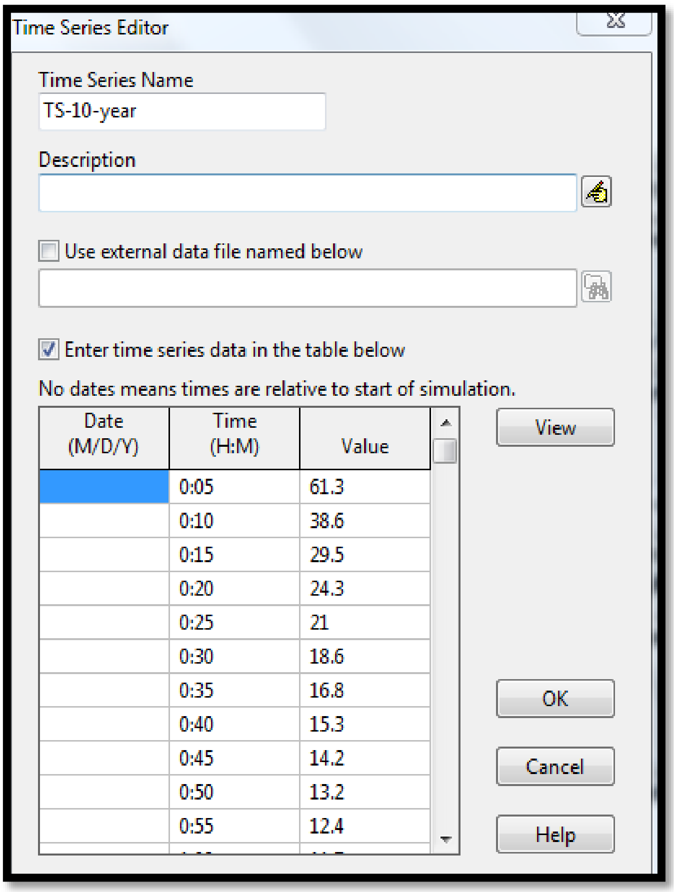

Figure 3.8: An example of data entry using a time series.

3.4.3 Hydraulic Data

Hydraulic data for Al-Ameer District were collected from Al-Najaf Sewage Directorate that include pipelines, inspection manhole, and their characteristics. Hydraulic data have been drawn in GIS ARCMAP as bitmap and line shapes files. After plotting and reviewing the data, the network was imported into SWMM software.

3.4.3.1 Pipe Parameters

The spatial distribution, upstream and downstream height of each pipe must be provided in the model to obtain the slope and determine the direction of fluid flow. The drainage system for the study area consists of

343 pipes of different diameters from (315 mm, 400 mm, 500 mm to 600 mm) distributed according to the capacity of the main and sub-areas, and the pipe lengths range from 30 m to 70 m. Note that the pipe material is polyvinyl chloride (PVC) and the values of Manning coefficient of pipe roughness are given in Table 3.6 (McGhee & Steel, 1991), where the Manning value for PVC (plastic pipe) is 0.009. All information was obtained from (D.S.N). The network consists of four main diameters as shown in Figure(3.9).

Table 3.6: Manning roughness coefficient for pipe(McCuen et al., 1996).

n_p	The material of pipe
0. 009	Plastic pipe
0. 009	Well-planed timber evenly laid
0.01	Neat cement. Very smooth pipe
0.012	Unplanned timber. Cast-iron pipe of ordinary roughness
0.013	Well-laid brickwork. Good concrete. Riveted steel pipe. Well-laid vitrified clay pipe
0.015	Vitrified tile and concrete pipe poorly jointed and unevenly settled. Average brick work
0.017	Rough brick. Tuberculate iron pipe
0.02	smooth earth or firm gravel
0.03	Ditches and rivers in good order, some stones and weeds
0.04	Ditches and rivers with rough bottoms and much vegetation

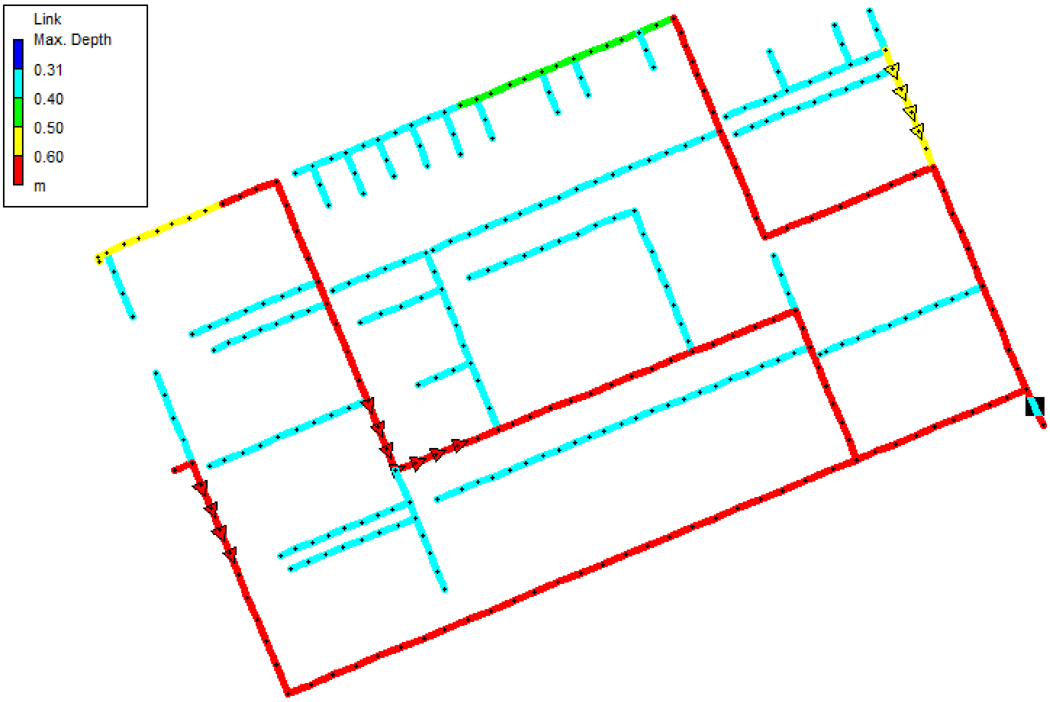

Figure 3.9: Pipes diameters of stormwater drainage system(SWMM).

3.4.3.2 Manholes properties

The most important information required in the manhole is the maximum depth, inlet, outlet, invert level, and dimensions of the manhole. The stormwater drainage network for the study area contains 343 manholes of sizes (60 * 90) cm and (60 * 55) cm. A part from that, manholes are very important in simulation because SWMM provides the flood volume in each manhole. There are seven types of reinforced concrete manholes in the stormwater drainage system of Al-Ameer district that are AS, BS, CS, BD, CD, CD1, and special manhole. Figure (3.10) manhole ID, Figure (3.11) shows the manhole type distribution ,and design details in Table 3.7.

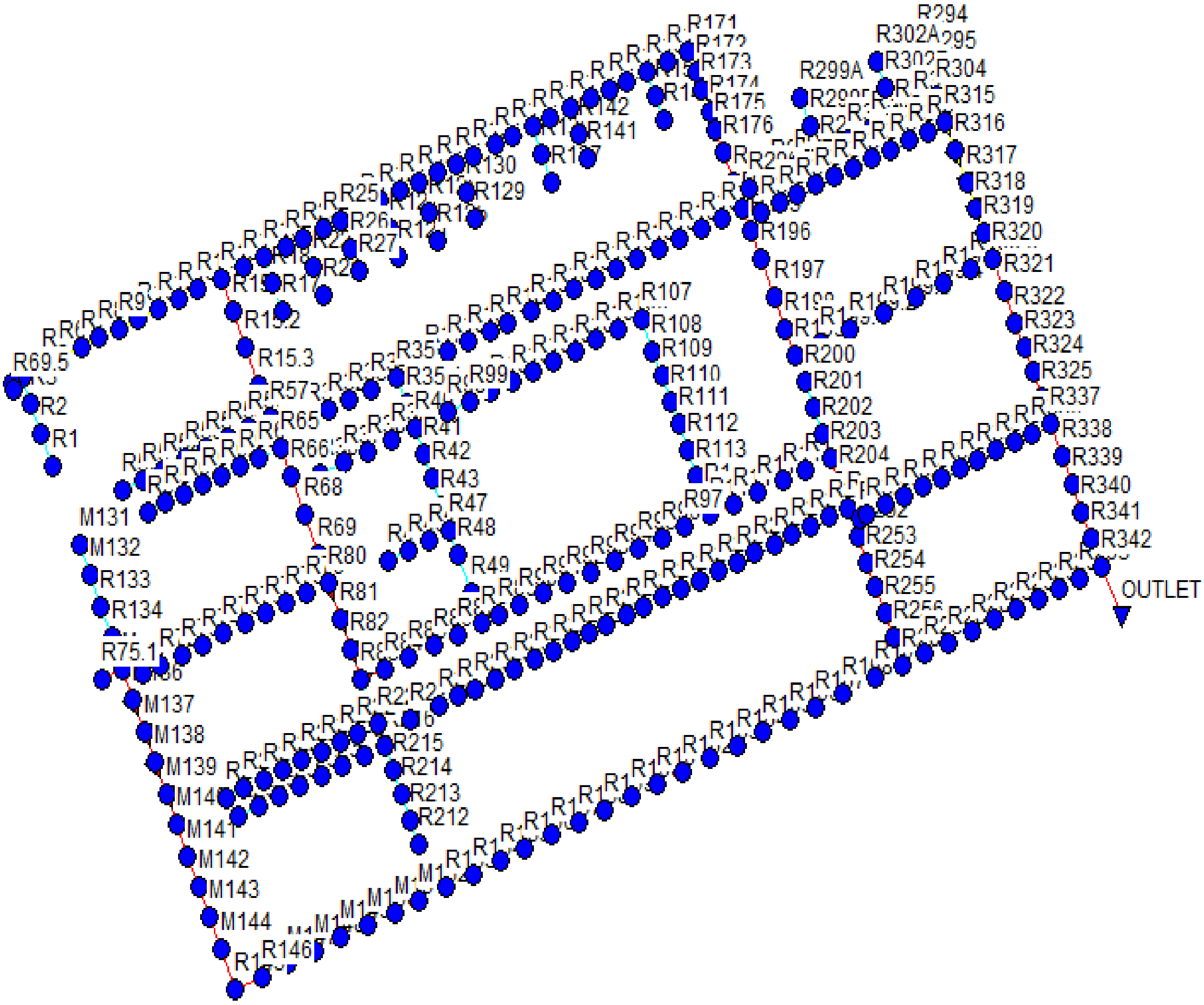

Figure 3.10: Manholes ID in stormwater drainage system in AL-Ameer District(SWMM).

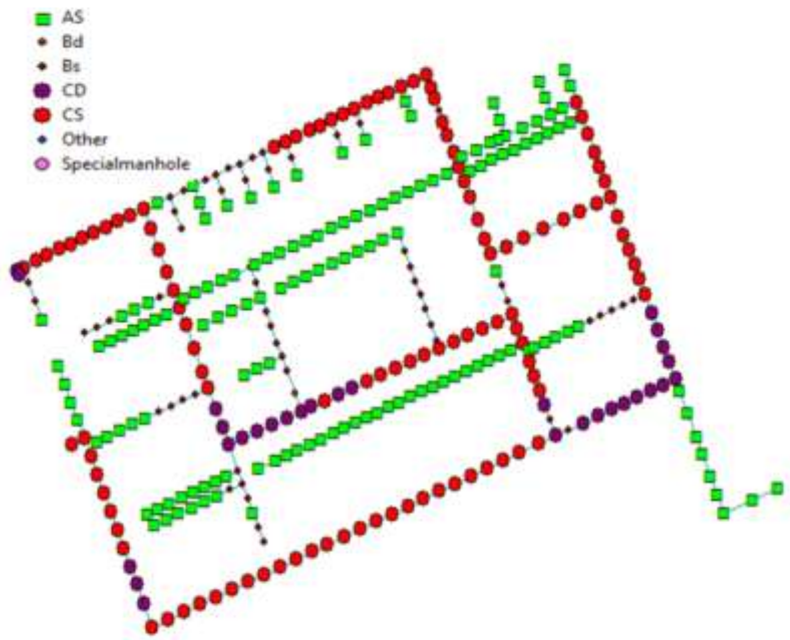

Figure 3.11: The distribution and types of manholes in the study area(GIS).

Table 3.7: Design details of manholes in the study are(D.S.N).

Type of MH	Invert depth (m)	Dia. of Outgoing pipe (mm)	Number of Incoming Pipes	Dia. of chamber Ring (cm)or diminution
A_S	1.25-1.69	200-400	Any number	Rectangular (60*90)cm
B_S	1.70-2.99	200-400	<2	110
B_d	>3.25	200-400	<2	110
C_S	1.70-3.24	200-400 450-700	>3 Any number	150
C_d	>3.25	200-400 450-700	3or more Any number	150
C_{d1} **(Special MH)**	>2.00	800-1000	Any number	According to the design

3.5 System flow routing

Flow routing is a method that uses known or assumed hydrographs at one or more upstream points to determine the time and amount of any event in a drainage system. SWMM utilizes the conservation of mass and momentum equations for open channel conduits using three levels of sophistication, (Rossman, 2010). The SWMM allows the modeler to choose the level of sophistication with which the equations are solved. Steady flow routing, kinematic flow routing, and dynamic flow routing are the three levels of flow routing in SWMM. The dynamic flow routing was chosen in this study because it can account for pressurized flow, channel storage, flow reversal, backwater, and entrance/exit losses, therefore it takes into consideration the most theoretically precise outcomes. The full flow closed pipe represents pressurized flow in dynamic routing, and flooding occurs when the water depth at the node exceeds the maximum allowable depth.

3.6 Infiltration

Infiltration can be calculated using three distinct formulas in the SWMM model: Horton, Green-Ampt, and SCS curve number. The Green-Ampt model was employed in this study since it is more physically based. (Gironás et al., 2009). The Green-Ampt method is simplify, empirical model to represent the infiltration process. It develops from the application of Darcy’s law and the law of conservation of mass. Green-Ampt supposes an existence of a sharp wetting front in the soil column creating separation in the soil where the above wetting front is fully saturated and the soil below is at the initial moisture content (Rawls et al., 1983). This method is a function of the soil's hydraulic conductivity, soil suction head, porosity and initial moisture deficit of the soil. In the study area, sand soil was the dominant type of soil that has been selected as a part of the infiltration model(Ali et al., 2016).

3.7 Additional input data

There is an additional flow discharged into the stormwater drainage system from neighboring areas. First, this includes surface runoff flowed from the main street of Al-Kufa/Al-Najaf, discharged into three inlet manholes at the north of study area stormwater drainage system, as shown in Figure (3.12). The main street of Al-Kufa-Al-Najaf in not served by any stormwater drainage system, and branch roads are acting as open channels discharging stormwater to the study area stormwater drainage system. The street system is collecting the surface runoff generated from rainfall, where rational method is used to calculate the peak discharge values at each junction inlet, and were approximately 0.046 m^3/sec.

Figure 3.12: The surface runoff from Al-Kufa/Al-Najaf Street to the study area(GIS).

The surface runoff was calculated using the rational [equation3.3] as follows:

$$\boldsymbol{Q = \frac{1}{3.6}\, C * I * A} \qquad \textbf{[3.3]}$$

Where:

Q is the maximum discharge rate (m^3/s). The runoff coefficient C, which is the ratio of the runoff rate to the rainfall rate, is determined from Table 3.8. I is the average rainfall intensity (mm/hr), calculated from IDF curve after calculating the time of concentration (Tc). A represents the area of streets (km^2) that collects water to the design point. Tc is the time required for water to flow from the farthest hydraulic point in the catchment area. It can be calculated from the Kirpich equation (Doubleday et al., 2013):

$$\boldsymbol{T_c = 0.02 * L^{0.8} * (S)^{-0.4}} \qquad \textbf{[3.4]}$$

Where

Tc is Time of concentration (min);

L is the length of the distance to run over the ground (m); and

S= slope for catchment.

Table 3.8: Runoff Coefficients (Kadioglu & ŞEn, 2001).

Ground Cover	Runoff Coefficient, C
Lawns	0.05 - 0 35
Forest	0.05 -025
Cultivated land	0.08-0.41
Meadow	0.1 - 0 5
Parks, cemeteries	0.1 - 0 25
Unimproved areas	0.1 - 0 3
Pasture	0.12 - 0.62
Residential areas	0.3 - 0 75
Business areas	0.5 - 0 95
Industrial areas	0.5 - 0 9
Asphalt streets	0.7 - 0 95
Brick streets	0.7 - 0 85
Roofs	0.75 -0.95
Lawns	0.7 - 0.95

After all, the Q can be calculated as shown below:

$Tc = 0.02 * 500^{0.8} * 0.005^{-0.4}$=24 min

From the IDF curve for the study area, for 24 min of concentration time and return period of 25 years, the rainfall intensity is 27 mm/hr.

$$\boldsymbol{Q = \frac{1}{3.6} * 0.82 * 27 * 7500 * 10^{-6} = 0.046\ \frac{m^3}{sec}}$$

Second, stormwater drainage system of study area is connected to neighboring Districts of Al-Eskan and Al-Ishtiraki, and discharge is to be 0.226 and 0.4 m^3/sec, respectively. All of these additional flows were input data as initial flow in the SWMM simulation. The calculation of the additional flow as input data was due to linking the stormwater drainage system in the study area with the Districts of Al-Eskan and Al-Ishtiraki, estimated as follows:

Pipe ID 69.5, $D = 500mm$, S=0.002 n = 0.009, and $\frac{\mathrm{d}}{\mathrm{D}} =$ assumed as 0.78. Through the ratio d/D and Figure (3.13) the value of (QP/Qf) = 0.93

$$\boldsymbol{Qf = \frac{0.312}{n} * (D)^{\frac{8}{3}} * (S)^{\frac{1}{2}}} \qquad \textbf{[3.5]}$$

$$\mathbf{Qf = \frac{0.312}{0.009} * (0.5)^{\frac{8}{3}} * (0.002)^{\frac{1}{2}} = 0.244\ \frac{m^3}{sec}}$$

$$\mathbf{Qp = 0.93 * 0.244 = 0.226\ \frac{m^3}{sec}}$$

Pipe ID 75.1, $D = 600\,mm$, S=0.0025, n = 0.009, and $\frac{d}{D} = assumed\ as\ 0.78$. From the ratio d/D and Figure (3.13) the value of Qp/Qf= 0.92, and

$$\boldsymbol{Qf = \frac{0.312}{0.009} * (0.6)^{\frac{8}{3}} * (0.0025)^{\frac{1}{2}} = 0.44\ \frac{m^3}{sec}}$$

$$\boldsymbol{Qp = 0.92 * 0.44 = 0.4\ \frac{m^3}{sec}}$$

Where

D = diameter of pipe (m).

S = slope of pipe.

n = Manning roughness in pipe.

Qf = flow in pipe when full ($\frac{m^3}{sec}$).

Qp= partial flow in pipe ($\frac{m^3}{sec}$).

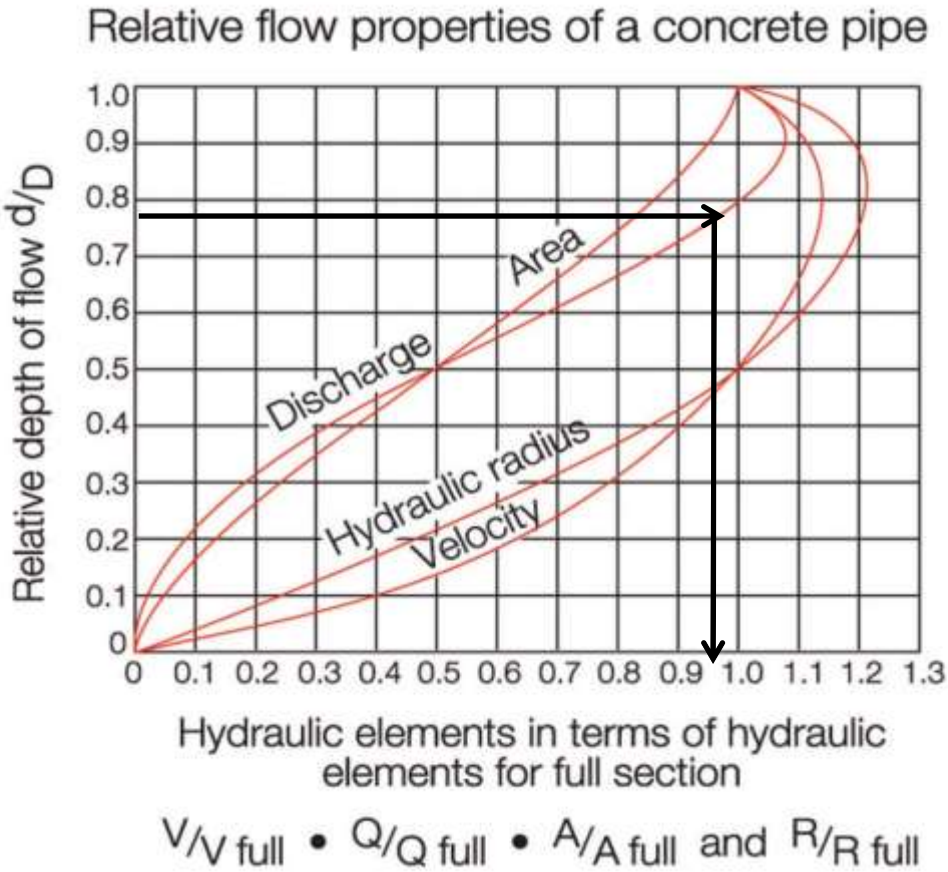

Figure 3.13: partial hydraulic elements(Fukuchi, 2006).

3.8 Model Validation

Validation is a process of comparing the model and its behavior to the real system. In this study, model validation was conducted by comparing predicted maximum discharge in pipes that acquired from SWMM program with real discharge pipes that acquired from Al-Najaf Sewage Directorate. As recommended by (Zwain et al., 2020), mean of normal squared error (NMSE) and correlation coefficient (R) were selected statistical parameters for model validation. NMSE (Eq. 3.7) measures of mean relative scatter and reflect both systematic and systematic (random) errors, and R (Eq. 3.8) reflects the linear relationship between two variables and is thus insensitive to either an additive or a multiplicative factor.

$$NMSE = \frac{\overline{(C_{\circ} - C_p)^2}}{\overline{C_{\circ}} - \overline{C_p}} \qquad \textbf{[3.6]}$$

$$R = \frac{\overline{(C_{\circ} - \overline{C_{\circ}})(C_P - \overline{C_p})}}{\sigma C_{\circ}\ \sigma C_P} \qquad \textbf{[3.7]}$$

Where:

Cp is predicted data, Co is observed data, $\overline{C}$ is average data over the dataset, and σC is standard deviation over the dataset.

3.9 Prospected Design Scenarios

According to the actual land-use of the study area in 2008, 50% of it is designed as a sub-catchment that contributes to the surface runoff. However, this designed land-use ratio is changing over time as the land use of the area is changing. The area is facing urban expansion; this includes the conversion of public parks into residential areas and commercial centers due to land limitation, and home yards are transferred into houses due to the land high price and family extension. Therefore, an increase in surface runoff beyond designed quantities is expecting to occur over time, but its rate is not exactly specified as the urban expansion is taking place in irregular forms. Hence, to study the effect of land-use and determine expected flooding, the designed sub-catchment area was varied as 50, 75, and 100 %. In recent years, Al-Najaf Governorate is witnessing an increase in rainfall intensities within a short rainfall duration due to climate change effect. Therefore, the effect of rainfall intensities was simulated using SWMM at different return periods of 2, 5, 10, 25 years. As well as, the effect of topography on runoff represented by the land slope was studied, thereby changing the sub-catchment as 0.1%, 0.2%, 0.3%, 0.4%, and 0.5%.

Part of that, concentration time is commonly used in the design of hydraulic flood flow, precisely estimated peak discharge, and flood hydrograph. Three critical manholes in different areas selected to determine the effect of time concentration on flooding: the first located upstream (R15), the second in the middle of the study area (R250), and the third downstream (R315). After identifying the problem in the stormwater drainage system, a solution of changing pipes diameter might be proposed with simulation using SWMM.

3.10 Dimensional Analysis

After studying the most important variables that cause flooding in AL-Ameer District, a mathematical model is found to clarify the relationship between flood flow and the variables that affect the flood:

$$Qf = f(Qc, Sc, Sp, I, Tc, d, D, Ac, \rho) \quad \textbf{[3.8]}$$

In this study, there are ten variables: pipe diameter, peak flood, concentration time, average catchment slope, catchment area, pipe slope, manhole depth, mass density, catchment flow , and precipitation. These variables, their symbols, units and dimensions are given in Table 3.9. It is noted that among the ten variables, there are three geometric factors of a kinetic nature, Qc, Qf and I. By kinetic means, the properties that include time. With only one variable representing the properties of the fluid and also there are three variables related to the shape are Ac, D, and d. It is clear that there are three basic dimensions (L, T and M). While two of them are dimensionless (Sc, Sp), depending on the fundamental dimensions with three recurring variables fixed and according to their influence, which includes (Qc, ρ, I) there are seven dimensionless products (10 - 3 = 7).

Table 3.9: The definition of dimensional analysis variables.

Name of Variable	Symbol	Unit	Dimension
Rainfall intensity	I	mm\hr	$L\ T^{-1}$
Pipe diameter	D	m	L
Flooding peak	Qf	m^3\s	$L^3\ T^{-1}$
Time of concentration	Tc	min	T
Catchment average slope	Sc	m\m	1
Catchment area	Ac	m^2	L^2
Pipe slope	Sp	m\m	1
Manhole depth	d	m	L
Catchment flow	QC	m^3\s	$L^3\ T^{-1}$
$mass\ density$	ρ	Kg/m^3	M L^{-3}

$\pi_1 = Sp$

$\pi_2 = Sc$

$$\pi_3 = I^x * {Q_c}^y * \rho^z * Tc^1 \qquad \textbf{[3.9]}$$

$$M^0\ L^0\ T^0 = (L * T^{-1})^x * (L^3 * T^{-1})^y * (M * L^{-3})^Z * (T)^1 \qquad \textbf{[3.10]}$$

For Mass (M) Term

0 = Z → $\therefore Z = 0$

For Length (L) Term

0 = x+3y-3z

x+3y = 0 …….(a)

For Time (T) Term

0 = - x- y+1

x+y =1 ……….(b)

Through the simultaneous equations (a) and (b), the variable x and y were obtained

X = 1.5

Y = - 0.5

$$\pi_3 = \frac{I^{1.5} * T}{{Q_c}^{0.5}}$$

$$\pi_4 = I^x * {Q_c}^y * \rho^z * {A_c}^1 \quad \textbf{[3.11]}$$

$$M^0\ L^0\ T^0 = (L * T^{-1})^x * (L^3 * T^{-1})^y * (M * L^{-3})^Z * (L^2)^1 \quad \textbf{[3.12]}$$

For Mass (M) Term

0 = Z → $\therefore Z = 0$

For Length (L) Term

0 = x+3y-3z+2

x+3y = -2 …….(c)

For Time(T) Term

0 = - x- y

x+y = 0 ……….(d)

Through the simultaneous equations (c), and (d) the variable x and y were obtained

X = 1

Y = - 1

$$\pi_4 = \frac{I * A_c}{Qc}$$

$$\pi_5 = I^x * {Q_c}^y * \rho^z * D^1$$ **[3.13]**

$$M^0\ L^0\ T^0 = (L * T^{-1})^x * (L^3 * T^{-1})^y * (M * L^{-3})^Z * (L)^1$$ **[3.14]**

For Mass (M) Term

0 = Z → $\therefore Z = 0$

For Length (L) Term

0 = x+3y-3z+1

x+3y = -1 …….(e)

For Time (T) Term

0 = - x- y

x = -y ……….(f)

Through the simultaneous equations (e), and (f) the variable x and y were obtained

x = 0.5

y =0.5

$$\pi_5 = \frac{I^{0.5} * D}{Qc^{0.5}}$$

$$\pi_6 = \frac{I^{0.5} * d}{Qc^{0.5}} \quad \textit{because same diamension}$$

$$\pi_7 = I^x * {Q_c}^y * \rho^z * {Q_f}^1$$ **[3.15]**

$$M^0\ L^0\ T^0 = (L * T^{-1})^x * (L^3 * T^{-1})^y * (M * L^{-3})^Z * (L^3 * T^{-1})^1$$

Eq. [3.17]

For Mass (M) Term

0 = Z → $\therefore Z = 0$

For Length (L) Term

0 = x+3y-3z+3

x+3y = -3 …….(g)

For Time(T) Term

0 = -x-y-1

x+ y = -1 ……….(h)

Through the simultaneous equations (g), and (h) the variable x and y were obtained

x = 0

y = -1

$$\pi_7 = \frac{Q_f}{Q_c}$$

Or using the Gauss-elimination method. This method is widely used in the computer business due to its ease of programming.

$$\begin{matrix} \boldsymbol{I} & \boldsymbol{\rho} & \boldsymbol{Q_c} \end{matrix}$$

Return variable matrix= $\begin{bmatrix} \mathbf{1} & \mathbf{-3} & \mathbf{+3} \\ \mathbf{0} & \mathbf{1} & \mathbf{0} \\ \mathbf{-1} & \mathbf{0} & \mathbf{-1} \end{bmatrix} \begin{matrix} \boldsymbol{I} \\ \boldsymbol{\rho} \\ \boldsymbol{Qc} \end{matrix} \;\vdots\; \begin{matrix} L \\ M \\ T \end{matrix}$

The main diameter of the return variable matrix is made equal to one and the top and bottom values of the main diameter equal to zero as shown in the table (3.10) and (3.11).

Table 3.10: shows the elements of the variables and their dimensions

		I	$\boldsymbol{\rho}$	Qc	Qf	Tc	Ac	$\boldsymbol{S.p}$	$\boldsymbol{S.G}$	D	d
L	I	1	-3	3	3	0	2	0	0	1	1
M	$\boldsymbol{\rho}$	0	1	0	0	0	0	0	0	0	0
T	$\boldsymbol{Qc}$	-1	0	-1	-1	1	0	0	0	0	0

Table 3.11 shows the dimensions of the repeating variables depending on the dependent variable

		I	ρ	Qc	Qf	Tc	Ac	$S.p$	$S.G$	D	d
L	I	1	0	0	0	-3/2	-1	0	0	-1/2	-1/2
M	ρ	0	1	0	0	0	0	0	0	0	0
T	Qc	0	0	1	1	1/2	1	0	0	1/2	1/2

After substituting all values, the final equation is formed as shown below:

$$Q_f = Q_c * f\left[\frac{T_c I^{1.5}}{Q_c^{0.5}}, \frac{A_c I}{Q_c}, \frac{DI^{0.5}}{Q_c^{0.5}}, \frac{dI^{0.5}}{Q_c^{0.5}}, \frac{S.c}{S.p}\right] \qquad \textbf{[3.16]}$$

CHAPTER FOUR
RESULTS AND DISCUSSION

4.1 Introduction

The study findings obtained using physical and statistical models are described in this chapter. To achieve the objectives mentioned in Chapter 1, these findings are selected and analyzed. This chapter is divided into three sections: the results of the hydraulic output of the current network, the results of the network according to the area planned, and the results of the network analytical process management procedures. Finally, to achieve the goals of the analysis, the findings obtained are interpreted, addressed, and relationships formed mathematically to calculate the floods.

4.2 IDF Curve for Al-Najaf Governorate

Al-Najaf Governorate is facing a sever lack of hydrological data and several information is unavailable to conduct further research related to environmental engineering and hydrological analysis. In this study, a detailed procedure and data of IDF curve generation are shown in Table [3.1-3.3] An IDF curve has been successfully generated for Al-Najaf Governorate for the first time as shown in Figure (4.1). From Table 3.1, it was noticed that there is an increase in the maximum daily rainfall (mm) in the last 10 years. For example, in 2013 and 2015, maximum daily rainfall reached 64.5 and 33 mm, respectively. This could be due to the effect of climate change in Al-Najaf Governorate. Unfortunately, although precipitation extremes in several regions worldwide have increased, still there are uncertainty and limited data available. This will affect the infrastructure capability during precipitation extremes that is closely related to human health and safety, particularly sewer and stormwater drainage systems. For this reason, understanding changing precipitation extremes are essential for sanitary systems design. The accuracy and suitability of present infrastructure design concepts, which rely on an assumption of climatic data, are called into question by potential non-uniform and climate-induced changes on severe rainfall occurrences (Cheng & AghaKouchak, 2014).

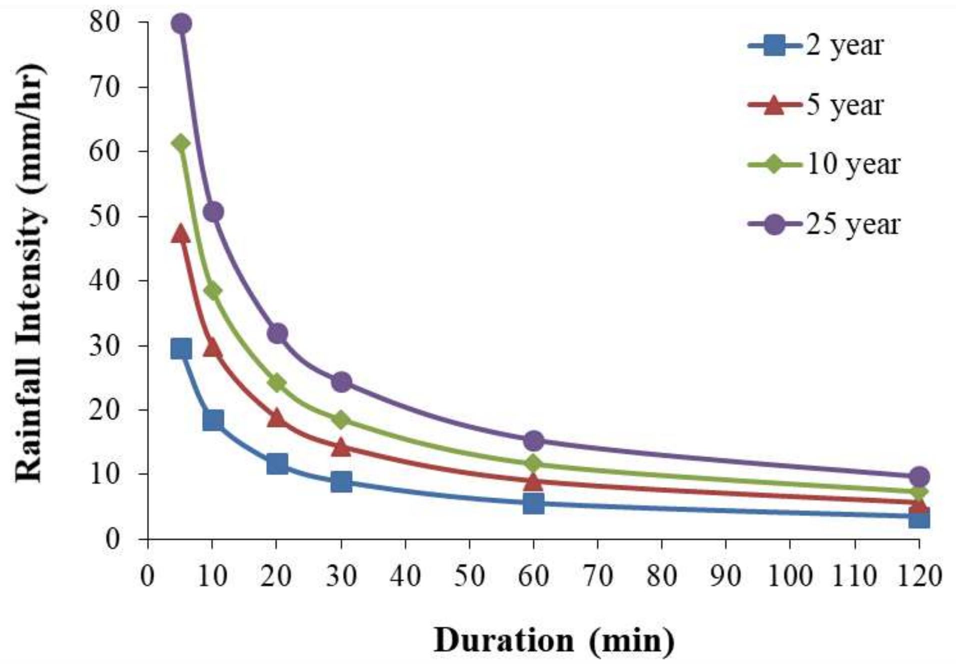

Figure 4.1: Intensity Duration Frequency (IDF) Curve for Al-Najaf city.

At any return period, the results in Figure (4.1). indicated that the rainfall intensity at short duration of 5 min was generally three times higher than duration of 30 min approximately . It is similarly noticed at time duration of 30 and 120 min, the rainfall intensity decreased about three times approximately also. The stormwater drainage system in AL-Ameer District had been designed in 2008 for a maximum rainfall intensity of 20 mm/h. Meanwhile, the study area has been exposed to the climate change effects. A noticeable increase in rainfall intensities has been recorded, especially after 2009. According to Figure 4.1, rainfall intensity of 20 mm/h is excessed at several occupations that include 2 years return period and below 10 min duration, 5 years return period and below than 20 min duration, 10 years return period and below than 30 min duration, 25 years return period and below than 35 min duration. Hence, it is expected that flooding areas are going to increase in the coming years, unless some effective solutions are introduced (Hassan et al., 2017).

4.3 Model Validation

The simulation of Al-Ameer district stormwater drainage system was validated using real data provided by (D.S.N) for one rain event and predicted data by SWMM. Statistical results of NMSE and R values are shown in Table 4.1, and predicted data over actual data are shown in Figure (4.2). The validation results showed that NMSE was 0.002 that is very close to ideal fit of zero. The R value was 0.95, and it which shows a positive correlation and very close to ideal value of 1. Linear correlation in Figure (4.2), that showed a very well fitted data of predicted data over actual data. Therefore, the results above indicated that the SWMM simulation predicted data very close to actual data, hence, no model calibration is needed as this stage.

Table 4.1: Effect of land-use assessment of AL-Ameer District stormwater drainage system throughout 2 hours of rainfall duration.

Parameter	Value	Ideal fit	NOTE
NMSE	0.002	Zero	It is close to zero, the model fits well.
R	0.95	1	It is close to 1, the model fits well.

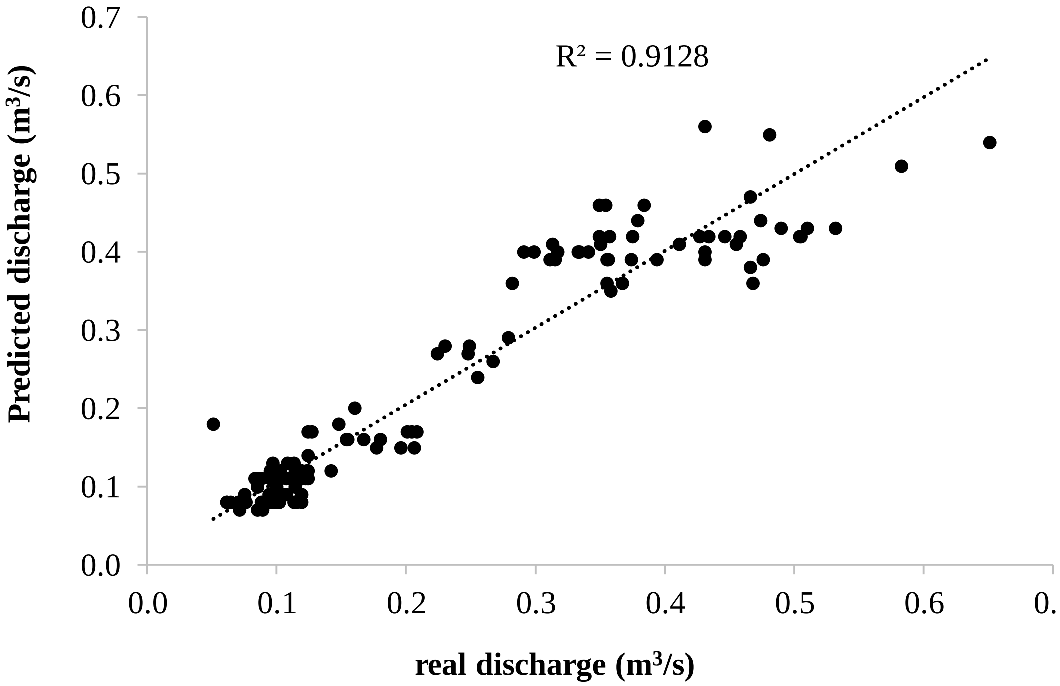

Figure 4.2: Linear relationship between predicted data over real discharge.

Likewise, (Oreskes et al., 1994) had studied the Verification and validation of numerical models of natural systems are impossible. This is because natural systems are never closed and because model results are always non unique. Models can be confirmed by the demonstration of agreement between observation and prediction, but confirmation is inherently partial. Complete confirmation is logically precluded by the fallacy of affirming the consequent and by incomplete access to natural phenomena. Models can only be evaluated in relative terms, and their predictive value is always open to question. The primary value of models is heuristic. Likewise, (Zwain et al., 2020) had studied system in Muharram Aisha-sewage treatment plant (MA-STP) was studied using the TOXCHEM model. Sensitivity analysis at different aeration flowrate, H2S loading rates, wastewater pH, wastewater temperature, and wind speed was studied. The predicted data were validated against actual results, where all the data were validated within the limits, and the statistical evaluation of normalized mean square error (NMSE), geometric variance (VG), and correlation coefficient (R) were close to the ideal fit.

4.4 Effect of Land-use on Stormwater Drainage System

In order to study the effect of land-use on the stormwater drainage system in AL-Ameer District, different ratios of sub-catchment areas that contribute to the surface runoff were taking into consideration. This is because the actual land-use in AL-Ameer District is not well known due to random development. At a constant rainfall intensity of 10 years return period and throughout 2 hours of rainfall duration, different sub-catchments areas of 50, 75, and 100% were simulated using SWMM, and results are shown in Table 4.2. Increasing the sub-catchment area from 50 to 75% led to an increment of impervious surfaces of 33%, while enlarging the sub-catchment area from 75 to 100% increased the impervious surfaces by 25%. Table 4.2 details the assessment of AL-Ameer District stormwater drainage system. By increasing the sub-catchment area from 50 to 100%, an increment in total surface runoff from 20380 to 37350 m^3, total flooding from 10513 to 26032 m^3, and number of flooded manholes from 70 to 95 have occurred, respectively.

able 4.2: Effect of land-use assessment of AL-Ameer District stormwater drainage system throughout 2 hours of rainfall duration.

Return Period (Years)	Sub-catchment (%)	Total Surface runoff (m^3)	Maximum flooded manhole volume (m^3)	Total flooding (m^3)	Number of flooded manholes
10	50	20380	1703 (R315)*	10513	70
10	75	29150	2074 (R315)*	18414	84
10	100	37350	2222 (R315)*	26032	95

*Name of manhole

Notably for almost 2 hours, manhole R315 indicated in Figure (4.3) was mostly flooded with maximum flooding volume of 1703, 2074, and 2222 m^3 for 50, 75, and 100%, respectively. It's worthy to report that data obtained in Table 4.2 occurred at any time throughout the 2 hours duration and not after 2 hours. It also important to note that any change in land-use, for example increasing the area of sub-catchment, will lead extra flooding volumes that the stormwater drainage system may not be able to withstand it. Similarly, Kong et al. (2017b) reported the effect of land-use changes on stormwater management using SWMM simulation. They found that a 33.3% reduction in pervious surfaces (increased of impervious surfaces) result in 92.9% increase in surface runoff, 31.7% increase in peak flow, and 35 min earlier of peak runoff time. In addition, Hu et al. (2020) observed that urbanization increased impervious surfaces in Beijing's central area, leading to increment in surface runoff and flooding. They correlated impervious surfaces rise with surface runoff increase, leading to flooding risk in the area.

The After-2-hours duration, it is expected that the stormwater drainage system AL-Ameer District will discharge most of excess stormwater, but remaining flooding may be considered a risk warning. After 2 hours, Figure 4.3(a-c) illustrates the locations of flooding in AL-Ameer District, type of flooding, and percentage of flooded manholes, for sub-catchments areas of 50, 75, and 100%, respectively. The type of flooding from manholes is divided into five stages according to the SWMM simulation, as recommended by Hassan et al. (2017):

- Stage 1 (no flooding) ranges from (0 to 0.001 m^3/s).
- Stage 2 (very light flooding) ranges from (greater than 0.001 to 0.01 m^3/s).
- Stage 3 (medium flooding) ranges from (greater than 0.01 to 0.02 m^3/s).
- Stage 4 (high flooding) ranges from (greater than 0.02 to 0.04 m^3/s).
- Stage 5 (very high flooding) for (greater than 0.04 m^3/s).

Figure 4.3 (a) shows the assessment of stormwater drainage system at 50% of sub-catchment area, 2 hours of rainfall duration, 10 years of return period, and rainfall intensity of 7.36 mm/hour. Figure 4.3 (a) reveals that the number of flooded manholes were 13 manholes out of 343 total manholes, and ratio of flooded manholes is 4% only and non-flooded is 96%. According to the flooding flow rate, the flooded manholes stages were 21% of medium flooding (Stage 3), 50% of high flooding (Stage 4), and 29% of very high flooding (Stage 5). Among all manholes, R315 at downstream of the system was the most flooded manholes with flooding stage 5 and remains flooded for 1.7 hour of rainfall duration. The total flooded area in the study area after 2 hours was 25965 m^2. It is concluded that the system at 50% sub-catchment area is fairly average during the flood period of 2 hours.

Figure 4.3 (b) displays the behavior of stormwater drainage system at 75% of sub-catchment area, 2 hours of rainfall duration, 10 years of return period, and rainfall intensity of 7.36 mm/hour. It is observed that 25 manholes were flooded, constitute 8% of 343 total manholes, in which 16% were slightly flooded with Stage 2, 16% were fairly flooded with Stage 3, 24% were highly flooded with Stage 4, and 44% were the very highly flooded with Stage 5. It’s interesting to report that the flooding mostly observed in the downstream of the study area (North-East direction) and total flooded area after 2 hours increased to 33750 m^2. In this regard, it can be concluded that the system hardly withstand the surface runoff generated from 75% of sub-catchment, and flood is therefore considered relatively high.

By considering 100% of sub-catchment area, Figure 4.3 (c) reveals a deterioration in the system performance, in which 36 manholes were flooded that represent 11% out of 343 total number. Flooding stages were distributed as 14% very light flooding (Stage 2), 11% medium flooding (Stage 3), 32% high flooding (Stage 4), and mostly 43% very high flooding (Stage 5). The flooding condition in this case was the worse due to increased impervious surfaces and reduced green areas. The downstream area (North-East direction) was completely flooded, and total flooding area rose to 54900 m^2. Flooding water level is very high, might even enters properties, causing damage to property and infrastructure. Accordingly, it’s concluded that the system can’t withstand a sub-catchment area of 100% and flooding was very high at 2 hours of rainfall. After all, it was observed that flooding map has expanded as a result of urbanization and change in land use from pervious to impervious surfaces. Likewise,(Shanableh et al.,

2018) revealed a positive correlation between urbanization and floods, in which flooding increased substantially in areas where land-use has changed to residential area. They also reported that flooding increased by 60% in 10 years due to rapid urbanization.

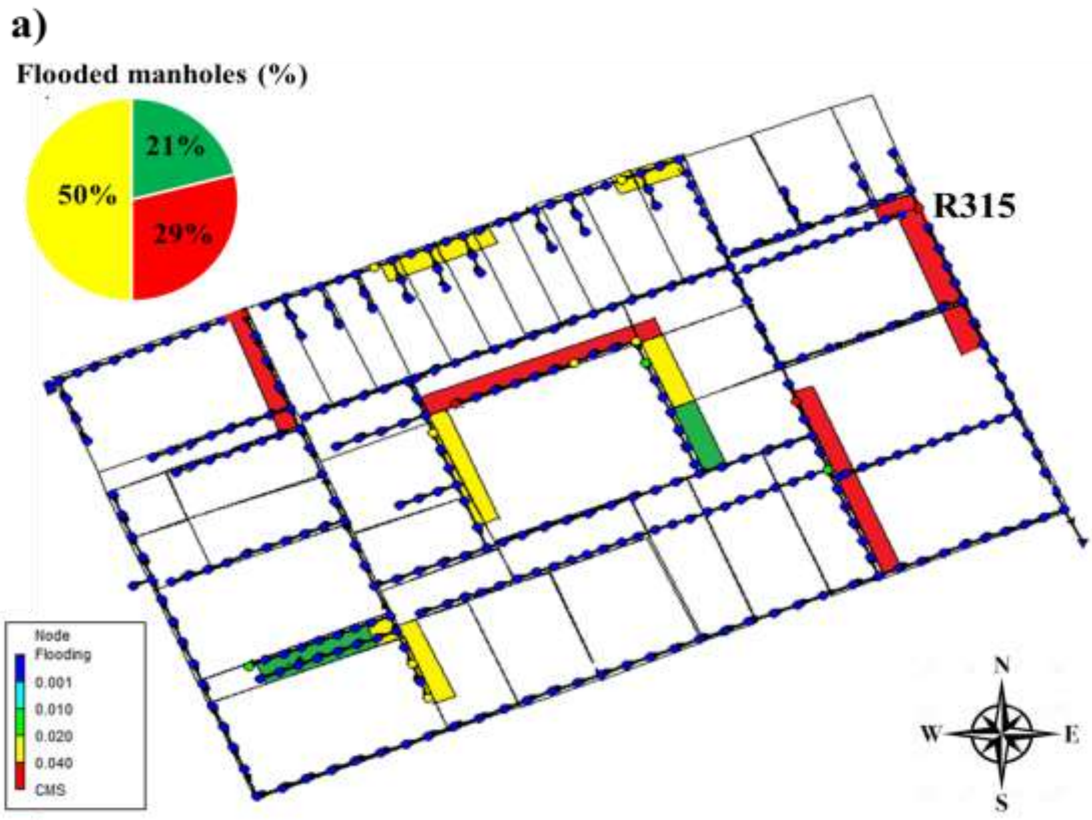

b)

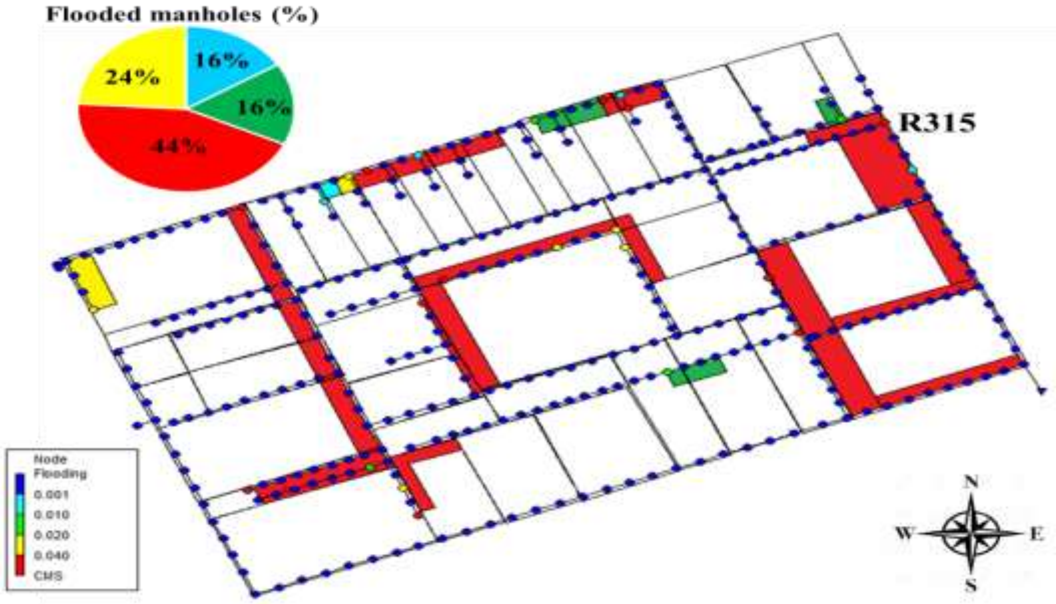

c)

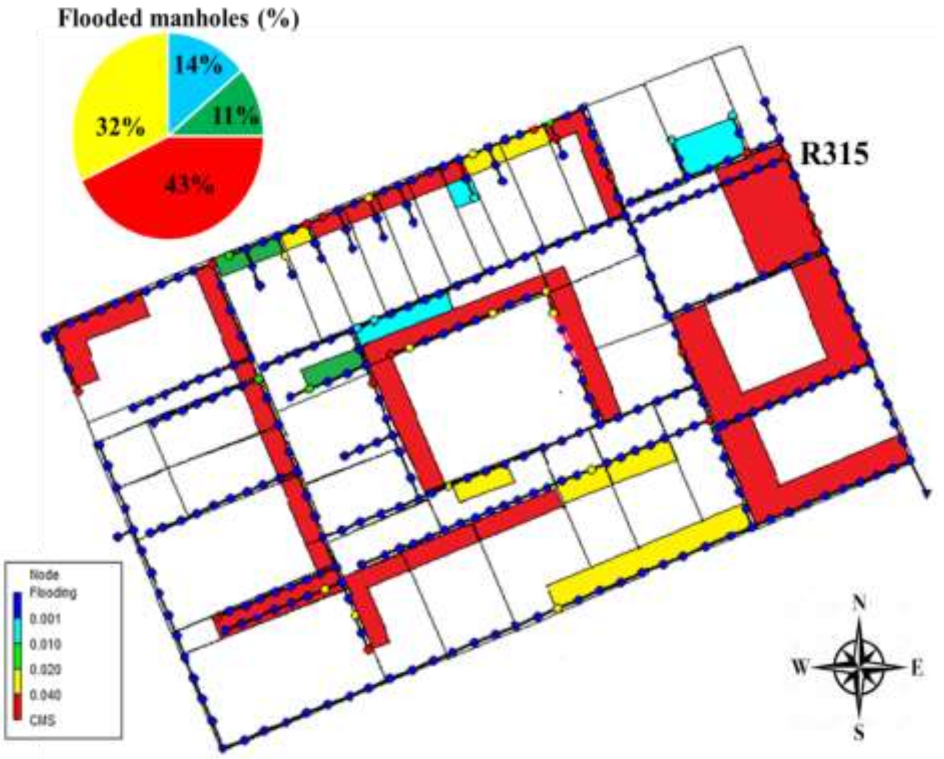

Figure 4.3: Effect of land-use on AL-Ameer District stormwater drainage system at 10 years return period and a) 50% sub-catchment, b) 75% sub-catchment and c) 100% sub-catchment.

4.5 Effect of Climate Change on Stormwater Drainage System

Climate change have a direct influence on increased rainfall intensity that will affect surface runoff generation. Different return period of 2, 5, 10, and 25 years that represent a series of rainfall intensities were selected as a response to climate change effect. Throughout 2 hours of rainfall duration, the assessment results are tabulated in Table 4.3, and rainfall intensities can be obtained from the IDF curve in Figure (4.1). It is observed that increasing the return period has dramatically increased the surface runoff generated in the study area. For example, when the return period shifted from 2 to 5 years, the total surface runoff rose from 14120 and 27110 m^3 (representing 48% of raise), and total flooding increased from 5914 to 17591 m^3, accounting 66.66 % of increment. When higher return period is selected, higher flooding volume and number of flooded manholes were observed. For instance at 25 years of return period, the surface runoff and total flooding were 52006 m^3 and 41230 m^3, respectively. This mean that 21% only of the surface runoff is discharged by the system and 79% of it is flooded, indicating the failure of the system.

Hence, from the results in Table 4.3, it is expected that the system may withstand climate change effect only for the next 10 years. In general, the greater return period, the greater flooding volume occurred. Similarly, an increase in peak runoff was observed then the total rainfall was increased due to increasing return period (Babaei et al., 2018). In support of that, (Anni et al., 2020) reported that number of flooded manholes and volume of flooding increased by 47% and 48% when the return period increased from 10 to 25 years. In like manner, Hassan et al. (2017) noticed a positive correlation between climate change and increased rainfall intensity, where they reported an increase in flooding by 47% as effect of climate change in the last 8 years

Table 4.3 : Effect of climate change assessment of AL-Ameer District stormwater drainage system throughout 2 hours of rainfall duration.

Sub-catchment (%)	Return Period (Years)	Total Surface runoff (m^3)	Maximum flooded manhole volume (m^3)	Total flooding (m^3)	Number of flooded manholes
100	2	14120	1306 (R315)*	5914	26
100	5	27110	1835 (R315)*	17591	72
100	10	37350	2222 (R315)*	26032	95
100	25	52006	2295 (R319)*	41230	106

*Name of manhole

For more realistic evaluation of stormwater drainage system, the system was assessed after 2 hours of rainfall duration. Figure (4.4) showed flooded manholes, flooding magnitude, and flooding locations. Flooding may occur whenever that water discharge at manholes or sewers exceeds the maximum designed values. At 2 years of return period, Figure 4.4 (a) displayed that 15 manholes out 343 total were flooded, and they consisted of 4% of the total manholes. Flooded manholes distributed as 7% of very light flooding, 20% of medium flooding, 40% of high flooding, and 33% very high flooding. Again, R315 manhole was mostly flooded for about 1.51 hr. It is noticed that flooding in small quantities was mainly in the downstream, and therefore surface runoff can be well controlled at this return period.

Figure 4.4 (b) assesses the stormwater drainage system at the end of 2 hours rainfall duration and 5 years of return period. The flooded manholes were 26 out of 343 manholes, which is equivalent to 8% the total manholes. Flooded manholes are classified as 14% very light flooding, 11% medium flooding, 26% high flooding, and 46% very high flooding.

Very high flooding locations were scattered mainly in downstream (east direction) and few locations in the center and upstream (west direction), In addition, flooding occurred mostly in main sewer lines, and manhole R315 had the longest duration flood of very high flood. Increased flooding magnitude is due to increased rainfall intensity, however, the system still can withstand return period of 5 years with climate change effect.

Figure 4.4 (c) shows the condition of the stormwater drainage system at return period of 10 years. The number of flooded manholes reached 36 out of 343, representing 11% of total manholes numbers. It is distributed as 13% very light flooding, 11% medium flooding, 32% high flooding, and 44% high flooding. However, it is noticed that the number of flooded manholes is less important than the magnitude of manholes flooding. For example, the magnitude flooding in manhole 315 (Stage 5) is as much as five other manholes (Stage 5). Therefore, flooding area drawing was used to illustrate flooding magnitude, in which maximum flooding occurs in the downstream (north-east and south-east directions) area and in the main sewer that passes through the center of the area. At 10 years return period, the system seems to fail to discharge excess rainfall, resulting in the accumulation of stormwater at downstream. Flooding quantities are highly increased and flooding depth is expected to rise more than 13 cm (curbstone height) and may enter the houses, causing damage to infrastructure and properties.

At return period of 25 years, Figure 4.4 (d) showed that 48 manholes out of 343 were flooded, and they consisted of 14% of the total manholes. Again, increased number of flooding manholes do not affect the area as much as flooding magnitude. Therefore, flooding magnitude were distributed as 5% very light flooding, 15% medium flooding, 26% high flooding, and 54% high flooding. A major system failure was observed, where 26% of AL-Ameer District was flooded. Many locations were flooded, not only in downstream, but also in the center and upstream. Figure 4.4(d) also showed that stormwater entering the housing, causing damage to infrastructure and properties. It worth to report that branch sewers were also flooded in addition to main sewers. High quantities of flooding is due to the expected high rainfall intensity of 80 mm/hr at the begging of rain storm. The system fail to discharge surface run off because it was beyond the design capacity. This indicate that climate change effect was not considered in future prediction of rainfall intensities needed for storm system design. Hence, climate change effect should be integrated in the generation of IDF curves (Noor et al., 2018) . It is concluded that this prediction of rainfall intensity is one of the most risk warning expected intensities and has sever effects on the system and properties.

Moreover, more areas were flooded when the return period increased further. Likewise, (Babaei et al., 2018). observed when the return period increased from 2 to 5 years and then from 5 to 10 years, more areas were flooded each time and drainage system should be expanded by 20% to prevent flooding. On the other hand, most of stormwater drainage systems are designed to serve a certain maximum value of rainfall intensity based on pervious hydrological data. Meanwhile in recent years, rainfall total amounts are less than before, but rainfall intensities are 4 times higher than the deigned once due to the effect of climate change (Nile et al., 2019).

a)

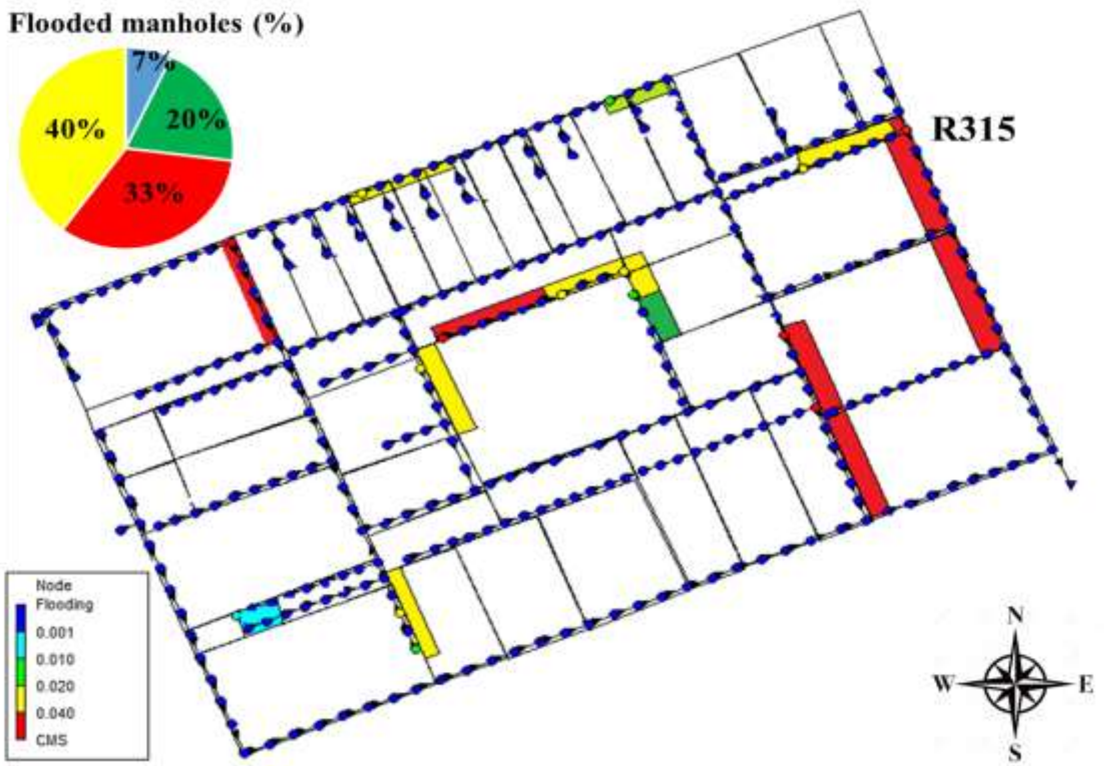
Flooded manholes (%)
7%
20%
40%
33%
R315
Node
Flooding
0.001
0.010
0.020
0.040
CMS
N
W
E
S

b)


Flooded manholes (%)
14%
29%
11%
46%
R315
Node
Flooding
0.001
0.010
0.020
0.040
CMS
N
W
E
S

c)

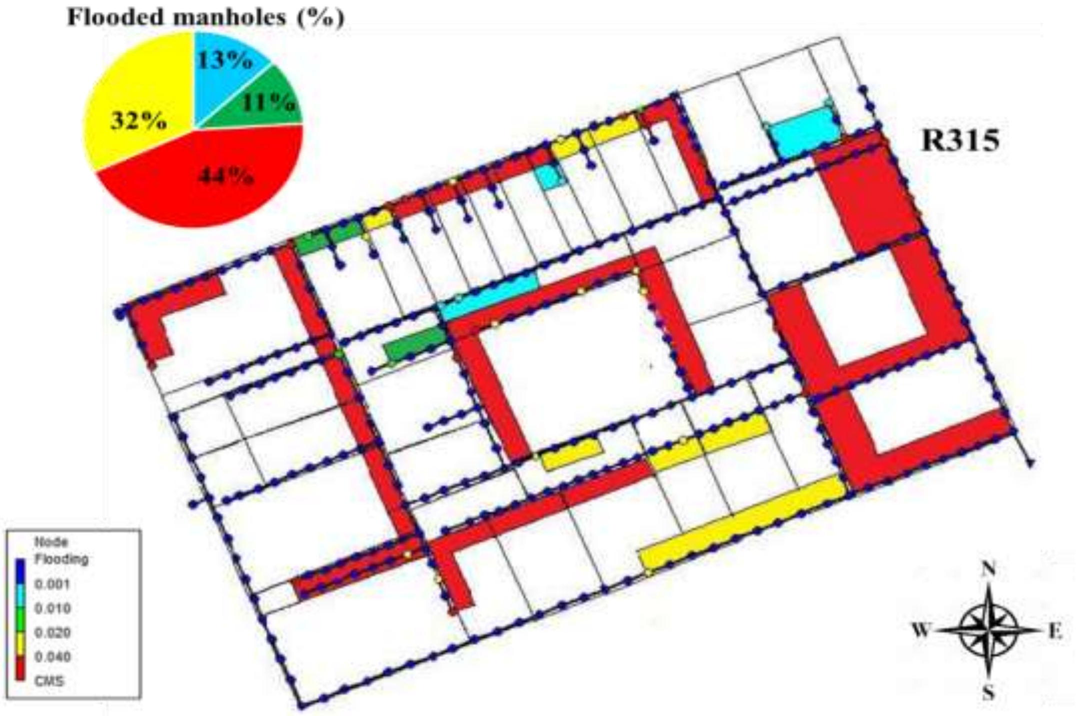

d)

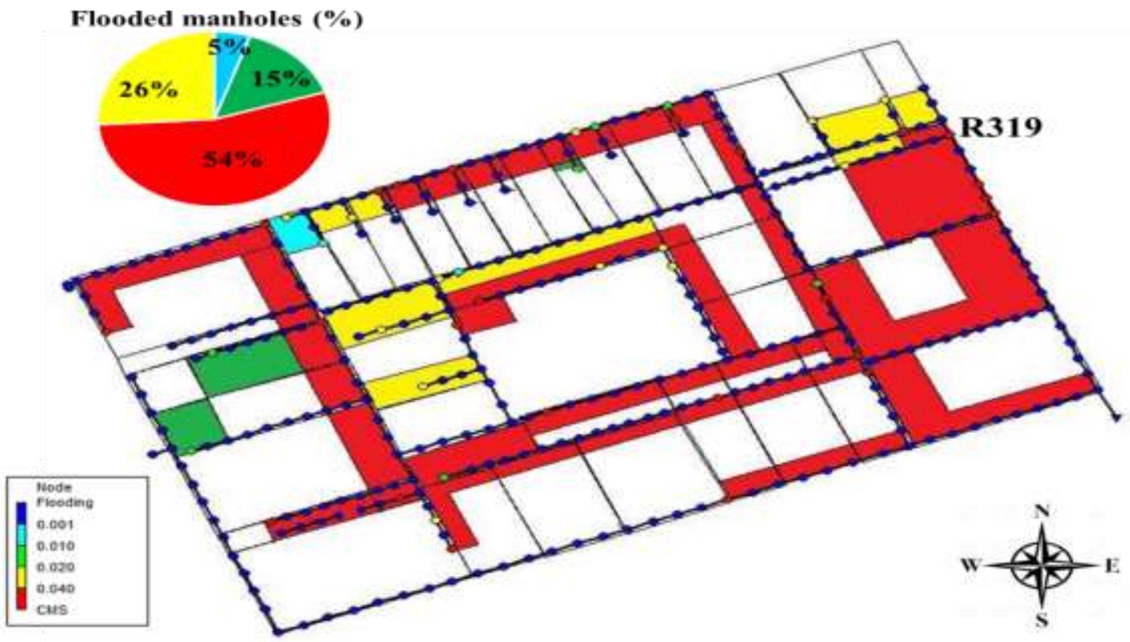

Figure 4.4: Effect of climate change on AL-Ameer District stormwater drainage system at 100% sub-catchment and a) 2 years return period, b) 5 years return period, c) 10 years return period, and d) 25 years return period.

4.6 Effect of Topography on Stormwater Drainage System

In order to study the effect of the topography presented by sub-catchment slope on the stormwater drainage system in the AL-Ameer region, different proportions of sub-catchment slopes contributing to the runoff were taken into consideration. At two hours of rainfall duration, different rainfall intensities at return period of 2, 5, 10, and 25 years were selected and slope of sub-catchments were changed from 0.5% to 0.4%, 0.3%, 0.2%, and 0.1%. The results of topography effects at different rerun period on flooding are shown in Figure (4.5). In general, inclination has increased flooding in the study area. Reducing the slope of the sub-catchments, with no change in the slope of the designed pipes, has reduced flooding.

At return period of 2 years, the total flood volumes were 5914 m^3 and 3309 m^3 for slopes of 0.5% and 0.1%, respectively. The results indicate that the volume of flooding decreased by 44 % then the slope decreased. At return period of 5 years, the total flood volumes were 17591 m^3 and 12513 m^3 for slopes of 0.5% and 0.1%, respectively. This indicate that the volume of flooding decreased by 29% then the slope decreased. At return period of 10 years, the total flood volumes were 26032 m^3 and 20477 m^3 for slopes of 0.5% and 0.1%, respectively. This indicate that the volume of flooding decreased by 21 % then the slope decreased. At return period of 25 years, the total flood volumes were 41230 m^3 and 32512 m^3 for slopes of 0.5% and 0.1%, respectively. This indicate that the volume of flooding decreased by 21% when the slope decreased.

In general, sub-catchment slope positively affected flooding at all rainfall intensities, but it had less effect at low rainfall intensities. In 2 years return period, the effect of sub-catchment slope was limited with high flood reduction, whereas low sub-catchment slope had a little effect on flooding at return period of 10 and 25 years. Finally, it is noted that high sub-catchment slope leads to further increase in surface runoff, resulting in flooding. Therefore, the designers must match the sub-catchment with network pipes slops to reduce floods. Similarly, Salvan et al. (2016) recommended that detailed information on topography is needed in order to come out with best design. They found that topography has a major influence on flood determination for both of drainage pipe networks and open channel systems.

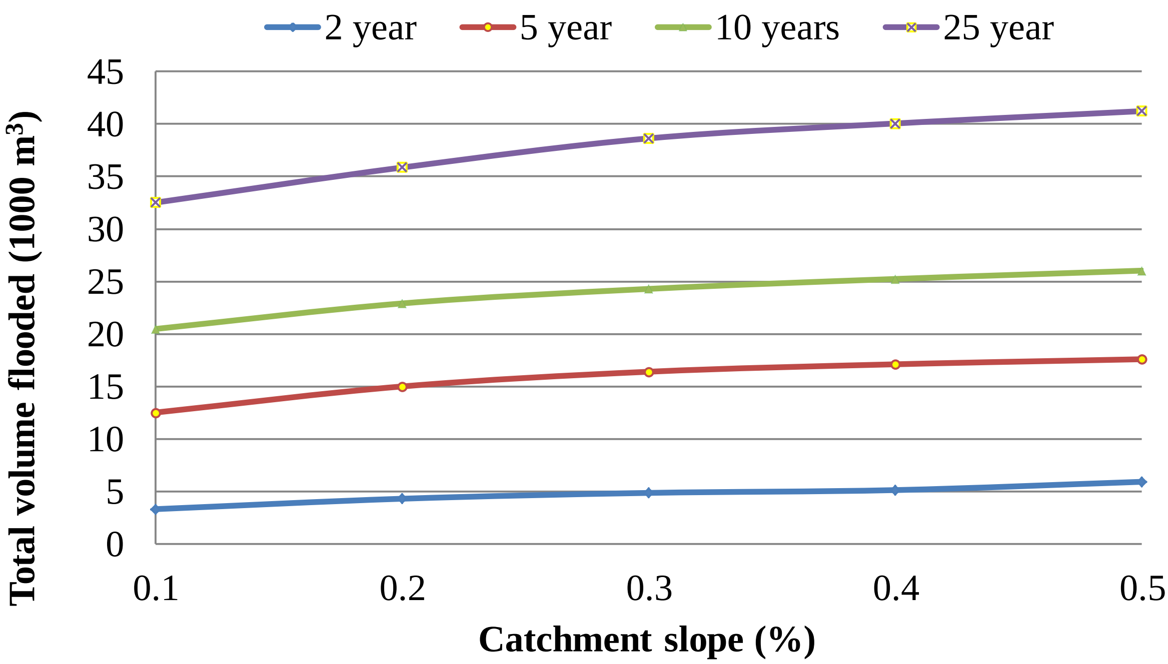

Figure 4.5: Effect topography on AL-Ameer district stormwater drainage system at different slopes of 0.5, 0.4, 0.3, 0.2, and 0.1%, and 2, 5, 10 and 25 years of return period.

4.7 Effect of Concentration Time on Stormwater Drainage System

Time of concentration is commonly used in hydraulic flood flow design, precise estimated peak discharge, and flood hydrograph. Three flood-experiencing manholes were selected to determine the time of flood: first is located upstream (R15), second is in the center of study area (R250), and third in the downstream (R315). At return period of 10 years, Figure (4.6) shows the maximum flood occurs downstream in manhole R315 after 20 minutes, upstream in manhole R15 after 25 minutes, and study area center in manhole R250 after 20 minutes and reaches maximum after one hour. These results showed that the flood time occurs downstream before the upstream, indicating that the downstream area suffers from topographical and design problems.

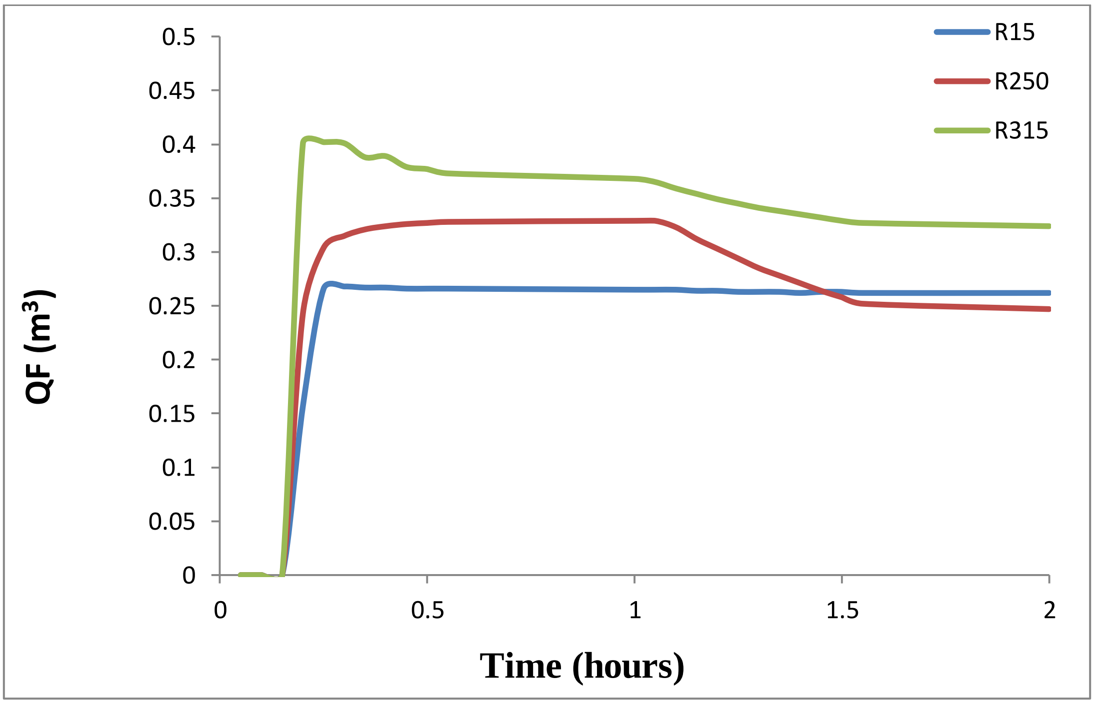

Figure 4.6: Effect of time concentration on AL-Ameer District stormwater drainage system.

In order to explain why manhole R315 flooded before manhole R15, Figure (4.7) shows the slope of the sub-catchments is in opposite direction to the direction of flow in pipes, as well as, the depth of the manhole is short . In similar way, Zhu et al. (2019) utilized permeable pavement to reduce part of the peak runoff and delay flood peak time. Permeable pavement will allow the infiltration of stormwater, reducing the surface runoff.

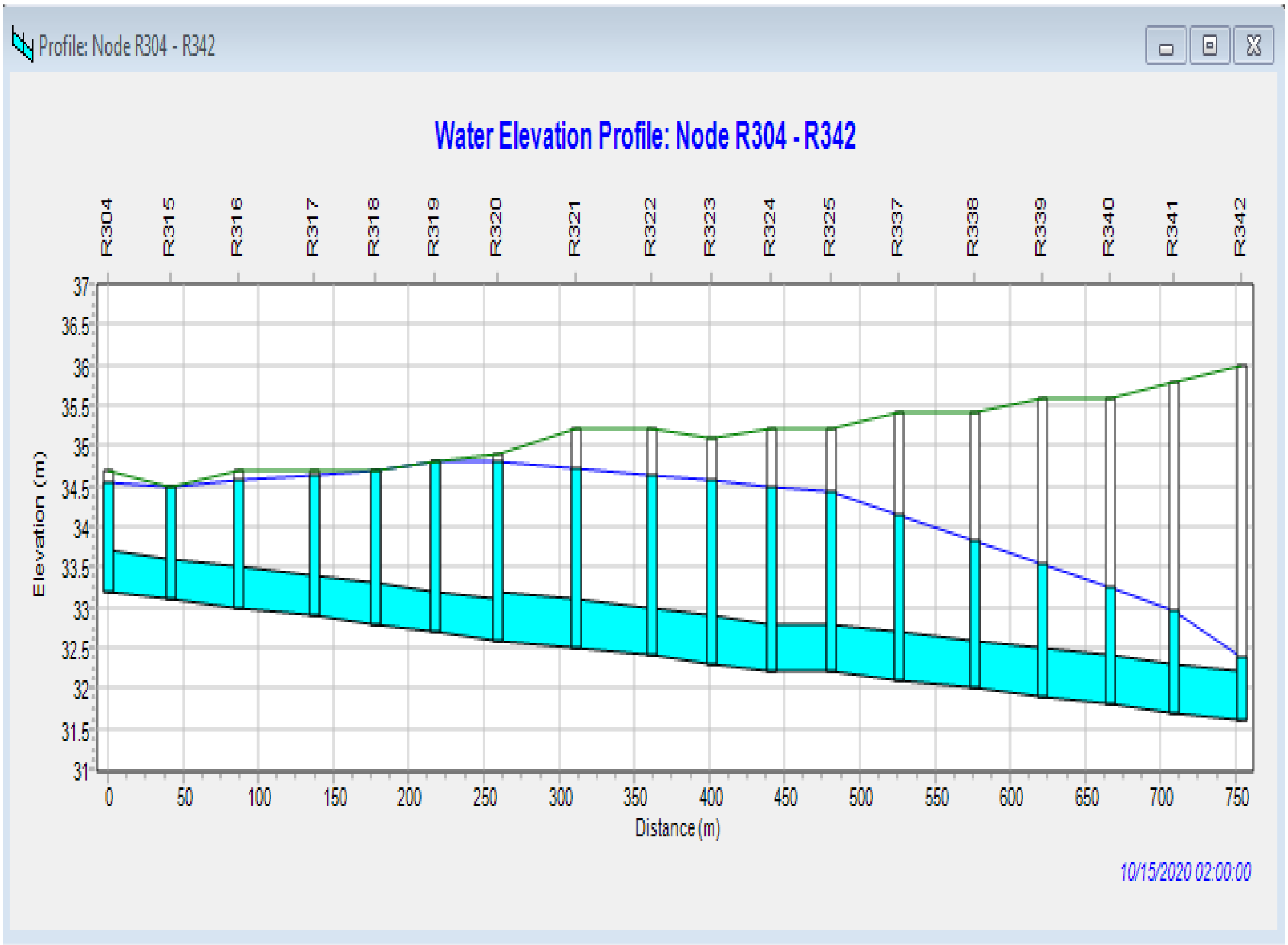

Figure 4.7: Downstream sewers in AL-Ameer District and depth of water in Manholes.

4.8 Effect of Pipe Diameter on Flooding in Downstream

After discussing all the impacts on the stormwater drainage system in the AL-Ameer region, the redesign of the main downstream line, which has a length of 850 m and consists of 16 pipes with different design diameters, was considered. This is because manholes on this line are mostly flooded at downstream drainage network area. At return period of 10 years and 2 hours rainfall duration, different design diameters were simulated using SWMM, the solution scenario was evaluated in node R315 and the results are shown in Figure 4.8 (a, b, c and d). Figure 4.8 (a) shows the condition of the current designed downstream line. Consecutively, the number of pipes after node 315 are 5 with diameter of 500 mm, and 11 with diameter of 600 mm (Figure 4.7). The results showed that the maximum flood flow occurred after 20 min was 0.43 m^3/s, the flood flow dropped from 0.43 to 0.31 m^3/s for a duration of 100 minutes, and the total flooding volume was 4000 m^3 after 2 hours.

In order to provide further discharge after the flooded manhole (R315), Figure 4.8 (b) shows the condition of redesigned stormwater drainage system after changing the pipes diameter from 500 mm to 600 mm, and from 600 to 700 mm. The results showed that the total maximum flood flow was 0.5 m3/s after 25 minutes, then gradually decreased to 0.38 m^3/s after two hours, and the total amount of flooding after 2 hours was 3252 m^3. This indicate that change occurred in total flood volume only and it was decreased by 18.7%.

Figure 4.8 (c) shows the drainage system condition after changing the pipes diameter from 500 mm to 700 mm, and from 600 to 800 mm. The results showed that the maximum flood flow was 0.55 m^3/s after 35 minutes, and decreased to 0.19 m^3/s after two hours. The total amount of flooding after 2 hours was 2193 m^3, which show that the total flood volume decreased by 45%.

Figure 4.8 (d) shows the flood condition after changing the diameter from 500 to 800 mm, and from 600 to 1000 mm. The results showed that the maximum flood flow was 0.09 m^3/s after 35 minutes, and surprisingly there was no flood after two hours. Furthermore, the total amount of flooding during 2 hours was 115 m^3. It is worth to report that the total flood volume during two hours decreased by 97%. Therefore, this design can be considered as a solution scenario to totally solve the flooding problem in AL-Ameer District stormwater drainage system. It is best solution

Likewise, in order to mitigate flooding occurred in drainage network due to climate change, Ngamalieu-Nengoue et al. (2019) studied the rehabilitation of the drainage network by substituting some pipes with other larger diameters. This solution was found to highly reduce flooding in the study area. Although replacing pipes is an expensive proposition, the expenses of installation will be covered by the costs of flood damage. As a result, a set of optimal solutions can be applied based on the goals that decision- makers want to achieve Rainwater pouds.

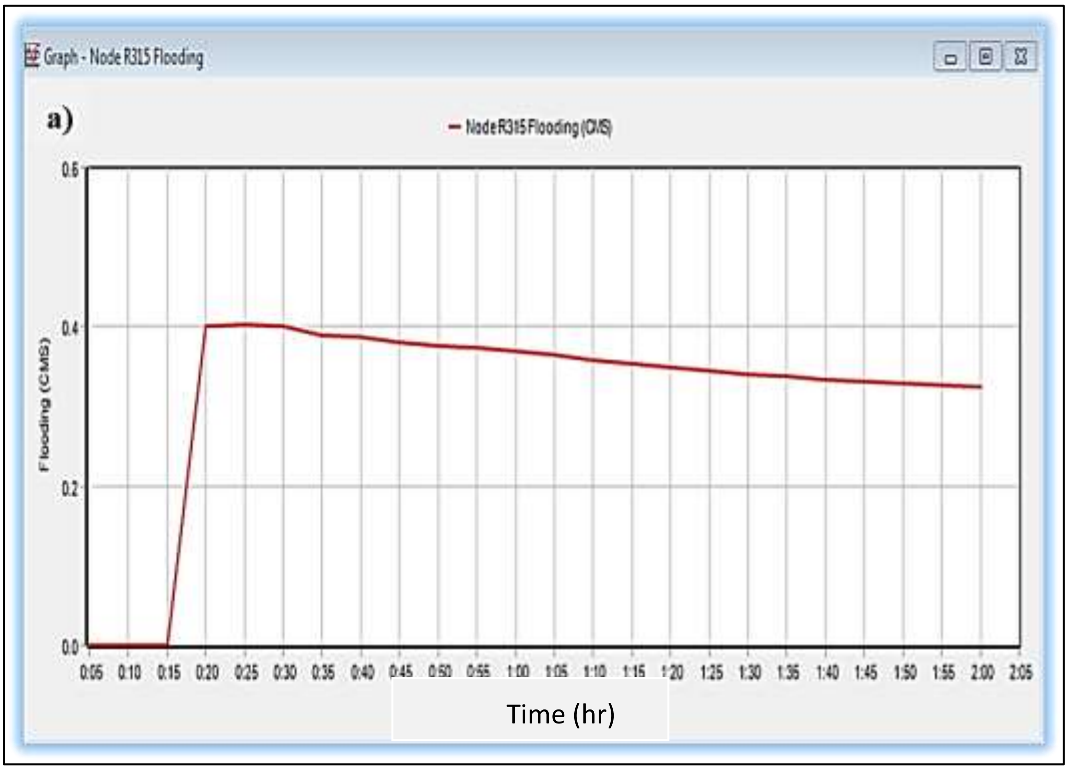
Graph - Node R315 Flooding
a)
Node R315 Flooding (CMS)
Flooding (CMS)
0.6
0.4
0.2
0.0
0:05 0:10 0:15 0:20 0:25 0:30 0:35 0:40 0:45 0:50 0:55 1:00 1:05 1:10 1:15 1:20 1:25 1:30 1:35 1:40 1:45 1:50 1:55 2:00 2:05
Time (hr)


Graph - Node R315 Flooding
b)
Node R315 Flooding (CMS)
Flooding (CMS)
0.6
0.4
0.2
0.0
0:05 0:10 0:15 0:20 0:25 0:30 0:35 0:40 0:45 0:50 0:55 1:00 1:05 1:10 1:15 1:20 1:25 1:30 1:35 1:40 1:45 1:50 1:55 2:00 2:05
Time (hr)

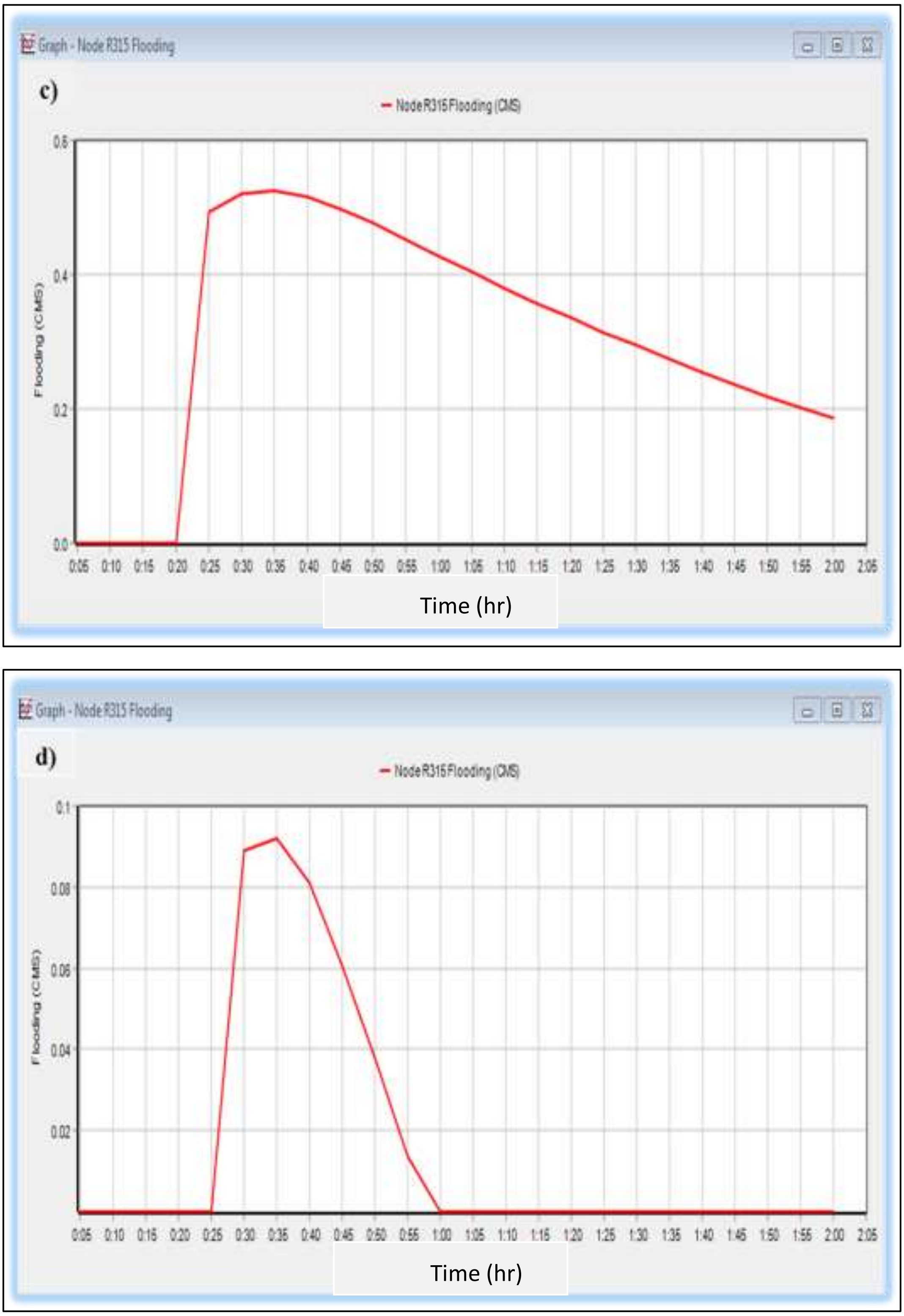

Figure 4.8. a,b,c, and d: Effect of different pipes diameters on the flooding in downstream.

4.9 Flood equation through dimensional analysis

Defining dimensional analysis is a very effective method to use in analyzing and understanding engineering problems. For computing dimensionless parameters, the dimensional analysis is useful and provides a response to the set of parameters affecting the problem in the study area.

In order to reduce the limits of the variables in equation [3.16] by dividing the fourth term by the third term, the effect of the second term for areas has been canceled, and the effect of its data will be taken into account when calculating the runoff.

$$\frac{Q_f}{Q_c} = f\left[\frac{T_c I^{1.5}}{Q_c^{0.5}}, \frac{d}{D}, \frac{S.c}{S.p}\right]$$

Y = f $(X_{1,} X_{2,} X_3)$

Where:

$X_1 = \frac{T_c I^{1.5}}{Q_c^{0.5}}$; $X_2 = \frac{S.c}{S.p}$; $X_3 = \frac{d}{D}$; $Y = \frac{Q_f}{Q_c}$ $X1, X2,$ and $X3 \neq 0$

After taking a sample of the data and making a simulation of the network using SWMM and using a program Data fit V.9, an approximate equation was found for calculating the flood in any aperture based on the variables of density, diameter, slope, area, runoff, and storage depth.

$$\mathbf{Q}_{\boldsymbol{F}} = \frac{\boldsymbol{Q_C}}{\mathbf{exp}(\frac{\mathbf{4.704 * 10^{-6}}}{X_1} + \frac{\mathbf{0.126}}{X_2} + \frac{\mathbf{0.676}}{X_3} - \mathbf{0.180})}$$

This approximate mathematical model is a guide to assessing, analyze and determine the flood in the study area, as it includes all the variables that affect the flood; they help designers to find possible solutions to address problems as quickly as possible without resorting to programs.

CHAPTER FIVE
CONCLUSIONS AND FUTURE RECOMMENDATIONS

5.1 Conclusions

The stormwater drainage system faces significant challenges due to climate change, topography, land-use change, increased urbanization, as well as land misuse, which has led to an increase in the impervious area and consequently an increase in the volume of runoff. These changes caused failure to address rain discharges whose severity exceeded design capacity. The inundation and escalation of these floods have environmental, economic, and health implications. This study analysed and evaluated the stormwater drainage system in AL-Ameer District of AL-Najaf city during heavy rains and developed plans and solutions that can reduce or mitigate floods using new strategies. The conclusions have been made based on the results reported previously. They can be summarized as follow:

1. An IDF curve that integrates the climate change effect has been successfully produced for Al-Najaf city in Iraq for the first time.
2. SWMM simulation was validated over designed stormwater flow rates in the system, with an NMSE value of 0.002 and an R-value of 0.95, without the need for model calibration.
3. Random urban development in AL-Ameer District has changed land use from pervious to impervious areas, causing an increase in surface runoff, flood volume, and the number of flooded manholes.
4. The sub-catchment slope had a positive effect on flooding in all rainfall intensity. In the 2-year return period, flooding was significantly reduced, while the sub-catchment slope had little impact on flooding in the 10- to 25-year return period.

5. When checking the flood time, it was noted that the manhole R315 was flooded before the manhole R15, because the slope of the sub-catchment is in the opposite direction to the direction of flow in the pipes, as well as the depth of the manhole is short.
6. In order to provide more discharge after the submerged orifice (R315), the flood condition was observed after changing the diameter from 500 to 800 mm, and from 600 to 1000 mm. It was concluded that the total flood volume in two hours was reduced by 97%. Therefore, this design can be considered as a solution scenario to completely solve the flood problem in the rainwater drainage system in the sub-catchment area.

5.2 Future Recommendations

1. It is recommended to maintain green lands to improve rainwater infiltration and increase previous surfaces and thus reduce runoff resulting in reduced flood volume.

2. Changing the diameter from 500 to 800 mm and from 600 to 1000 mm downstream can be considered as a solution scenario to completely solve the flood problem in the rainwater drainage system in the Al-Ameer District.

3. Municipal administrations must activate building permit laws and follow up the implementation of home gardens with a percentage of no less than 20% of the building area.

4. A new mitigation solution is proposed to reduce the impact of flooding in the downstream area through the installation of lift pumps. the solution is cost-effective and is a new approach to flood mitigation in Iraq.

5. It is recommended to implement barriers in the form of open, rectangular channels towards the width of the street that contribute to delaying the

surface runoff heading to the downstream, with dimensions and number estimated according to the size of the flood and the speed of flow.

Refrences

Agnese, C., Baiamonte, G., Corrao, C. 2007. Overland flow generation on hillslopes of complex topography: analytical solutions. *Hydrological Processes: An International Journal*, **21**(10), 1308-1317.

Al-Awadi, A.T. 2016. Assessment of intensity duration frequency (IDF) models for Baghdad city, Iraq. *Journal of Applied Sciences Research*, **12**(2), 7-11.

Ali, T. S., & Fakhraldin, M. K. (2016). Soil parameters analysis of Al-Najaf City in Iraq: case study. J Geotech Eng, 3(1), 56-62.

Anni, A.H., Cohen, S., Praskievicz, S. 2020. Sensitivity of urban flood simulations to stormwater infrastructure and soil infiltration. *Hydrology*, **588**, 125028.

Babaei, S., Ghazavi, R., Erfanian, M. 2018. Urban flood simulation and prioritization of critical urban sub-catchments using SWMM model and PROMETHEE II approach. *Physics Chemistry of the Earth, Parts A/B/C*, **105**, 3-11.

Behrouz, M.S., Zhu, Z., Matott, L.S., Rabideau, A.J. 2020. A new tool for automatic calibration of the Storm Water Management Model (SWMM). *Journal of Hydrology*, **581**, 124436.

Bell, C.D., McMillan, S.K., Clinton, S.M., Jefferson, A.J. 2016. Hydrologic response to stormwater control measures in urban watersheds. *Journal of Hydrology*, **541**, 1488-1500.

Bisht, D.S., Chatterjee, C., Kalakoti, S., Upadhyay, P., Sahoo, M., Panda, A. 2016. Modeling urban floods and drainage using SWMM and MIKE URBAN: a case study. *Natural hazards*, **84**(2), 749-776.

Buckingham, E. 1914. On physically similar systems; illustrations of the use of dimensional equations. *Physical review* **4**(4), 345.

Butler, D., Digman, C.J., Makropoulos, C., Davies, J.W. 2018. *Urban drainage*. Crc Press.

Cantone, J., Schmidt, A. 2011. Improved understanding and prediction of the hydrologic response of highly urbanized catchments through development of the Illinois Urban Hydrologic Model. *Water Resources Research*, **47**(8).

Chabaeva, A., Civco, D.L., Hurd, J.D. 2009. Assessment of impervious surface estimation techniques. *Hydrologic Engineering*, **14**(4), 377-387.

Cheng, L., AghaKouchak, A. 2014. Nonstationary precipitation intensity-duration-frequency curves for infrastructure design in a changing climate. *Scientific reports*, **4**(1), 1-6.

Chin, D.A. 2019. Relative performance of intensity-duration-frequency functions. *Journal of Hydrologic Engineering*, **24**(4), 04019006.

Doubleday, G., Sebastian, A., Luttenschlager, T., Bedient, P.B. 2013. Modeling hydrologic benefits of low impact development: A distributed hydrologic model of the Woodlands, Texas. *the American Water Resources Association*, **49**(6), 1444-1455.

Elsebaie, I.H. 2012. Developing rainfall intensity–duration–frequency relationship for two regions in Saudi Arabia. *King Saud University-Engineering Sciences*, **24**(2), 131-140.

Elshorbagy, A., Lindenas, K., Azinfar, H. 2018. Risk-based quantification of the impact of climate change on storm water infrastructure. *Water Science*, **32**(1), 102-114.

Federation, W.E., Engineers, A.S.o.C. 1992. *Design and construction of urban stormwater management systems*. American Society of Civil Engineers and Water Environment Federation.

Fukuchi, T. 2006. Hydraulic Elements Chart for Pipe Flow Using New Definition of Hydraulic Radius. *Journal of Hydraulic Engineering*, **132**(9), 990-994.

Gironás, J., Roesner, L.A., Davis, J., Rossman, L.A., Supply, W. 2009. *Storm water management model applications manual*. National Risk Management Research Laboratory, Office of Research and ….

Gironás, J., Roesner, L.A., Rossman, L.A., Davis, J. 2010. A new applications manual for the Storm Water Management Model (SWMM). *Environmental Modelling Software*, **25**(6), 813-814.

Gribbin, J.E. 2013. *Introduction to Hydraulics & Hydrology: With Applications for Stormwater Management*. Cengage Learning.

Hallema, D.W., Moussa, R., Sun, G., McNulty, S.G. 2016. Surface storm flow prediction on hillslopes based on topography and hydrologic connectivity. *Ecological Processes*, **5**(1), 1-13.

Haris, H., Chow, M., Usman, F., Sidek, L., Roseli, Z., Norlida, M. 2016. Urban stormwater management model and tools for designing stormwater management of green infrastructure practices. *IOP conference series: earth and environmental science*. IOP Publishing. pp. 012022.

Hassan, W.H., Nile, B.K., Al-Masody, B.A. 2017. Climate change effect on storm drainage networks by storm water management model. *Environmental Engineering Research*, **22**(4), 393-400.

Hu, S., Fan, Y., Zhang, T. 2020. Assessing the effect of land use change on surface runoff in a rapidly urbanized city: A case study of the central area of Beijing. *Landscape*, **9**(1), 17.

Jiang, L., Chen, Y., Wang, H. 2015. Urban flood simulation based on the SWMM model. *Proceedings of the International Association of Hydrological Sciences*, **368**, 186-191.

Kadioglu, M., ŞEn, Z. 2001. Monthly precipitation-runoff polygons and mean runoff coefficients. *Hydrological Sciences Journal,* **46**(1), 3-11.

Khadka, S., Basnet, K. 2019. Storm water management of barahi chowk area, lakeside, pokhara, nepal using swmm. *2nd International Conference on Engineering & Technology*. pp. 320-325.

Kim, R., Park, S., Lee, H. 2015. The Application Evaluation of Autodesk Storm and Sanitary Analysis for the Low Impact Development Design in the Park Area. *International Journal of Multimedia Ubiquitous Engineering*, **10**(10), 167-176.

Kong, F., Ban, Y., Yin, H., James, P., Dronova, I. 2017a. Modeling stormwater management at the city district level in response to changes in land use and low impact development. *Environmental Modelling Software*, **95**, 132-142.

Kong, F., Ban, Y., Yin, H., James, P., Dronova, I. 2017b. Modeling stormwater management at the city district level in response to changes in land use and low impact development. *Environmental Modelling Software Eng*, **95**, 132-142.

Koutsoyiannis, D., Kozonis, D., Manetas, A. 1998. A mathematical framework for studying rainfall intensity-duration-frequency relationships. *Hydrology*, **206**(1-2), 118-135.

Kundzewicz, Z.W., Robson, A.J. 2004. Change detection in hydrological records—a review of the methodology/revue méthodologique de la détection de changements dans les chroniques hydrologiques. *Hydrological sciences j*, **49**(1), 7-19.

Leandro, J., Schumann, A., Pfister, A. 2016a. A step towards considering the spatial heterogeneity of urban key features in urban hydrology flood modelling. *Journal of Hydrology*, **535**, 356-365.

Leandro, J., Schumann, A., Pfister, A. 2016b. A step towards considering the spatial heterogeneity of urban key features in urban hydrology flood modelling. *Hydrology,* **535**, 356-365.

Lockie, T. 2009. Catchment modelling using SWMM. *Modelling Stream at the 49th Water New Zealand Annual Conference and Expo*.

Mah, D.Y., Putuhena, F.J., Said, S. 2007. Use of infoworks river simulation (RS) in Sungai Sarawak Kanan modeling. *the Institution of Engineers, Malaysia,* **68**(1), 1-10.

McCuen, R.H., Johnson, P.A., Ragan, R.M. 1996. Highway hydrology: Hydraulic design series No. 2.

McGhee, T.J., Steel, E.W. 1991. *Water supply and sewerage*. McGraw-Hill New York.

Miles, B.C. 2014. Small-scale residential stormwater management in urbanized watersheds: A geoinformatics-driven ecohydrology modeling approach, The University of North Carolina at Chapel Hill.

Ngamalieu-Nengoue, U.A., Martínez-Solano, F.J., Iglesias-Rey, P.L., Mora-Meliá, D. 2019. Multi-objective optimization for urban drainage or sewer networks rehabilitation through pipes substitution and storage tanks installation. *Water,* **11**(5), 935.

Nhat, L.M., Tachikawa, Y., Takara, K. 2006. Establishment of intensity-duration-frequency curves for precipitation in the monsoon area of Vietnam. *Annuals of Disas. Prev. Res. Inst*, 93-103.

Nile, B.K. 2018. Effectiveness of hydraulic and hydrologic parameters in assessing storm system flooding. *Advances in Civil Engineering,* **2018**.

Nile, B.K., Hassan, W.H., Alshama, G.A. 2019. Analysis of the effect of climate change on rainfall intensity and expected flooding by using

ANN and SWMM programs. *ARPN Journal of Engineering and Applied Sciences*, **14**(5), 974-984.

Noor, M., Ismail, T., Chung, E.-S., Shahid, S., Sung, J.H. 2018. Uncertainty in Rainfall Intensity Duration Frequency Curves of Peninsular Malaysia under Changing Climate Scenarios. *Water*, **10**(12), 1750.

Ogden, F., Pradhan, N., Downer, C., Zahner, J. 2011. Relative importance of impervious area, drainage.

Olsson, J., Berggren, K., Olofsson, M., Viklander, M. 2009. Applying climate model precipitation scenarios for urban hydrological assessment: A case study in Kalmar City, Sweden. *mospheric Research*, **92**(3), 364-375.

Oreskes, N., Shrader-Frechette, K., & Belitz, K. (1994). Verification, validation, and confirmation of numerical models in the earth sciences. Science, 263(5147), 641-646.

Park, S., Lee, K., Park, I., Ha, S. 2008. Effect of the aggregation level of surface runoff fields and sewer network for a SWMM simulation. *Desalination*, **226**(1-3), 328-337.

Pauleit, S., Ennos, R., Golding, Y. 2005. Modeling the environmental impacts of urban land use and land cover change—a study in Merseyside, UK. *Landscape urban planning*, **71**(2-4), 295-310.

Pendergast, S.D., McCuen II, B.W. 1996. Visual field loss after macular hole surgery. *Ophthalmology*, **103**(7), 1069-1077.

Qi, M., Huang, H., Liu, L., Chen, X. 2020. Spatial heterogeneity of controlling factors' impact on urban pluvial flooding in Cincinnati, US. *Applied Geography*, **125**, 102362.

Rathnam, E.V., Jayakumar, K., Cunnane, C. 2001. Runoff computation in a data scarce environment for urban stormwater management-a case study. *Proceedings of the Congress-International Association For Hydraulic Research*. pp. 446-454.

Rawls, W.J., Brakensiek, D.L., Miller, N. 1983. Green-Ampt infiltration parameters from soils data. *hydraulic engineering*, **109**(1), 62-70.

Reddy, G.M., Reddy, V.D. 2014. Theoretical investigations on dimensional analysis of ball bearing parameters by using Buckingham pi-theorem. *Procedia Engineering*, **97**, 1305-1311.

Rosenzweig, B.R., McPhillips, L., Chang, H., Cheng, C., Welty, C., Matsler, M., Iwaniec, D., Davidson, C.I. 2018. Pluvial flood risk and opportunities for resilience. *Wiley Interdisciplinary Reviews: Water*, **5**(6), e1302.

Rossman, L.A. 2010. *Storm water management model user's manual, version 5.0*. National Risk Management Research Laboratory, Office of Research and ….

Rossman, L.A., Supply, W. 2006. *Storm water management model, quality assurance report: dynamic wave flow routing*. US Environmental Protection Agency, Office of Research and Development ….

Salarpour, M., Rahman, N.A., Yusop, Z. 2011. Simulation of flood extent mapping by InfoWorks RS-case study for tropical catchment. *Software Eng*, **5**, 127-135.

Salvan, L., Abily, M., Gourbesville, P., Schoorens, J. 2016. Drainage system and detailed urban topography: towards operational 1D-2D modelling for stormwater management. *Procedia Engineering*, **154**, 890-897.

Sansom, J., Renwick, J.A. 2007. Climate change scenarios for New Zealand rainfall. *Applied Meteorology Climatology*, **46**(5), 573-590.

Schubert, J.E., Sanders, B.F., Smith, M.J., Wright, N.G. 2008. Unstructured mesh generation and landcover-based resistance for hydrodynamic modeling of urban flooding. *Advances in Water Resources*, **31**(12), 1603-1621.

Shanableh, A., Al-Ruzouq, R., Yilmaz, A.G., Siddique, M., Merabtene, T., Imteaz, M.A. 2018. Effects of land cover change on urban floods and rainwater harvesting: a case study in Sharjah, UAE. *Water*, **10**(5), 631.

Shen, J., Zhang, Q. 2014. Parameter estimation method for SWMM under the condition of incomplete information based on GIS and RS. *EJGE. Pp*, 6095-6108.

Sheng, J., Wilson, J.P. 2009. Watershed urbanization and changing flood behavior across the Los Angeles metropolitan region. *Natural Hazards*, **48**(1), 41-57.

Solomon, S., Manning, M., Marquis, M., Qin, D. 2007. *Climate change 2007-the physical science basis: Working group I contribution to the fourth assessment report of the IPCC*. Cambridge university press.

Sun, Y., Wendi, D., Kim, D.E., Liong, S.-Y. 2019. Deriving intensity–duration–frequency (IDF) curves using downscaled in situ rainfall assimilated with remote sensing data. *Geoscience Letters*, **6**(1), 1-12.

Troch, P.A., Paniconi, C., Emiel van Loon. 2003. Hillslope-storage Boussinesq model for subsurface flow and variable source areas along complex hillslopes: 1. Formulation and characteristic response. *Water Resources Research*, **39**(11).

Wang, X. 2021. *Water Resources and Hydraulics*. Cambridge University Press.

Wang, C., & Li, S. S. (2018). Hydraulic jump and resultant flow choking in a circular sewer pipe of steep slope. Water, 10(11), 1674.

Westra, S., Fowler, H., Evans, J., Alexander, L., Berg, P., Johnson, F., Kendon, E., Lenderink, G., Roberts, N. 2014. Future changes to the intensity and frequency of short-duration extreme rainfall. *Reviews of geophysics*, **52**(3), 522-555.

Wong, S.T.J.G.A. 1978. Toward achieving dimensional homogeneity in hydrologic analysis. **10**(3), 262-272.

Yang, Q., Dai, Q., Han, D., Zhu, X., Zhang, S. 2018. Impact of the storm sewer network complexity on flood simulations according to the stroke scaling method. *Water*, **10**(5), 645.

Yannopoulos, S.I., Lyberatos, G., Theodossiou, N., Li, W., Valipour, M., Tamburrino, A., Angelakis, A.N. 2015. Evolution of water lifting devices (pumps) over the centuries worldwide. *Water*, **7**(9), 5031-5060.

Zhu, H., Yu, M., Zhu, J., Lu, H., Cao, R. 2019. Simulation study on effect of permeable pavement on reducing flood risk of urban runoff. *International journal of transportation science technology*, **8**(4), 373-382.

Zwain, H.M., Almurshedi, K.R., Vakili, M., Dahlan, I., Naje, A.S. 2021. Water Quality and Radionuclides Content Assessment of the Al-Najaf Sea: Case Study. *Ecological Engineering*, **22**(2).

Zwain, H.M., Nile, B.K., Faris, A.M., Vakili, M., Dahlan, I. 2020. Modelling of hydrogen sulfide fate and emissions in extended aeration sewage treatment plant using TOXCHEM simulations. *Scientific Reports*, **10**(1), 22209.

APPENDIX A

Stormwater drainage system Data about the sub-catchment area input to the model(GIS).

element(ID)	Area(ha)	Average slope (%)	Drainage node ID	impervious Area(%)	Manning's roughness
Sub-01	8.85	0.5	R1	75	0.013
Sub-02	1.8	0.5	R50	75	0.013
Sub-03	3.21	0.5	R58	75	0.013
Sub-04	1.3	0.5	M131	75	0.013
Sub-05	3.33	0.5	R71	75	0.013
Sub-06	1.37	0.5	M135	75	0.013
Sub-07	8.36	0.5	R217	75	0.013
Sub-08	2.19	0.5	R205	75	0.013
Sub-09	8.83	0.5	R212	75	0.013
Sub-10	2.41	0.5	R37	75	0.013
Sub-11	3.91	0.5	R44	75	0.013
Sub-12	3.06	0.5	R83	75	0.013
Sub-13	1.98	0.5	R88	75	0.013
Sub-14	3.53	0.5	R227	75	0.013
Sub-15	4.19	0.5	R159	75	0.013
Sub-16	5.11	0.5	R162	75	0.013
Sub-17	2.65	0.5	R94	75	0.013
Sub-18	3.98	0.5	R178	75	0.013
Sub-19	12.96	0.5	R98	75	0.013
Sub-20	2.1	0.5	R194	75	0.013
Sub-21	3.44	0.5	R199	75	0.013
Sub-22	3.35	0.5	R200	75	0.013
Sub-23	1.44	0.5	R315	75	0.013
Sub-24	8.27	0.5	R319	75	0.013
Sub-25	9.72	0.5	R325	75	0.013
Sub-26	8.73	0.5	R341	75	0.013
Sub-27	3.36	0.5	R299A	75	0.013
Sub-28	3.7	0.5	R302A	75	0.013

Sub-29	1.83	0.5	R294	75	0.013
Sub-30	3.82	0.5	R165	75	0.013
Sub-31	5.11	0.5	R168	75	0.013
Sub-32	3.64	0.5	R169	75	0.013
Sub-33	1.78	0.5	R16	75	0.013
Sub-34	2.28	0.5	R17	75	0.013
Sub-35	1.72	0.5	R21	75	0.013
Sub-36	2.14	0.5	R27	75	0.013
Sub-37	1.89	0.5	R121	75	0.013
Sub-38	1.95	0.5	R125	75	0.013
Sub-39	1.94	0.5	R129	75	0.013
Sub-40	1.42	0.5	R137	75	0.013
Sub-41	2.58	0.5	R171	75	0.013
Sub-42	2.62	0.5	R149	75	0.013
Sub-43	2.17	0.5	R141	75	0.013

APPENDIX B

Stormwater drainage system Data about the sewer manhole input into the model (GIS).

node ID	X Coordinate	Y Coordinate	Invert Elevation	Ground/Rim (Max) Elevation(m)	MAX depth (m)	Initial water Elevation(m)	Minimum Pipe Cover (m)	Surcharge Elevation (m)
M131	439131.34	3541394.01	40.3	41.7	1.4	40.3	1.09	41.7
M132	439149.57	3541349.82	40.2	41.3	1.1	40.2	0.79	41.3
M135	439206.78	3541211.16	39.4	41.6	2.2	39.4	1.6	41.6
M136	439225.2	3541166.51	39.3	41.6	2.3	39.3	1.7	41.6
M137	439244.66	3541119.37	39.2	41.8	2.6	39.2	2	41.8
M138	439263.73	3541073.15	39.1	41.7	2.6	39.1	2	41.7
M139	439282.8	3541026.93	38.9	41.6	2.7	38.9	2.1	41.6
M140	439301.87	3540980.71	38.8	41.6	2.8	38.8	2.2	41.6
M141	439320.94	3540934.49	38.7	41.8	3.1	38.7	2.5	41.8
M142	439340.01	3540888.27	38.6	41.8	3.2	38.6	2.6	41.8
M143	439357.67	3540845.47	38.4	41.9	3.5	38.4	2.9	41.9
M144	439378.15	3540795.83	38.3	41.9	3.6	38.3	3	41.9
M147	439495.59	3540775.51	37.9	41.5	3.6	37.9	2.1	41.5
M148	439541.82	3540794.54	37.7	41.1	3.4	37.2	1.9	41.1
M149	439588.05	3540813.58	37.6	41	3.4	37.6	2.8	41
M150	439634.29	3540832.62	37.5	40.7	3.2	37.5	2.6	40.7
M151	439681.45	3540852.04	37.4	40.6	3.2	37.4	2.6	40.6
M152	439724.91	3540869.93	37.3	40.4	3.1	37.3	2.5	40.4
R1	439084.32	3541510.69	39.5	41	1.5	39.5	1.19	41
R10	439234.53	3541728.59	37.6	39.6	2	34.8	1.5	37.6
R100	439849.37	3541620.67	36.6	38.1	1.5	36.6	1.19	38.1
R101	439886.35	3541635.9	36.5	38.1	1.6	36.5	1.29	38.1
R102	439923.34	3541651.14	36.4	37.9	1.5	36.4	1.19	37.9
R103	439960.32	3541666.38	36.2	37.8	1.6	36.2	1.29	37.8
R104	439997.31	3541681.61	36.1	37.4	1.3	36.1	0.99	37.4
R105	440034.29	3541696.85	35.8	37.4	1.6	35.8	1.29	37.4

R106	440071.28	3541712.09	35.8	37.4	1.6	35.8	1.29	37.4
R107	440112.88	3541729.23	35.7	37.3	1.6	35.7	1.29	37.3
R108	440132.9	3541680.69	35.5	37.3	1.8	35.5	1.49	37.3
R109	440148.16	3541643.72	35.4	37.5	2.1	35.4	1.79	37.5
R110	440163.41	3541606.74	35.3	37.7	2.4	35.3	2.09	37.7
R111	440177.67	3541572.17	35.1	37.7	2.6	35.1	2.29	37.7
R112	440192.77	3541535.56	34.9	37.8	2.9	34.9	2.59	37.8
R113	440209.24	3541495.62	34.8	37.8	3	34.8	2.69	37.8
R114	440224.42	3541458.83	34.7	37.8	3.1	34.7	2.79	37.8
R115	440233	3541438.03	34.3	37.7	3.4	34.3	2.8	37.7
R116	440273.85	3541454.33	34.2	37.6	3.4	34.2	2.8	37.6
R117	440315.46	3541470.93	34.1	37.2	3.1	34.2	2.4	37.2
R118	440359.39	3541488.46	34	37	3	34.1	2.3	37
R119	440400.26	3541504.76	33.9	36.9	3	34	2.3	36.9
R12	439268.06	3541742.15	37.5	39.5	2	37.5	1.4	39.5
R120	439624.41	3541889.15	36.5	38.3	1.8	36.5	1.49	38.3
R121	439689.49	3541819.51	37.1	38.8	1.7	37.1	1.39	38.8
R122	439672.71	3541860.19	36.6	38.6	2	36.6	1.69	38.6
R123	439655.47	3541901.97	36.4	38.3	1.9	36.4	1.59	38.3
R124	439691.52	3541916.85	36.3	38.2	1.9	36.3	1.59	38.2
R125	439757.53	3541845.21	36.8	38.6	1.8	36.8	1.49	38.6
R126	439740.75	3541885.89	36.5	38.3	1.8	36.5	1.49	38.3
R127	439722.67	3541929.71	36.1	38.1	2	36.1	1.69	38.1
R128	439757.52	3541944.09	36	38.1	2.1	36	1.7	38.1
R129	439823.35	3541874.98	36.6	38.2	1.6	36.6	1.29	38.2
R13	439303.89	3541757.14	37.4	39.5	2.1	37.4	1.5	39.5
R130	439806.23	3541916.48	36.4	38.1	1.7	36.4	1.39	38.1
R131	439789.41	3541957.25	35.9	38.1	2.2	35.9	1.8	38.1
R132	439818.99	3541969.46	35.8	37.9	2.1	35.8	1.7	37.9
R133	439168.64	3541303.6	40	41.3	1.3	40	0.99	41.3
R134	439187.71	3541257.38	39.8	41.5	1.7	39.8	1.39	41.5
R135	439857.63	3541985.41	35.7	37.8	2.1	35.7	1.7	37.8
R136	439887.4	3541997.68	35.6	37.6	2	35.6	1.6	37.6
R137	439955.54	3541930.57	36	37.5	1.5	36	1.19	37.5
R138	439938.71	3541971.79	35.8	37.6	1.8	35.8	1.49	37.6

R139	439922.27	3542012.07	35.5	37.5	2	35.5	1.6	37.5
R14	439338.1	3541771.22	37.3	39.4	2.1	37.3	1.5	39.4
R140	439954.51	3542025.37	35.4	37.3	1.9	35.4	1.5	37.3
R141	440019.2	3541964.54	35.8	37.4	1.6	35.8	1.29	37.4
R142	440003.87	3542001.7	35.5	37.3	1.8	35.5	1.49	37.3
R143	439988.35	3542039.33	35.3	37.2	1.9	35.3	1.5	37.2
R144	440024.86	3542054.39	35.2	37	1.8	35.2	1.4	37
R145	439402.63	3540737.24	38.1	41.6	3.5	38.1	2.9	41.6
R146	439449.35	3540756.47	38	41.5	3.5	38	2.9	41.5
R147	440057.31	3542067.77	35.1	36.9	1.8	35.1	1.4	36.9
R148	440086.43	3542079.78	35.1	36.6	1.5	35.1	1.1	36.6
R149	440152.68	3542021.98	35.2	36.8	1.6	35.2	1.29	36.8
R15	439379.71	3541788.35	37.2	39.2	2	37.2	1.4	39.2
R15.1	439400.15	3541738.8	37.2	39.4	2.2	37.2	1.6	39.4
R15.2	439422.16	3541685.46	37.1	39.5	2.4	37.1	1.8	39.5
R15.3	439445.04	3541629.99	37	39.5	2.5	37	1.9	39.5
R150	440137.69	3542058.31	35.1	36.5	1.4	35.1	1.09	36.5
R151	440122.67	3542094.73	35	36.5	1.5	35	1.1	36.5
R152	440158.91	3542109.68	34.9	36.5	1.6	34.9	1.2	36.5
R153	439771.14	3540888.97	37.2	40.3	3.1	37.2	2.5	40.3
R154	439818.3	3540908.39	37	40	3	37	2.4	40
R155	439865.46	3540927.81	36.9	39.9	3	36.9	2.4	39.9
R156	439909.38	3540945.89	36.8	39.7	2.9	36.8	2.3	39.7
R157	439956.54	3540965.31	36.7	39.5	2.8	36.7	2.2	39.5
R158	440002.77	3540984.35	36.5	39.4	2.9	36.5	2.3	39.4
R159	440049	3541003.39	36.4	39.3	2.9	36.4	2.3	39.3
R16	439417.54	3541803.77	37.5	39.2	1.7	37.5	1.39	39.2
R160	440095.24	3541022.42	36.3	39.1	2.8	36.3	2.2	39.1
R161	440141.47	3541041.46	37.2	38.8	1.6	37.2	1	38.8
R162	440185.86	3541059.74	36	38.7	2.7	36	2.1	38.7
R163	440233.02	3541079.16	35.9	38.5	2.6	35.9	2	38.5
R164	440279.25	3541098.19	35.8	38.5	2.7	35.8	2.1	38.5
R165	440325.48	3541117.23	35.7	38.3	2.6	35.7	2	38.3
R166	440371.72	3541136.27	35.5	38.2	2.7	35.5	2.1	38.2
R167	440417.95	3541155.31	35.4	37.9	2.5	35.4	1.9	37.9

R168	440465.11	3541174.73	35.3	37.8	2.5	35.3	1.9	37.8
R169	440521.51	3541197.95	35.1	37.7	2.6	35.1	2	37.7
R17	439486.79	3541738.56	37.4	39.4	2	37.4	1.69	39.4
R171	440194.96	3542124.55	34.8	36.4	1.6	34.8	1	36.4
R172	440207.58	3542092.47	34.6	36.4	1.8	34.6	1.2	36.4
R173	440218.45	3542066.12	34.6	36.3	1.7	34.6	1.1	36.3
R174	440231.23	3542035.15	34.5	36.3	1.8	34.5	1.2	36.3
R175	440242.67	3542007.42	34.5	36.3	1.8	34.5	1.2	36.3
R176	440256.78	3541973.22	34.4	36.2	1.8	34.4	1.2	36.2
R177	440274.95	3541929.17	34.3	36.3	2	34.3	1.4	36.3
R178	439699.86	3541648.86	37.5	38.9	1.4	37.5	1.09	38.9
R179	439736.83	3541664.13	37.3	38.7	1.4	37.3	1.09	38.7
R18	439468.68	3541782.47	37.2	39.3	2.1	37.2	1.79	39.3
R180	439773.8	3541679.4	37.2	38.6	1.4	37.2	1.09	38.6
R181	439810.77	3541694.67	37	38.5	1.5	37	1.19	38.5
R182	439847.74	3541709.94	36.9	38.2	1.3	36.9	0.99	38.2
R183	439880.09	3541723.3	36.8	38.2	1.4	36.8	1.09	38.2
R184	439921.68	3541740.48	36.6	38.1	1.5	36.6	1.19	38.1
R185	439958.66	3541755.73	36.5	38.1	1.6	36.5	1.29	38.1
R186	439995.64	3541770.97	36.3	37.9	1.6	36.3	1.29	37.9
R187	440032.16	3541786.03	36.1	37.6	1.5	36.1	1.19	37.6
R188	440069.14	3541801.27	35.9	37.3	1.4	35.9	1.09	37.3
R189	440106.12	3541816.52	35.8	37.1	1.3	35.8	0.99	37.1
R19	439453.73	3541818.71	37.1	39.2	2.1	37.1	1.79	39.2
R190	440143.1	3541831.77	35.6	37.1	1.5	35.6	1.19	37.1
R191	440180.08	3541847.01	35.5	36.9	1.4	35.5	1.09	36.9
R192	440217.06	3541862.26	35.4	36.8	1.4	35.4	1.09	36.8
R193	440254.04	3541877.5	35	36.6	1.6	35	1.29	36.6
R194	440290.1	3541892.37	34.3	36.3	2	34.3	1.4	36.3
R195	440304.19	3541858.26	34.2	36.3	2.1	34.2	1.5	36.3
R196	440321.2	3541817.03	34.1	36.3	2.2	34.1	1.6	36.3
R197	440344.58	3541760.36	34	36.4	2.4	34	1.8	36.4
R198	440364.03	3541713.22	34	36.3	2.3	34	1.7	36.3
R199	440380.04	3541674.39	33.4	36.3	2.9	33.4	2.3	36.3
R199.1	440426.79	3541693.5	33.3	36.2	2.9	33.3	2.3	36.2

R199.2	440477.5	3541714.39	33.2	36.1	2.9	33.2	2.3	36.1
R199.3	440534.54	3541737.9	33.1	36	2.9	33.1	2.3	36
R199.4	440591.59	3541761.42	33	35.7	2.7	33	2.1	35.7
R199.5	440640.22	3541781.47	32.9	35.5	2.6	32.9	2	35.5
R199.6	440688.43	3541801.34	32.8	35.3	2.5	32.8	1.9	35.3
R2	439065.25	3541556.91	39.1	40.8	1.7	39.1	1.39	40.8
R20	439493.48	3541835.12	37	39.1	2.1	37	1.79	39.1
R200	440397.7	3541634.22	34.4	36.6	2.2	35.9	0.38	36.6
R201	440413.45	3541596.04	34.2	36.4	2.2	35	1.09	36.4
R202	440429.2	3541557.86	34	36.6	2.6	34.6	1.69	36.6
R203	440444.15	3541521.86	33.8	36.7	2.9	33.1	2.2	36.7
R204	440458.65	3541486.45	33.7	36.6	2.9	33.8	2.2	36.6
R205	439407.55	3540993.91	39.7	41.1	1.4	39.7	1.09	41.1
R206	439443.48	3541008.29	39.5	41	1.5	39.5	1.19	41
R207	439479.69	3541022.77	39.4	41	1.6	39.4	1.29	41
R208	439517.11	3541037.74	39.3	40.8	1.5	39.3	1.19	40.8
R209	439553.5	3541052.3	39.2	40.5	1.3	39.2	0.99	40.5
R21	439556.19	3541764.9	37.5	39.1	1.6	37.5	1.29	39.1
R210	439590.64	3541067.16	39	40.6	1.6	39	1.29	40.6
R211	439627.78	3541082.02	38.4	40.2	1.8	38.4	1.49	40.2
R212	439725.29	3540950.59	39	40.6	1.6	39	1.29	40.6
R213	439709.77	3540988.22	38.8	40.5	1.7	38.8	1.39	40.5
R214	439694.52	3541025.19	38.7	40.3	1.6	38.7	1.29	40.3
R215	439680.03	3541060.32	38.4	40.3	1.9	38.4	1.59	40.3
R216	439664.96	3541096.84	38.3	40.2	1.9	38.3	1.59	40.2
R217	439388.14	3541021.34	39.8	41.2	1.4	39.8	1.09	41.2
R218	439419.2	3541034.15	39.6	41.1	1.5	39.6	1.19	41.1
R219	439452.29	3541047.8	39.5	41	1.5	39.5	1.19	41
R22	439539.36	3541805.7	37.4	38.9	1.5	37.4	1.19	38.9
R220	439487.24	3541062.22	39.4	40.9	1.5	39.4	1.19	40.9
R221	439520.33	3541075.87	39.3	40.8	1.5	39.3	1.19	40.8
R222	439553.24	3541089.45	39.2	40.6	1.4	39.2	1.09	40.6
R223	439586.06	3541102.98	39.1	40.5	1.4	39.1	1.09	40.5
R224	439618.04	3541116.18	38.9	40.4	1.5	38.9	1.19	40.4
R225	439651.32	3541129.9	38.1	40.4	2.3	38.1	1.99	40.4

R227	439708.93	3541135.78	38.5	40.1	1.6	38.5	1.29	40.1
R228	439758.43	3541156.06	38.3	40	1.7	38.3	1.39	40
R229	439793.22	3541170.32	38.2	39.9	1.7	38.2	1.39	39.9
R23	439522.32	3541847.02	36.8	38.9	2.1	36.8	1.79	38.9
R230	439820.98	3541181.7	38.1	39.8	1.7	38.1	1.39	39.8
R231	439858.27	3541196.98	38	39.6	1.6	38	1.29	39.6
R232	439891.31	3541210.52	37.8	39.5	1.7	37.8	1.39	39.5
R233	439926.47	3541224.92	37.7	39.3	1.6	37.7	1.29	39.3
R234	439958.21	3541237.93	37.6	39.3	1.7	37.6	1.39	39.3
R235	439990.59	3541251.2	37.5	39.2	1.7	37.5	1.39	39.2
R236	440022.61	3541264.32	37.4	39	1.6	37.4	1.29	39
R237	440052.68	3541276.64	37.3	38.8	1.5	37.3	1.19	38.8
R238	440086.46	3541290.48	37.1	38.8	1.7	37.1	1.39	38.8
R239	440118.1	3541303.45	37	38.6	1.6	37	1.29	38.6
R24	439559.11	3541862.2	36.7	38.7	2	36.7	1.69	38.7
R240	440150.77	3541316.84	36.9	38.6	1.7	36.9	1.39	38.6
R241	440183.15	3541330.11	36.8	38.5	1.7	36.8	1.39	38.5
R242	440214	3541342.5	36.7	0	-36.7	0	0	0
R243	440247	3541356.27	36.2	38.2	2	36.6	1.29	38.2
R244	440278.83	3541369.32	36.1	38.1	2	36.5	1.29	38.1
R245	440310.85	3541382.44	36	37.7	1.7	36.4	0.99	37.7
R246	440344.16	3541396.09	35.6	37.6	2	36	1.29	37.6
R247	440374.23	3541408.41	35.2	37.2	2	35.6	1.29	37.2
R248	440406.9	3541421.8	34.8	37.1	2.3	35.6	1.19	37.1
R249	440441.13	3541435.82	34.2	36.9	2.7	35.4	1.19	36.9
R25	439588.22	3541874.22	36.6	38.5	1.9	36.6	1.59	38.5
R250	440473.98	3541449.29	33.6	36.5	2.9	33.7	2.2	36.5
R252	440491.91	3541405.84	33.4	36.5	3.1	33.6	2.3	36.5
R253	440507.04	3541369.14	33.25	36.7	3.45	33.6	2.5	36.7
R254	440522.14	3541332.53	33.15	36.7	3.55	33.5	2.6	36.7
R255	440537.86	3541294.44	33.05	36.8	3.75	33.4	2.8	36.8
R256	440552.92	3541257.93	32.9	36.9	4	33.4	2.9	36.9
R26	439605.19	3541833.08	36.8	38.7	1.9	36.8	1.59	38.7
R27	439619.19	3541799.15	37.3	38.7	1.4	37.3	1.09	38.7
R285	440569.5	3541217.71	32.75	37.4	4.65	33.3	3.5	37.4

R286	440607.42	3541233.32	32.65	37.2	4.55	33.2	3.4	37.2
R287	440649.03	3541250.46	32.55	37	4.45	33.1	3.3	37
R288	440690.91	3541267.71	32.45	36.8	4.35	33	3.2	36.8
R289	440730.21	3541283.89	32.35	36.7	4.35	32.9	3.2	36.7
R290	440767.2	3541299.12	32.25	36.6	4.35	32.8	3.2	36.6
R291	440805.11	3541314.73	32.15	36.6	4.45	32.7	3.3	36.6
R292	440842.84	3541330.26	32	36.4	4.4	32.5	3.3	36.4
R293	440879.09	3541345.19	31.9	36.4	4.5	31.9	3.9	36.4
R294	440594.48	3542139.24	33.7	34.8	1.1	33.7	0.79	34.8
R295	440611.07	3542099.02	33.6	34.8	1.2	33.6	0.89	34.8
R296	440340.31	3541938.11	34.4	36	1.6	34.4	1.29	36
R296A	440299.54	3541921.3	34.6	36.2	1.6	34.6	1.29	36.2
R297	440381.72	3541955.2	34.3	35.9	1.6	34.3	1.29	35.9
R298	440403.45	3541964.16	34.1	35.7	1.6	34.1	1.29	35.7
R299	440425.17	3541973.12	34.1	35.7	1.6	34.1	1.29	35.7
R299A	440391.23	3542055.39	34.4	35.6	1.2	34.4	0.89	35.6
R299B	440408.77	3542012.87	34.2	35.7	1.5	34.2	1.19	35.7
R3	439046.37	3541602.67	39.1	40.8	1.7	39.1	1.39	40.8
R30	439495.54	3541564.55	38.2	39.6	1.4	38.2	1.09	39.6
R300	440472.24	3541992.53	34	35.5	1.5	34	1.19	35.5
R301	440515.31	3542010.3	33.8	35.5	1.7	33.8	1.39	35.5
R302	440557.1	3542027.54	33.7	35	1.3	33.7	0.99	35
R302A	440523.81	3542108.24	33.9	35.3	1.4	33.9	1.09	35.3
R302B	440540.21	3542068.49	33.8	35.2	1.4	33.8	1.09	35.2
R303	440590.52	3542041.33	33.6	35	1.4	33.6	1.09	35
R304	440628.42	3542056.96	33.2	34.7	1.5	33.2	1	34.7
R305	440320.67	3541885.45	34.9	36.5	1.6	34.9	1.29	36.5
R306	440353.03	3541898.79	34.8	36.1	1.3	34.8	0.99	36.1
R307	440385.47	3541912.18	34.7	36.1	1.4	34.7	1.09	36.1
R308	440418.29	3541925.72	34.6	35.9	1.3	34.6	0.99	35.9
R309	440449.45	3541938.57	33.7	0	-33.7	0	0	0
R31	439528.82	3541578.27	38.1	39.5	1.4	38.1	1.09	39.5
R310	440482.08	3541952.03	34.2	35.5	1.3	34.2	0.99	35.5
R311	440515.08	3541965.64	34.1	35.5	1.4	34.1	1.09	35.5
R312	440547.25	3541978.91	33.8	35.3	1.5	33.8	1.19	35.3

R313	440579.42	3541992.18	33.5	35	1.5	33.5	1.19	35
R314	440611.78	3542005.53	33.3	34.7	1.4	33.3	1.09	34.7
R315	440644.13	3542018.87	33.1	34.5	1.4	32.8	0.9	34.5
R316	440661.33	3541977.18	33	34.7	1.7	33	1.2	34.7
R317	440680.55	3541930.59	32.9	34.7	1.8	32.9	1.3	34.7
R318	440696.26	3541892.5	32.8	34.7	1.9	32.8	1.4	34.7
R319	440711.25	3541856.17	32.7	34.8	2.1	32.7	1.6	34.8
R32	439565.79	3541593.53	38	39.3	1.3	38	0.99	39.3
R320	440727.26	3541817.35	32.6	34.9	2.3	32.6	1.7	34.9
R321	440747.02	3541769.46	32.5	35.2	2.7	32.5	2.1	35.2
R322	440766.08	3541723.24	32.4	35.2	2.8	32.4	2.2	35.2
R323	440781.34	3541686.26	32.3	35.1	2.8	32.3	2.2	35.1
R324	440796.59	3541649.28	32.2	35.2	3	32.2	2.4	35.2
R325	440811.84	3541612.31	32.2	35.2	3	32.2	2.4	35.2
R326	440493.37	3541434.6	35.1	36.8	1.7	35.1	1.39	36.8
R327	440506.64	3541440.08	35	36.8	1.8	35	1.49	36.8
R328	440538.99	3541453.44	34.9	36.6	1.7	34.9	1.39	36.6
R329	440570.88	3541466.6	34.8	36.2	1.4	34.8	1.09	36.2
R33	439603.23	3541608.97	37.8	39.2	1.4	37.8	1.09	39.2
R330	440605.08	3541480.72	34.5	36.2	1.7	34.5	1.39	36.2
R331	440636.97	3541493.89	34.4	36.1	1.7	34.4	1.39	36.1
R332	440668.4	3541506.86	34.3	36.1	1.8	34.3	1.49	36.1
R333	440700.19	3541519.99	34.2	36	1.8	34.2	1.49	36
R334	440732.55	3541533.35	34.1	35.9	1.8	34.1	1.49	35.9
R335	440763.97	3541546.32	34	35.8	1.8	34	1.49	35.8
R336	440795.86	3541559.49	33.9	35.6	1.7	33.9	1.39	35.6
R337	440828.21	3541572.85	32.1	35.4	3.3	32.1	2.7	35.4
R338	440847.58	3541525.89	32	35.4	3.4	32	2.8	35.4
R339	440864.82	3541484.1	31.9	35.6	3.7	31.9	3.1	35.6
R34	439640.21	3541624.22	37.5	39	1.5	37.5	1.19	39
R340	440882.02	3541442.41	31.8	35.6	3.8	31.8	3.2	35.6
R341	440898.11	3541403.4	31.7	35.8	4.1	31.7	3.5	35.8
R342	440915.75	3541362.46	31.8	36	4.2	31.8	3.6	36
R35	439685.23	3541642.8	37.4	38.9	1.5	36.6	1.19	38.9
R35.1	439702.18	3541601.86	37.1	39	1.9	37.1	1.59	39

R36	439551.85	3541498.2	37.8	39.8	2	37.8	1.69	39.8
R37	439593.45	3541515.36	37.6	39	1.4	37.6	1.09	39
R38	439635.05	3541532.52	37.5	39	1.5	37.5	1.19	39
R39	439676.65	3541549.68	37.3	39	1.7	37.3	1.39	39
R4	439030.59	3541640.94	38.2	40.6	2.4	38.2	1.9	40.6
R40	439716.86	3541566.27	37	39	2	36.3	1.69	39
R41	439732.04	3541529.48	36.9	38.8	1.9	36.9	1.59	38.8
R42	439747.29	3541492.5	36.8	39	2.2	36.8	1.89	39
R43	439764.07	3541451.83	36.6	39.1	2.5	36.6	2.19	39.1
R44	439669.29	3541371.62	38.3	39.7	1.4	38.3	1.09	39.7
R45	439706.73	3541387.07	38.1	39.7	1.6	38.1	1.29	39.7
R46	439741.86	3541401.56	38	39.5	1.5	38	1.19	39.5
R47	439778.56	3541416.7	36.5	39.3	2.8	36.5	2.49	39.3
R48	439793.81	3541379.72	36.3	39.1	2.8	36.3	2.49	39.1
R49	439816.69	3541324.25	36.1	39.5	3.4	36.1	3.09	39.5
R4A	439012.65	3541632.32	38.2	40.7	2.5	38.2	2	40.7
R5	439066.98	3541658.2	38	40.3	2.3	38	1.8	40.3
R50	439206.67	3541475.96	39.3	40.7	1.4	39.3	1.09	40.7
R51	439242.72	3541490.83	38.6	40.6	2	38.6	1.69	40.6
R52	439279.05	3541505.81	38.5	40.2	1.7	38.5	1.39	40.2
R53	439316.49	3541521.26	38.4	40	1.6	38.4	1.29	40
R54	439353	3541536.32	38.2	39.9	1.7	38.2	1.39	39.9
R55	439391.65	3541552.26	38.1	39.7	1.6	38.1	1.29	39.7
R56	439426.77	3541566.75	37.4	39.5	2.1	37.4	1.79	39.5
R57	439464.68	3541582.38	36.8	39.5	2.7	36.8	2.1	39.5
R58	439250.57	3541443.22	39.2	40.4	1.2	39.2	0.89	40.4
R59	439282	3541456.19	39	40.2	1.2	39	0.89	40.2
R6	439097.21	3541672.07	37.9	40.1	2.2	37.9	1.7	40.1
R60	439315.28	3541469.92	38.6	40.1	1.5	38.6	1.19	40.1
R61	439347.63	3541483.26	38.4	40.1	1.7	38.4	1.39	40.1
R62	439379.99	3541496.61	38.3	39.9	1.6	38.3	1.29	39.9
R63	439412.34	3541509.96	38.2	39.7	1.5	38.2	1.19	39.7
R64	439444.7	3541523.3	38.1	39.5	1.4	38.1	1.09	39.5
R65	439482.6	3541538.94	36.6	39.3	2.7	36.6	2.1	39.3
R66	439500.45	3541495.65	36.5	39.6	3.1	36.5	2.5	39.6

R68	439524.1	3541438.33	36.4	39.7	3.3	36.4	2.7	39.7
R69	439548.5	3541379.17	36.3	39.7	3.4	36.3	2.8	39.7
R69.5	439017.36	3541622.71	38.3	40.6	2.3	38.3	1.8	40.6
R7	439134.2	3541687.29	37.8	40	2.2	37.8	1.7	40
R71	439242.09	3541204.09	39.5	41	1.5	39.5	1.19	41
R72	439272.8	3541216.76	39.4	41	1.6	39.4	1.29	41
R73	439309.96	3541232.09	39.3	40.9	1.6	39.3	1.29	40.9
R74	439347.12	3541247.42	39.2	40.6	1.4	39.2	1.09	40.6
R75	439383.64	3541262.48	39	40.4	1.4	39	1.09	40.4
R75.1	439170.7	3541196.36	39.6	41.8	2.2	39.6	1.6	41.8
R76	439420.62	3541277.74	38.9	40.3	1.4	38.9	1.09	40.3
R77	439457.13	3541292.8	37.9	40.2	2.3	37.9	1.99	40.2
R78	439492.54	3541307.41	37.8	40.1	2.3	37.8	1.99	40.1
R79	439529.24	3541322.54	37.7	40	2.3	37.7	1.99	40
R8	439165.64	3541700.23	37.8	40	2.2	37.8	1.7	40
R80	439565.66	3541337.57	36.2	39.7	3.5	37.6	2.9	39.7
R81	439587.63	3541284.32	36.1	39.8	3.7	36.1	3.1	39.8
R82	439606.35	3541238.93	36	40	4	36	3.4	40
R83	439624.39	3541195.21	35.9	40	4.1	35.9	3.5	40
R84	439664.88	3541211.36	35.8	39.9	4.1	35.8	3.5	39.9
R85	439707.14	3541228.22	35.8	39.8	4	35.8	3.4	39.8
R86	439750.38	3541245.47	35.7	39.6	3.9	35.7	3.3	39.6
R87	439792.41	3541262.24	35.6	39.4	3.8	35.6	3.2	39.4
R88	439835.23	3541279.33	35.5	39.4	3.9	35.5	3.3	39.4
R89	439863.15	3541290.47	35.5	39	3.5	35.5	2.9	39
R9	439199.86	3541714.32	37.7	39.8	2.1	37.7	1.6	39.8
R90	439900.3	3541305.29	35.4	38.6	3.2	35.4	2.6	38.6
R91	439942.1	3541321.97	35.3	38.6	3.3	35.3	2.7	38.6
R92	439982.04	3541337.9	35.3	38.6	3.3	35.3	2.7	38.6
R93	440023.83	3541354.58	35.2	38.4	3.2	35.2	2.6	38.4
R94	440064.7	3541370.88	35.1	38.2	3.1	35.1	2.5	38.2
R95	440107.43	3541387.93	35	38	3	35	2.4	38
R96	440148.29	3541404.23	35	37.9	2.9	35	2.3	37.9
R97	440189.35	3541420.61	34.9	37.9	3	34.9	2.4	37.9
R98	439775.4	3541590.2	36.9	38.2	1.3	36.9	0.99	38.2

R99	439812.38	3541605.43	36.8	38.1	1.3	36.8	0.99	38.1

APPENDIX C

Stormwater drainage system Data about the sewer pipes input into the model(GIS).

Link ID	From (Inlet) Node	To (Outlet) Node	Length (m)	Inlet Invert Elevation (m)	Outlet Invert Elevation (m)	Average Slope (%)	Pipe Diameter or Height (m)	Manning's Roughness
1	R1	R2	50	39.50	39.10	0.8	0.315	0.009
2	R2	R3	49.5	39.10	39. 01	0.09	0.315	0.009
3	R3	R4	41.35	39.10	38.20	0.2	0.315	0.009
4	R4	R5	47	38.20	38.00	0.43	0.5	0.009
5	R5	R6	32.5	38.00	37.90	0.31	0.5	0.009
6	R6	R7	40	37.90	37.80	0.25	0.5	0.009
7	R7	R8	34	37.80	37.79	0.01	0.5	0.009
8	R8	R9	37	37.80	37.70	0.27	0.5	0.009
9	R9	R10	37.5	37.70	37.60	0.27	0.5	0.009
10	R10	R12	37	37.60	37.50	0.27	0.5	0.009
11	R12	R13	38	37.50	37.40	0.26	0.6	0.009
12	R13	R14	37	37.40	37.30	0.27	0.6	0.009
13	R14	R15	45	37.30	37.20	0.22	0.6	0.009
15	R15	R15.1	53.6	37.20	37.19	0.01	0.6	0.009
15.1	R15.1	R15.2	57.7	37.20	37.10	0.17	0.6	0.009
15.2	R15.2	R15.3	60	37.10	37.00	0.17	0.6	0.009
15.3	R15.3	R57	51.5	37.00	36.80	0.39	0.6	0.009
16	R16	R19	38.9	37.50	37.10	0.2	0.315	0.009
17	R17	R18	47.5	37.40	37.20	0.42	0.315	0.009
18	R18	R19	39.2	37.20	37.10	0.26	0.315	0.009
19	R19	R20	43	37.10	37.00	0.23	0.315	0.009
20	R20	R23	31.2	37.00	36.80	0.64	0.315	0.009
21	R21	R22	43.4	37.50	37.40	0.23	0.315	0.009

22	R22	R23	44.7	37.40	36.80	0.2	0.315	0.009
23	R23	R24	39.8	36.8	36.7	0.25	0.315	0.009
24	R24	R25	31.5	36.70	36.60	0.32	0.315	0.009
25	R25	R120	36.9	36.60	36.50	0.27	0.315	0.009
26	R26	R25	44.5	36.80	36.60	0.45	0.315	0.009
27	R27	R26	36.7	37.30	36.80	0.2	0.315	0.009
30	R30	R31	36	38.20	38.10	0.28	0.315	0.009
31	R31	R32	40	38.10	38.00	0.25	0.315	0.009
32	R32	R33	40.5	38.00	37.80	0.49	0.315	0.009
33	R33	R34	40	37.80	37.50	0.75	0.315	0.009
34	R34	R35	48.7	37.50	37.40	0.21	0.315	0.009
35	R35	R35.1	42	37.40	37.10	0.71	0.315	0.009
35.1	R35.1	R40	38.5	37.10	37.00	0.26	0.315	0.009
36	R36	R37	45	37.80	37.60	0.44	0.315	0.009
37	R37	R38	45	37.60	37.50	0.22	0.315	0.009
38	R38	R39	45	37.50	37.30	0.44	0.315	0.009
39	R39	R40	43.5	37.30	37.00	0.69	0.315	0.009
40	R40	R41	39.8	37.00	36.90	0.25	0.315	0.009
41	R41	R42	40	36.90	36.80	0.25	0.315	0.009
42	R42	R43	44	36.80	36.60	0.45	0.315	0.009
43	R43	R47	38	36.60	36.50	0.26	0.315	0.009
44	R44	R45	40.5	38.30	38.10	0.49	0.315	0.009
45	R45	R46	38	38.10	38.00	0.26	0.315	0.009
46	R46	R47	39.7	38.00	36.50	3.78	0.315	0.009
47	R47	R48	40	36.50	36.30	0.5	0.315	0.009
48	R48	R49	60	36.30	36.10	0.33	0.315	0.009
49	R49	R88	48.6	36.10	35.50	1.23	0.315	0.009
50	R50	R51	39	39.30	38.60	1.79	0.315	0.009
51	R51	R52	39.3	38.60	38.50	0.25	0.315	0.009
52	R52	R53	40.5	38.50	38.40	0.25	0.315	0.009
53	R53	R54	39.5	38.40	38.20	0.51	0.315	0.009
54	R54	R55	41.8	38.20	38.10	0.24	0.315	0.009

55	R55	R56	38	38.10	37.40	0.2	0.315	0.009
56	R56	R57	41	37.40	36.80	0.2	0.315	0.009
57	R57	R65	47	36.80	36.60	0.43	0.6	0.009
58	R58	R59	34	39.20	39.00	0.59	0.315	0.009
59	R59	R60	36	39.00	38.60	0.2	0.315	0.009
60	R60	R61	35	38.60	38.40	0.57	0.315	0.009
61	R61	R62	35	38.40	38.30	0.29	0.315	0.009
62	R62	R63	35	38.30	38.20	0.29	0.315	0.009
63	R63	R64	35	38.20	38.10	0.29	0.315	0.009
64	R64	R65	41	38.10	36.60	3.66	0.315	0.009
65	R65	R66	50	36.60	36.50	0.2	0.6	0.009
66	R66	R68	62	36.50	36.40	0.16	0.6	0.009
68	R68	R69	64	36.40	36.30	0.16	0.6	0.009
69	R69	R80	45	36.30	36.20	0.22	0.6	0.009
69.5	R69.5	R4A	10.7	38.30	38.20	0.2	0.5	0.009
71	R71	R72	34.3	39.50	39.40	0.29	0.315	0.009
72	R72	R73	40.2	39.40	39.30	0.25	0.315	0.009
73	R73	R74	40.2	39.30	39.20	0.25	0.315	0.009
74	R74	R75	39.5	39.20	39.00	0.51	0.315	0.009
75	R75	R76	40	39.00	38.90	0.25	0.315	0.015
75.1	R75.1	M135	39	39.60	39.40	0.25	0.6	0.015
76	R76	R77	39.5	38.90	37.90	2.53	0.315	0.009
77	R77	R78	38.3	37.90	37.80	0.26	0.315	0.009
78	R78	R79	39.7	37.80	37.70	0.25	0.315	0.009
79	R79	R80	39.4	37.70	36.20	3.81	0.315	0.009
80	R80	R81	57.6	36.20	36.10	0.17	0.6	0.009
81	R81	R82	49.1	36.10	36.00	0.2	0.6	0.009
82	R82	R83	47.3	36.00	35.90	0.21	0.6	0.009
83	R83	R84	43.6	35.90	35.80	0.23	0.6	0.009
84	R84	R85	45.5	35.81	35.80	0.01	0.6	0.009
85	R85	R86	46.55	35.80	35.70	0.21	0.6	0.009
86	R86	R87	45.25	35.70	35.60	0.22	0.6	0.009

87	R87	R88	46.1	35.60	35.50	0.22	0.6	0.009
88	R88	R89	32.7	35.51	35.50	0.01	0.6	0.009
89	R89	R90	40	35.50	35.40	0.25	0.6	0.009
90	R90	R91	45	35.40	35.30	0.22	0.6	0.009
91	R91	R92	43	35.30	35.29	0.01	0.6	0.009
92	R92	R93	45	35.30	35.20	0.22	0.6	0.009
93	R93	R94	44	35.20	35.10	0.23	0.6	0.009
94	R94	R95	46	35.10	35.00	0.22	0.6	0.009
95	R95	R96	44	35.01	35.00	0.01	0.6	0.009
96	R96	R97	44.2	35.00	34.90	0.23	0.6	0.009
97	R97	R115	47	34.90	34.30	1.28	0.6	0.009
98	R98	R99	40	36.90	36.80	0.25	0.315	0.009
99	R99	R100	40	36.80	36.60	0.5	0.315	0.009
100	R100	R101	40	36.60	36.50	0.25	0.315	0.009
101	R101	R102	40	36.50	36.40	0.25	0.315	0.009
102	R102	R103	40	36.40	36.20	0.5	0.315	0.009
103	R103	R104	40	36.20	36.10	0.25	0.315	0.009
104	R104	R105	40	36.10	35.80	0.75	0.315	0.009
105	R105	R106	40	35.80	35.80	0.01	0.315	0.009
106	R106	R107	45	35.80	35.70	0.22	0.315	0.009
107	R107	R108	52.5	35.70	35.50	0.38	0.315	0.009
108	R108	R109	40	35.50	35.40	0.25	0.315	0.009
109	R109	R110	40	35.40	35.30	0.25	0.315	0.009
110	R110	R111	37.4	35.30	35.10	0.53	0.315	0.009
111	R111	R112	39.6	35.10	34.90	0.51	0.315	0.009
112	R112	R113	43.2	34.90	34.80	0.23	0.315	0.009
113	R113	R114	39.8	34.80	34.70	0.25	0.315	0.009
114	R114	R115	22.5	34.70	34.30	1.78	0.315	0.009
115	R115	R116	42.5	34.30	34.20	0.24	0.6	0.009
116	R116	R117	44.8	34.20	34.19	0.01	0.6	0.009
117	R117	R118	47.3	34.20	34.10	0.21	0.6	0.009
118	R118	R119	44	34.10	34.00	0.23	0.6	0.009

119	R119	R203	47	34.00	33.90	0.21	0.6	0.009
120	R120	R123	33.6	36.50	36.40	0.3	0.315	0.009
121	R121	R122	44	37.10	36.60	1.14	0.315	0.009
122	R122	R123	45.2	36.60	36.40	0.44	0.315	0.009
123	R123	R124	39	36.40	36.30	0.26	0.315	0.009
124	R124	R127	33.7	36.30	36.10	0.59	0.315	0.009
125	R125	R126	44	36.80	36.50	0.68	0.315	0.009
126	R126	R127	47.4	36.50	36.10	0.84	0.315	0.009
127	R127	R128	37.7	36.10	36.00	0.27	0.315	0.009
128	R128	R131	34.5	36.00	35.90	0.29	0.4	0.009
129	R129	R130	44.9	36.60	36.40	0.45	0.315	0.009
130	R130	R131	44.1	36.40	35.90	1.13	0.315	0.009
131	R131	R132	32	35.90	35.80	0.31	0.4	0.009
132	R132	R135	41.8	35.80	35.70	0.24	0.4	0.009
133	R133	R134	50	40.00	39.80	0.4	0.315	0.009
134	R134	M135	50	39.80	39.40	0.8	0.315	0.009
135	R135	R136	32.2	35.70	35.60	0.31	0.4	0.009
136	R136	R139	40.6	35.60	35.50	0.25	0.4	0.009
137	R137	R138	44.5	36.00	35.80	0.45	0.315	0.009
138	R138	R139	43.5	35.80	35.50	0.69	0.315	0.009
139	R139	R140	32	35.50	35.40	0.31	0.4	0.009
140	R140	R143	36.6	35.40	35.30	0.27	0.4	0.009
141	R141	R142	40.2	35.80	35.50	0.75	0.315	0.009
142	R142	R143	40.7	35.50	35.30	0.49	0.315	0.009
143	R143	R144	39.5	35.30	35.20	0.25	0.4	0.009
144	R144	R147	35.1	35.20	35.10	0.28	0.4	0.009
145	R145	R146	45.5	38.10	38.00	0.22	0.6	0.009
146	R146	M147	50	38.00	37.90	0.2	0.6	0.009
147	R147	R148	31.5	35.10	35.09	0.01	0.4	0.009
148	R148	R151	39.2	35.10	35.00	0.26	0.4	0.009
149	M149	M150	50	37.60	37.50	0.2	0.6	0.009
150	M150	M151	51	37.50	37.40	0.2	0.6	0.009

151	R151	R152	39.2	35.00	34.90	0.26	0.4	0.009
152	R152	R171	39	34.90	34.80	0.26	0.4	0.009
153	R153	R154	51	37.20	37.00	0.39	0.6	0.009
154	R154	R155	51	37.00	36.90	0.2	0.6	0.009
155	R155	R156	47.5	36.90	36.80	0.21	0.6	0.009
156	R156	R157	51	36.80	36.70	0.2	0.6	0.009
157	R157	R158	50	36.70	36.50	0.4	0.6	0.009
158	R158	R159	50	36.50	36.40	0.2	0.6	0.009
159	R159	R160	50	36.40	36.30	0.2	0.6	0.009
160	R160	R161	50	36.30	37.20	0.4	0.6	0.009
161	R161	R162	48	37.20	36.00	2.5	0.6	0.009
162	R162	R163	51	36.00	35.90	0.2	0.6	0.009
163	R163	R164	50	35.90	35.80	0.2	0.6	0.009
164	R164	R165	50	35.80	35.70	0.2	0.6	0.009
165	R165	R166	50	35.70	35.50	0.4	0.6	0.009
166	R166	R167	50	35.50	35.40	0.2	0.6	0.009
167	R167	R168	51	35.40	35.30	0.2	0.6	0.009
168	R168	R169	60	35.30	35.10	0.33	0.6	0.009
169	R169	R285	51.9	35.10	33.30	3.47	0.6	0.009
171	R171	R172	30	34.80	34.60	0.67	0.6	0.009
172	R172	R173	28.5	34.60	34.59	0.01	0.6	0.009
173	R173	R174	33.5	34.60	34.50	0.3	0.6	0.009
174	R174	R175	30	34.50	34.49	0.01	0.6	0.009
175	R175	R176	37	34.50	34.40	0.27	0.6	0.009
176	R176	R177	47.65	34.40	34.30	0.21	0.6	0.009
177	R177	R194	41.2	34.30	34.29	0.01	0.6	0.009
178	R178	R179	40	37.50	37.30	0.5	0.315	0.009
179	R179	R180	40	37.30	37.20	0.25	0.315	0.009
180	R180	R181	40	37.20	37.00	0.5	0.315	0.009
181	R181	R182	40	37.00	36.90	0.25	0.315	0.009
182	R182	R183	35	36.90	36.80	0.29	0.315	0.009
183	R183	R184	45	36.80	36.60	0.44	0.315	0.009

184	R184	R185	40	36.60	36.50	0.25	0.315	0.009
185	R185	R186	40	36.50	36.30	0.5	0.315	0.009
186	R186	R187	39.5	36.30	36.10	0.51	0.315	0.009
187	R187	R188	40	36.10	35.90	0.5	0.315	0.009
188	R188	R189	40	35.90	35.80	0.25	0.315	0.009
189	R189	R190	40	35.80	35.60	0.5	0.315	0.009
190	R190	R191	40	35.60	35.50	0.25	0.315	0.009
191	R191	R192	40	35.50	35.40	0.25	0.315	0.009
192	R192	R193	40	35.40	35.00	1	0.315	0.009
193	R193	R194	39	35.00	34.30	1.79	0.315	0.009
194	R194	R195	35.5	34.30	34.20	0.28	0.6	0.009
195	R195	R196	44.6	34.20	34.10	0.22	0.6	0.009
196	R196	R197	61.3	34.10	34.00	0.16	0.6	0.009
197	R197	R198	51	34.01	34.00	0.01	0.6	0.009
198	R198	R199	42	34.00	33.40	1.43	0.6	0.009
199	R199	R199.1	50.5	33.40	33.30	0.2	0.6	0.009
199	R199.1	R199.2	54.85	33.30	33.20	0.18	0.6	0.009
199	R199.2	R199.3	61.7	33.20	33.10	0.16	0.6	0.009
199	R199.3	R199.4	61.7	33.10	33.00	0.16	0.6	0.009
199	R199.4	R199.5	52.6	33.00	32.90	0.19	0.6	0.009
200	R199.5	R199.6	52.15	32.90	32.80	0.19	0.6	0.009
200	R199.6	R320	42	32.80	32.60	0.48	0.6	0.009
200	R200	R201	41.3	35.90	35.00	2.18	0.315	0.009
201	R201	R202	41.3	35.00	34.60	0.97	0.315	0.009
202	R202	R203	38.6	34.60	33.90	1.81	0.315	0.009
203	R203	R204	42.9	33.90	33.80	0.23	0.6	0.009
204	R204	R250	40.2	33.80	33.70	0.25	0.6	0.009
205	R205	R206	38.7	39.70	39.50	0.52	0.315	0.009
206	R206	R207	39	39.50	39.40	0.26	0.315	0.009
207	R207	R208	40.3	39.40	39.30	0.25	0.315	0.009
208	R208	R209	39.2	39.30	39.20	0.26	0.315	0.009
209	R209	R210	40	39.20	39.00	0.5	0.315	0.009

210	R210	R211	40	39.00	38.40	1.5	0.315	0.009
211	R211	R216	40	38.40	38.30	0.25	0.315	0.009
212	R212	R213	41	39.00	38.80	0.49	0.315	0.009
213	R213	R214	40	38.80	38.70	0.25	0.315	0.009
214	R214	R215	38	38.70	38.40	0.79	0.315	0.009
215	R215	R216	39.5	38.40	38.30	0.25	0.315	0.009
216	R216	R225	43	38.30	38.10	0.47	0.315	0.009
217	R217	R218	33.6	39.80	39.60	0.6	0.315	0.009
218	R218	R219	35.8	39.60	39.50	0.28	0.315	0.009
219	R219	R220	37.8	39.50	39.40	0.26	0.315	0.009
220	R220	R221	35.8	39.40	39.30	0.28	0.315	0.009
221	R221	R222	35.6	39.30	39.20	0.28	0.315	0.009
222	R222	R223	35.5	39.20	39.10	0.28	0.315	0.009
223	R223	R224	34.6	39.10	38.90	0.58	0.315	0.009
224	R224	R225	36	38.90	38.10	2.22	0.315	0.009
225	R225	R83	65	38.10	35.90	3.38	0.315	0.009
227	R227	R228	53.5	38.50	38.30	0.37	0.315	0.009
228	R228	R229	37.6	38.30	38.20	0.27	0.315	0.009
229	R229	R230	30	38.20	38.10	0.33	0.315	0.009
230	R230	R231	40.3	38.10	38.00	0.25	0.315	0.009
231	R231	R232	35.7	38.00	37.80	0.56	0.315	0.009
232	R232	R233	38	37.80	37.70	0.26	0.315	0.009
233	R233	R234	34.3	37.70	37.60	0.29	0.315	0.009
234	R234	R235	35	37.60	37.50	0.29	0.315	0.009
235	R235	R236	34.6	37.50	37.40	0.29	0.315	0.009
236	R236	R237	32.5	37.40	37.30	0.31	0.315	0.009
237	R237	R238	36.5	37.30	37.10	0.55	0.315	0.009
238	R238	R239	34.2	37.10	37.00	0.29	0.315	0.009
239	R239	R240	35.3	37.00	36.90	0.28	0.315	0.009
240	R240	R241	35	36.90	36.80	0.29	0.315	0.009
241	R241	R242	34	36.80	36.70	0.29	0.315	0.009
242	R242	R243	35	36.70	36.60	0.29	0.315	0.009

243	R243	R244	34.4	36.60	36.50	0.29	0.315	0.009
244	R244	R245	34.6	36.50	36.40	0.29	0.315	0.009
245	R245	R246	36	36.40	36.00	1.11	0.315	0.009
246	R246	R247	32.5	36.00	35.60	1.23	0.315	0.009
247	R247	R248	35.3	35.60	35.59	0.01	0.315	0.009
248	R248	R249	37	35.60	35.40	0.54	0.315	0.009
249	R249	R250	35.5	35.40	33.70	4.79	0.315	0.009
250	R250	R252	47	33.70	33.60	0.21	0.6	0.009
252	R252	R253	39.7	33.60	33.59	0.01	0.6	0.009
253	R253	R254	39.6	33.60	33.50	0.25	0.6	0.009
254	R254	R255	41.2	33.50	33.40	0.24	0.6	0.009
255	R255	R256	39.5	33.41	33.40	0.01	0.6	0.009
256	R256	R285	43.5	33.40	33.30	0.23	0.6	0.009
285	R285	R286	41	33.30	33.20	0.24	0.6	0.009
286	R286	R287	45	33.20	33.10	0.22	0.6	0.009
287	R287	R288	45.3	33.10	33.00	0.22	0.6	0.009
288	R288	R289	42.5	33.00	32.90	0.24	0.6	0.009
289	R289	R290	40	32.90	32.80	0.25	0.6	0.009
290	R290	R291	41	32.80	32.70	0.24	0.6	0.009
291	R291	R292	40.8	32.70	32.50	0.49	0.6	0.009
292	R292	R293	39.2	32.50	31.90	1.53	0.6	0.009
293	R293	R342	39.7	31.90	31.80	0.25	0.6	0.009
294	R294	R295	43.5	33.70	33.60	0.23	0.315	0.009
295	R295	R304	45.5	33.60	33.20	0.88	0.315	0.009
296	R296	R297	44.8	34.40	34.30	0.22	0.315	0.009
296A	R296A	R296	44.1	34.60	34.40	0.45	0.315	0.009
297	R297	R298	23.5	34.30	34.10	0.85	0.315	0.009
298	R298	R299	23.5	34.11	34.10	0.01	0.315	0.009
299	R299	R300	29.5	34.10	34.00	0.34	0.315	0.009
299A	R299A	R299B	46	34.40	34.20	0.43	0.315	0.009
299B	R299B	R299	43	34.20	34.10	0.23	0.315	0.009
300	R300	R301	46.6	34.00	33.80	0.43	0.315	0.009

301	R301	R302	45.2	33.80	33.70	0.22	0.315	0.009
302	R302	R303	31.4	33.70	33.60	0.32	0.315	0.009
302A	R302A	R302B	43	33.90	33.80	0.23	0.315	0.009
302B	R302B	R302	44.3	33.80	33.70	0.23	0.315	0.009
303	R303	R304	41	33.60	33.20	0.98	0.315	0.009
304	R304	R315	41.2	33.20	33.10	0.24	0.5	0.009
305	R305	R306	35	34.90	34.80	0.29	0.315	0.009
306	R306	R307	35.1	34.80	34.70	0.28	0.315	0.009
307	R307	R308	35.5	34.70	34.60	0.28	0.315	0.009
309	R310	R309	35.3	34.20	33.70	1.42	0.315	0.009
310	R310	R311	35.7	34.20	34.10	0.28	0.315	0.009
311	R311	R312	34.8	34.10	33.80	0.86	0.315	0.009
312	R312	R313	34.8	33.80	0.00	0.86	0.315	0.009
313	R313	R314	35	33.50	33.30	0.57	0.315	0.009
314	R314	R315	35	33.30	33.10	0.57	0.315	0.009
315	R315	R316	45.1	33.10	33.00	0.22	0.5	0.009
316	R316	R317	50.4	33.00	32.90	0.2	0.5	0.009
317	R317	R318	41.2	32.90	32.80	0.24	0.5	0.009
318	R318	R319	39.3	32.80	32.70	0.25	0.5	0.009
319	R319	R320	42	32.70	32.60	0.24	0.5	0.009
320	R320	R321	51.8	32.60	32.50	0.19	0.6	0.009
321	R321	R322	50	32.50	32.40	0.2	0.6	0.009
322	R322	R323	40	32.40	32.30	0.25	0.6	0.009
323	R323	R324	40	32.30	32.20	0.25	0.6	0.009
324	R324	R325	40	32.20	32.20	0.01	0.6	0.009
325	R325	R337	44.3	32.20	32.10	0.23	0.6	0.009
326	R326	R327	34.5	35.10	35.00	0.29	0.315	0.009
327	R327	R328	34.5	35.00	34.90	0.29	0.315	0.009
328	R328	R329	34.5	34.90	34.80	0.29	0.315	0.009
329	R329	R330	37	34.80	34.50	0.81	0.315	0.009
330	R330	R331	34.5	34.50	34.40	0.29	0.315	0.009
331	R331	R332	34	34.40	34.30	0.29	0.315	0.009

332	R332	R333	34.4	34.30	34.20	0.29	0.315	0.009
333	R333	R334	35	34.20	34.10	0.29	0.315	0.009
334	R334	R335	34	34.10	34.00	0.29	0.315	0.009
335	R335	R336	34.5	34.00	33.90	0.29	0.315	0.009
336	R336	R337	39	33.90	32.10	4.62	0.315	0.009
337	R337	R338	50.8	32.10	32.00	0.2	0.6	0.009
338	R338	R339	45.2	32.00	31.90	0.22	0.6	0.009
339	R339	R340	45.1	31.90	31.80	0.22	0.6	0.009
340	R340	R341	42.2	31.80	31.70	0.24	0.6	0.009
341	R341	R342	45	31.70	31.80	0.22	0.6	0.009
4A	R4A	R4	15	38.21	38.20	0.01	0.5	0.009
Link-07	R149	R150	39.3	35.20	35.10	0.25	0.315	0.009
Link-08	R150	R151	39.4	35.10	35.00	0.25	0.315	0.009
Link-22	R309	R308	33.7	33.70	34.60	0.5	0.315	0.009
Link-23	R309	R310	35.3	33.70	34.20	0.5	0.315	0.009
Link-24	R342	OUTLET	83.01	31.80	30.80	1.2	0.6	0.009
P131	M131	M132	47.8	40.30	40.20	0.21	0.315	0.009
P132	M132	R133	50	40.20	40.00	0.4	0.315	0.009
P135	M135	M136	48.3	39.40	39.30	0.21	0.6	0.009
P136	M136	M137	51	39.30	39.20	0.2	0.6	0.009
P137	M137	M138	50	39.20	39.10	0.2	0.6	0.009
P138	M138	M139	50	39.10	38.90	0.4	0.6	0.009
P139	M139	M140	50	38.90	38.80	0.2	0.6	0.009
P140	M140	M141	50	38.80	38.70	0.2	0.6	0.009
P141	M141	M142	50	38.70	38.60	0.2	0.6	0.009
P142	M142	M143	46.3	38.60	38.40	0.43	0.6	0.009
P143	M143	M144	53.7	38.40	38.30	0.19	0.6	0.009
P144	M144	R145	54.5	38.30	38.10	0.37	0.6	0.009
P147	M147	M148	49.99	37.90	37.70	0.4	1.5	0.009
P148	M148	M149	50	37.70	37.60	0.2	0.6	0.009
P151	M151	M152	47	37.40	37.30	0.21	0.6	0.009
P152	M152	R153	50	37.30	37.20	0.2	0.6	0.009

APPENDIX D

Table showing the data and matching to find the values of NMSE and R

ID	Peak	Design	Co avg	CO-Coavg	CP avg	CP-CPavg	(CO-CO avg) *(Cp-CP avg)	(C0-Cp)2	CoCp
	Flow	Flow							
		Capacity							
	O	P							
	co	cp							
10	0.230	0.28	0.22	0.010	0.224507	0.06	0.000542424	0.0025	0.0644
11	0.354	0.46	0.22	0.134	0.224507	0.24	0.031502988	0.011236	0.1628
12	0.384	0.46	0.22	0.164	0.224507	0.24	0.038567776	0.005776	0.1766
13	0.375	0.42	0.22	0.155	0.224507	0.20	0.030257354	0.002025	0.1575
16	0.468	0.36	0.22	0.248	0.224507	0.14	0.03357172	0.011664	0.1685
17	0.481	0.55	0.22	0.261	0.224507	0.33	0.084880311	0.004761	0.2646
20	0.064	0.08	0.22	-0.156	0.224507	-0.14	0.022575664	0.000256	0.0051
22	0.097	0.13	0.22	-0.123	0.224507	-0.09	0.011645664	0.001089	0.0126
23	0.089	0.08	0.22	-0.131	0.224507	-0.14	0.018962988	8.1E-05	0.0071
24	0.051	0.18	0.22	-0.169	0.224507	-0.04	0.00753172	0.016641	0.0092
25	0.097	0.08	0.22	-0.123	0.224507	-0.14	0.017806931	0.000289	0.0078
26	0.094	0.09	0.22	-0.126	0.224507	-0.13	0.016978199	0.000016	0.0085
34	0.089	0.07	0.22	-0.131	0.224507	-0.15	0.020275241	0.000361	0.0062
36	0.093	0.08	0.22	-0.127	0.224507	-0.14	0.018384959	0.000169	0.0074
38	0.113	0.08	0.22	-0.107	0.224507	-0.14	0.015494818	0.001089	0.009
39	0.112	0.11	0.22	-0.108	0.224507	-0.11	0.012392565	4E-06	0.0123
40	0.113	0.13	0.22	-0.107	0.224507	-0.09	0.010133551	0.000289	0.0147
41	0.070	0.08	0.22	-0.150	0.224507	-0.14	0.021708621	1E-04	0.0056
42	0.061	0.08	0.22	-0.159	0.224507	-0.14	0.023009185	0.000361	0.0049
44	0.061	0.08	0.22	-0.159	0.224507	-0.14	0.023009185	0.000361	0.0049
50	0.148	0.18	0.22	-0.072	0.224507	-0.04	0.003214537	0.001024	0.0266
54	0.109	0.11	0.22	-0.111	0.224507	-0.11	0.012736086	0.000001	0.012
59	0.124	0.12	0.22	-0.096	0.224507	-0.10	0.010056227	0.000016	0.0149
60	0.124	0.17	0.22	-0.096	0.224507	-0.05	0.005244959	0.002116	0.0211
61	0.123	0.12	0.22	-0.097	0.224507	-0.10	0.010160734	9E-06	0.0148
66	0.291	0.40	0.22	0.071	0.224507	0.18	0.012420452	0.011881	0.1164
67	0.282	0.36	0.22	0.062	0.224507	0.14	0.00837003	0.006084	0.1015
68	0.358	0.35	0.22	0.138	0.224507	0.13	0.017289748	6.4E-05	0.1253
69	0.357	0.42	0.22	0.137	0.224507	0.20	0.02673848	0.003969	0.1499
74	0.113	0.11	0.22	-0.107	0.224507	-0.11	0.012278058	9E-06	0.0124
78	0.114	0.08	0.22	-0.106	0.224507	-0.14	0.015350311	0.001156	0.0091
79	0.114	0.08	0.22	-0.106	0.224507	-0.14	0.015350311	0.001156	0.0091
84	0.349	0.42	0.22	0.129	0.224507	0.20	0.025174537	0.005041	0.1466

90	0.474	0.44	0.22	0.254	0.224507	0.22	0.054686649	0.001156	0.2086
93	0.434	0.42	0.22	0.214	0.224507	0.20	0.041791438	0.000196	0.1823
94	0.446	0.42	0.22	0.226	0.224507	0.20	0.044137354	0.000676	0.1873
100	0.122	0.11	0.22	-0.098	0.224507	-0.11	0.011247495	0.000144	0.0134
103	0.114	0.11	0.22	-0.106	0.224507	-0.11	0.012163551	0.000016	0.0125
108	0.100	0.10	0.22	-0.120	0.224507	-0.12	0.014968903	0	0.01
109	0.098	0.08	0.22	-0.122	0.224507	-0.14	0.017662424	0.000324	0.0078
110	0.096	0.08	0.22	-0.124	0.224507	-0.14	0.017951438	0.000256	0.0077
111	0.095	0.12	0.22	-0.125	0.224507	-0.10	0.013086931	0.000625	0.0114
112	0.095	0.11	0.22	-0.125	0.224507	-0.11	0.014339185	0.000225	0.0105
113	0.090	0.08	0.22	-0.130	0.224507	-0.14	0.01881848	1E-04	0.0072
114	0.072	0.08	0.22	-0.148	0.224507	-0.14	0.021419607	6.4E-05	0.0058
116	0.490	0.43	0.22	0.270	0.224507	0.21	0.05543679	0.0036	0.2107
118	0.455	0.41	0.22	0.235	0.224507	0.19	0.043549044	0.002025	0.1866
119	0.427	0.42	0.22	0.207	0.224507	0.20	0.040422988	4.9E-05	0.1793
120	0.411	0.41	0.22	0.191	0.224507	0.19	0.035387354	0.000001	0.1685
121	0.106	0.09	0.22	-0.114	0.224507	-0.13	0.015364114	0.000256	0.0095
123	0.098	0.11	0.22	-0.122	0.224507	-0.11	0.013995664	0.000144	0.0108
125	0.142	0.12	0.22	-0.078	0.224507	-0.10	0.0081751	0.000484	0.017
126	0.108	0.13	0.22	-0.112	0.224507	-0.09	0.010606086	0.000484	0.014
130	0.085	0.11	0.22	-0.135	0.224507	-0.11	0.015484255	0.000625	0.0094
132	0.208	0.17	0.22	-0.012	0.224507	-0.05	0.000666368	0.001444	0.0354
133	0.206	0.15	0.22	-0.014	0.224507	-0.07	0.001059889	0.003136	0.0309
134	0.085	0.10	0.22	-0.135	0.224507	-0.12	0.016836509	0.000225	0.0085
136	0.204	0.17	0.22	-0.016	0.224507	-0.05	0.000884396	0.001156	0.0347
138	0.083	0.11	0.22	-0.137	0.224507	-0.11	0.015713269	0.000729	0.0091
140	0.201	0.17	0.22	-0.019	0.224507	-0.05	0.001047917	0.000961	0.0342
141	0.167	0.16	0.22	-0.053	0.224507	-0.06	0.00343341	4.9E-05	0.0267
144	0.196	0.15	0.22	-0.024	0.224507	-0.07	0.001804959	0.002116	0.0294
145	0.180	0.16	0.22	-0.040	0.224507	-0.06	0.002594818	0.0004	0.0288
149	0.177	0.15	0.22	-0.043	0.224507	-0.07	0.003220593	0.000729	0.0266
155	0.315	0.39	0.22	0.095	0.224507	0.17	0.015684537	0.005625	0.1229
156	0.313	0.41	0.22	0.093	0.224507	0.19	0.017209044	0.009409	0.1283
157	0.311	0.39	0.22	0.091	0.224507	0.17	0.015022565	0.006241	0.1213
159	0.317	0.40	0.22	0.097	0.224507	0.18	0.016983269	0.006889	0.1268
160	0.299	0.40	0.22	0.079	0.224507	0.18	0.013824396	0.010201	0.1196
163	0.394	0.39	0.22	0.174	0.224507	0.17	0.02875848	0.000016	0.1537
164	0.333	0.40	0.22	0.113	0.224507	0.18	0.019791157	0.004489	0.1332
165	0.334	0.40	0.22	0.114	0.224507	0.18	0.019966649	0.004356	0.1336
166	0.431	0.56	0.22	0.211	0.224507	0.34	0.07071341	0.016641	0.2414
167	0.431	0.40	0.22	0.211	0.224507	0.18	0.036989466	0.000961	0.1724
168	0.431	0.39	0.22	0.211	0.224507	0.17	0.03488172	0.001681	0.1681
169	0.583	0.51	0.22	0.363	0.224507	0.29	0.103569607	0.005329	0.2973
175	0.349	0.46	0.22	0.129	0.224507	0.24	0.030325523	0.012321	0.1605
176	0.350	0.41	0.22	0.130	0.224507	0.19	0.024072283	0.0036	0.1435
178	0.119	0.11	0.22	-0.101	0.224507	-0.11	0.011591016	8.1E-05	0.0131
180	0.119	0.11	0.22	-0.101	0.224507	-0.11	0.011591016	8.1E-05	0.0131

181	0.119	0.08	0.22	-0.101	0.224507	-0.14	0.014627776	0.001521	0.0095
182	0.119	0.09	0.22	-0.101	0.224507	-0.13	0.013615523	0.000841	0.0107
183	0.115	0.11	0.22	-0.105	0.224507	-0.11	0.012049044	0.000025	0.0127
184	0.115	0.08	0.22	-0.105	0.224507	-0.14	0.015205804	0.001225	0.0092
185	0.111	0.11	0.22	-0.109	0.224507	-0.11	0.012507072	0.000001	0.0122
186	0.109	0.11	0.22	-0.111	0.224507	-0.11	0.012736086	0.000001	0.012
187	0.107	0.11	0.22	-0.113	0.224507	-0.11	0.0129651	9E-06	0.0118
189	0.100	0.11	0.22	-0.120	0.224507	-0.11	0.013766649	1E-04	0.011
194	0.466	0.47	0.22	0.246	0.224507	0.25	0.060335945	1.6E-05	0.219
195	0.458	0.42	0.22	0.238	0.224507	0.20	0.046483269	0.001444	0.1924
199	0.476	0.39	0.22	0.256	0.224507	0.17	0.042328903	0.007396	0.1856
200	0.466	0.38	0.22	0.246	0.224507	0.16	0.038216227	0.007396	0.1771
201	0.367	0.36	0.22	0.147	0.224507	0.14	0.019886931	4.9E-05	0.1321
202	0.355	0.36	0.22	0.135	0.224507	0.14	0.018261016	0.000025	0.1278
203	0.355	0.39	0.22	0.135	0.224507	0.17	0.022304255	0.001225	0.1385
204	0.356	0.39	0.22	0.136	0.224507	0.17	0.022469748	0.001156	0.1388
207	0.154	0.16	0.22	-0.066	0.224507	-0.06	0.004272002	3.6E-05	0.0246
209	0.532	0.43	0.22	0.312	0.224507	0.21	0.064067495	0.010404	0.2288
210	0.379	0.44	0.22	0.159	0.224507	0.22	0.034214818	0.003721	0.1668
211	0.101	0.11	0.22	-0.119	0.224507	-0.11	0.013652142	8.1E-05	0.0111
212	0.101	0.08	0.22	-0.119	0.224507	-0.14	0.017228903	0.000441	0.0081
213	0.101	0.08	0.22	-0.119	0.224507	-0.14	0.017228903	0.000441	0.0081
214	0.102	0.08	0.22	-0.118	0.224507	-0.14	0.017084396	0.000484	0.0082
215	0.088	0.11	0.22	-0.132	0.224507	-0.11	0.015140734	0.000484	0.0097
217	0.088	0.08	0.22	-0.132	0.224507	-0.14	0.019107495	6.4E-05	0.007
218	0.124	0.11	0.22	-0.096	0.224507	-0.11	0.01101848	0.000196	0.0136
220	0.124	0.14	0.22	-0.096	0.224507	-0.08	0.00813172	0.000256	0.0174
223	0.118	0.12	0.22	-0.102	0.224507	-0.10	0.010683269	4E-06	0.0142
229	0.114	0.12	0.22	-0.106	0.224507	-0.10	0.011101297	3.6E-05	0.0137
231	0.279	0.29	0.22	0.059	0.224507	0.07	0.003849326	0.000121	0.0809
232	0.114	0.10	0.22	-0.106	0.224507	-0.12	0.013225804	0.000196	0.0114
236	0.116	0.12	0.22	-0.104	0.224507	-0.10	0.010892283	1.6E-05	0.0139
241	0.107	0.09	0.22	-0.113	0.224507	-0.13	0.015229607	0.000289	0.0096
242	0.103	0.12	0.22	-0.117	0.224507	-0.10	0.012250875	0.000289	0.0124
243	0.103	0.09	0.22	-0.117	0.224507	-0.13	0.015767635	0.000169	0.0093
244	0.102	0.08	0.22	-0.118	0.224507	-0.14	0.017084396	0.000484	0.0082
245	0.102	0.09	0.22	-0.118	0.224507	-0.13	0.015902142	0.000144	0.0092
246	0.101	0.09	0.22	-0.119	0.224507	-0.13	0.016036649	0.000121	0.0091
248	0.100	0.09	0.22	-0.120	0.224507	-0.13	0.016171157	0.0001	0.009
249	0.102	0.09	0.22	-0.118	0.224507	-0.13	0.015902142	0.000144	0.0092
252	0.127	0.17	0.22	-0.093	0.224507	-0.05	0.005081438	0.001849	0.0216
253	0.160	0.20	0.22	-0.060	0.224507	-0.02	0.001475945	0.0016	0.032
267	0.651	0.54	0.22	0.431	0.224507	0.32	0.135906368	0.012321	0.3515
269	0.653	0.77	0.22	0.433	0.224507	0.55	0.236075523	0.013689	0.5028
270	0.098	0.08	0.22	-0.122	0.224507	-0.14	0.017662424	0.000324	0.0078
272	0.076	0.08	0.22	-0.144	0.224507	-0.14	0.020841579	0.000016	0.0061
276	0.075	0.09	0.22	-0.145	0.224507	-0.13	0.019533833	0.000225	0.0068

277	0.114	0.10	0.22	-0.106	0.224507	-0.12	0.013225804	0.000196	0.0114
280	0.071	0.07	0.22	-0.149	0.224507	-0.15	0.023056368	1E-06	0.005
284	0.155	0.16	0.22	-0.065	0.224507	-0.06	0.004207495	0.000025	0.0248
285	0.224	0.27	0.22	0.004	0.224507	0.05	0.00017172	0.002116	0.0605
294	0.267	0.26	0.22	0.047	0.224507	0.04	0.001660171	4.9E-05	0.0694
295	0.255	0.24	0.22	0.035	0.224507	0.02	0.000538762	0.000225	0.0612
296	0.248	0.27	0.22	0.028	0.224507	0.05	0.001263551	0.000484	0.067
297	0.249	0.28	0.22	0.029	0.224507	0.06	0.00159679	0.000961	0.0697
299	0.374	0.39	0.22	0.154	0.224507	0.17	0.025448621	0.000256	0.1459
300	0.341	0.40	0.22	0.121	0.224507	0.18	0.0211951	0.003481	0.1364
317	0.504	0.42	0.22	0.284	0.224507	0.20	0.055475945	0.007056	0.2117
318	0.505	0.42	0.22	0.285	0.224507	0.20	0.055671438	0.007225	0.2121
319	0.510	0.43	0.22	0.290	0.224507	0.21	0.059546649	0.0064	0.2193
327	0.085	0.07	0.22	-0.135	0.224507	-0.15	0.020893269	0.000225	0.006
328	0.085	0.10	0.22	-0.135	0.224507	-0.12	0.016836509	0.000225	0.0085
total	31.272	31.88							
avarage	0.220	0.225	0.220	0.000	0.225	0.000	0.022	0.002	0.072
standard	0.152	0.156							

APPENDIX E

Parameters of Green-Ampat for different soil types (Rawls et al., 1983).

Soil texture class	K	ψ	Φ	FC	WP wilting point
Sand	4.74	1.93	0.437	0.062	0.024
Loamy Sand	1.18	2.4	0.437	0.105	0.047
Sandy Loam	0.43	4.33	0.453	0.19	0.085
Loam	0.13	3.5	0.463	0.232	0.116
Silt Loam	0.26	6.69	0.501	0.284	0.135
Sandy Clay Loam	0.06	8.66	0.398	0.244	0.136
Clay Loam	0.04	8.27	0.464	0.31	0.187
Silty Clay Loam	0.04	10.63	0.471	0.342	0.21
Sandy Clay	0.02	9.45	0.43	0.321	0.221
Silty Clay	0.02	11.42	0.479	0.371	0.251
Clay	0.01	12.6	0.475	0.378	0.265

الخلاصة

تعتبر فيضانات نظام تصريف مياه الأمطار مشكلة رئيسية في التنمية الحضرية التي يمكن أن تتأثر باستخدام الأراضي وتغير المناخ والتضاريس. يمكن تقييم مشاكل الفيضانات بنجاح باستخدام نماذج المحاكاة مثل نموذج إدارة مياه العواصف (SWMM). في هذه الدراسة ، تم إجراء توليد منحنيات شدة-مدة-تردد (IDF) دمج تأثير تغير المناخ لمحافظة النجف في العراق لأول مرة. بالإضافة إلى ذلك ، تأثيرات الظروف المختلفة لاستخدام الأراضي (50 ، 75 ، 100٪) ، تغير المناخ (2 ، 5 ، 10 ، 25 سنة) ، منحدر التضاريس (0.5٪ إلى 0.4٪ ، 0.3٪ ، 0.2٪ ، و 0.1٪) ، وزمن التركيز (upstream and downstream) على نظام تصريف مياه الأمطار تم تقييمها باستخدام محاكاة SWMM. أشارت النتائج إلى أنه من خلال زيادة مساحة مستجمعات المياه الفرعية من 50 إلى 100٪ ، كان هناك زيادة في إجمالي الجريان من 20380 إلى 37350 مترًا مكعبًا ، وإجمالي الفيضانات من 10513 إلى 26032 مترًا مكعبًا على التوالي. استجابة لتغير المناخ ، أدى تغيير فترة العودة من 2 إلى 5 سنوات إلى زيادة الجريان الكلي من 120،14 إلى 110،27 متر مكعب (تمثل 48٪ من الزيادة) ، وزاد إجمالي الفيضانات من 5914 إلى 17591 متر مكعب (تمثل زيادة بنسبة 66.66٪). بشكل عام ، أثر منحدر المستجمعات الفرعية بشكل إيجابي على الفيضانات في جميع شدة هطول الأمطار ، ولكن كان تأثيرها أقل في شدة هطول الأمطار المنخفضة. في فترة العودة لمدة عامين ، كان تأثير منحدر المستجمعات الفرعية محدودًا مع انخفاض كبير في الفيضانات ، في حين كان للانحدار المنخفض للمستجمعات الفرعية تأثير ضئيل على الفيضانات في فترة العودة البالغة 10 و 25 عامًا. أخيرًا ، لوحظ ارتفاع منحدر المستجمعات الفرعية مما أدى إلى زيادة أخرى في الجريان السطحي ، مما يؤدي إلى الفيضانات. أظهرت النتائج أيضًا أن زمن حدوث الفيضان يحدث في اتجاه downstream قبل upstream ، مما يشير إلى أن منطقة downstream تعاني من مشاكل طبوغرافية وتصميمية. وقد تم توضيح ذلك من خلال الفيضان R315 قبل المانهول R15 لأن منحدر المستجمع الفرعي في الاتجاه المعاكس للتدفق في الأنابيب ، وكذلك عمق المانهول ، قصير. في الختام ، حيث تم تحديد مواقع وحجم الفيضانات ، فشل النظام في تصريف مياه الأمطار في بعض الظروف الحرجة ، وكان التأثير السلبي لتغير المناخ على نظام تصريف مياه الأمطار أكثر من تأثيرات استخدام الأراضي. أيضًا ، يجب على المصممين مطابقة المستجمعات الفرعية مع منحدرات أنابيب الشبكة لتقليل الفيضانات.

جمهورية العراق

وزارة التعليم العالي والبحث العلمي

جامعة كربلاء

كلية الهندسة

قسم الهندسة المدنية

تأثيرات الطبوغرافية، استخدام الاراض والتغير المناخي على تصريف مياه الامطار تحت شدات مطرية مختلفة في منطقة الأمير في مدينة النجف

رسالة مقدمة الى قسم الهندسة المدنية، جامعة كربلاء وهي جزء من متطلبات الحصول على درجة الماجستير في الهندسة المدنية (هندسة البنى التحتية)

من قبل :

سلام ناجي حسين

بكالوريوس في الهندسة المدنية 2006 / جامعة الكوفة

بأشراف

أ.د. باسم خليل نايل

أ.م.د. حيدر محمد نعمه